



MASTER THESIS

Synthesis of *N*- & *S*- heterocycle-based Monomers and their high-performance Materials

TECHNISCHE UNIVERSITÄT WIEN
Institute of Materials Chemistry
Advanced Organic Materials Research Group
Vienna, Austria
October 16, 2019

This thesis was carried out under the supervision of Assistant Prof.
Dipl.-Chem. Dipl.-Ing. Dr.rer.nat. Miriam Margarethe Unterlass, MSc

submitted by
PATRICK WALTER FRITZ, BSc

born on March 17th, 1993 in Bregenz
matriculation number 01325048
Reitweg 16, 6830 Rankweil

"Organic chemists are masterful at exercising control in zero dimensions. One subculture of organic chemists has learned to exercise control in one dimension. There are polymer chemists, the chain builders... but in two or three dimensions, it's a synthetic wasteland"

Roland Hoffmann

Abstract

Organic polymers can be tuned to fulfill a plethora of tasks. Both polyimides (PIs) and polythiophenes (PTs) are highly functional polymers. PIs are high-performance polymers (HPPs) featuring high chemical, thermal and mechanical stability. Hence, they can be used for applications, which require materials to withstand extreme conditions (*e.g.* as insulators in electronic devices). PTs, on the other hand, become conductive upon oxidation, which enables them to be used in electronic devices (*e.g.* organic light-emitting diodes (OLEDs) or organic photovoltaics (OPVs)). However, both in synthesis, as well as in processing of these materials toxic solvents and catalysts are required, resulting in an overall environmentally harmful product. For PIs, hydrothermal polymerization (HTP) and solid-state polymerization (SSP), are suitable methods to avoid toxic solvents and catalysts. Whereas SSP is a solvent-free method, HTP utilizes only water as a solvent. HTP utilizes the changing properties of water upon heating to $T > 100\text{ }^{\circ}\text{C}$ in a confined reaction vessel, which enables the synthesis of PIs, as well as enhances their crystallinity. As solvents are one of the main contributors when evaluating the "greenness" of a procedure, using an ubiquitous, non-toxic solvent such as water greatly increases the green characteristics of a procedure.

This diploma thesis deals with the development and synthesis of both amine- and thiophene-based precursors and their environmentally friendly polymerization towards highly functional materials.

The goal of the first part was to synthesize PI-based 3D covalent organic frameworks (COFs). This work shows that the conditions (temperature, reaction time, and concentration), as well as the used monomers, affect the polymerization significantly. It was also found, that under hydrothermal conditions aniline is eliminated from the amine precursor of choice, tetra(4-aminophenyl)methane, complicating the characterization significantly. Besides HTP, SSP of prepared monomer salts was conducted as an alternative procedure.

The second part addressed the preparation of solid-state polymerizable thiophene precursors as only a few examples of such precursors/polymers are reported. However, these polymers usually lack processability because their solubility is rather low. To address this problem, a variety of strategies were tested to assess the suitability of thiophene-based systems for SSP, while the product should retain some degree of solubility. Hence, trithiophenes were designed to feature a tuneable thiophene system while also containing moieties that should enable SSP.

Kurzfassung

Organische Polymere stellen eine Materialklasse dar, welche sich besonders durch ihre Flexibilität auszeichnet. Polyimide (PIs) sind Hochleistungspolymere, welche sich besonders durch ihre mechanischen Eigenschaften, sowie durch ihre hohe chemische und thermische Stabilität auszeichnen. Daher können sie für Anwendungen unter extremen Bedingungen (z.B. als Isolatoren auf Leiterplatten) verwendet werden. Polythiophene (PTs) können durch Oxidation elektrisch leitfähig gemacht werden und eignen sich daher zur Verwendung in elektronischen Bauteilen (z.B. organische Leuchtdioden (OLEDs) oder organische Solarzellen (OPVs)). Allerdings muss im Allgemeinen sowohl für die Synthese als auch die Verarbeitung dieser Polymere auf giftige organische Lösemittel und Katalysatoren zurückgegriffen werden. Hydrothermale Polymerisation (HTP) und Festphasenpolymerisation (SSP vom engl. solid-state polymerization) stellen im Fall von Polyimiden attraktive Alternativen dar, um giftige Lösemittel zu vermeiden. SSP ist eine lösemittelfreie Methode, während bei HTP Wasser als einziges Lösemittel verwendet wird. Dabei nutzt hydrothermale Synthese (HTS) die sich verändernden Eigenschaften von Wasser bei Temperaturen über 100 °C, aus um die Synthese sowie die Kristallisation von PIs zu ermöglichen. Da bei der Beurteilung der Umweltfreundlichkeit einer Synthese bzw. eines Prozesses Lösemittel einen großen Einfluss haben, bietet es sich an ein ubiquitäres, ungiftiges Lösemittel wie Wasser zu nutzen um ein umweltfreundlicheres Verfahren zu erhalten.

Diese Diplomarbeit setzt sich mit der Synthese von amin- und thiophenbasierten Monomeren und deren umweltfreundlicher Polymerisation zu hochfunktionellen Materialien auseinander.

Das Ziel des ersten Teils dieser Arbeit war die Synthese von PI-basierten kristallinen, organischen Gerüstverbindungen (COFs vom engl. covalent organic frameworks). Diese Arbeit untersucht welchen Einfluss die verwendeten Reaktionsbedingungen (Temperatur, Reaktionszeit und Konzentration) sowie die Wahl der Monomere auf die Polymerisation haben. Es wurde zudem gezeigt, dass unter hydrothermalen Bedingungen eine Anilin-Gruppe vom verwendeten Ausgangsstoff (Tetra(4-aminophenylmethan)) abgespalten werden kann, was die Charakterisierung signifikant erschwert. Neben HTP wurde auch SSP als alternative Methode zur Polymerisation von Monomersalzen herangezogen.

Der zweite Teil dieser Arbeit beschäftigt sich mit der Synthese von festphasenpolymerisierbaren Thiophen-Monomeren. Zum Zeitpunkt dieser Arbeit sind nur wenige Monomere bekannt, welche sich entsprechend polymerisieren lassen. Zudem weisen die entsprechenden Polymere oft nur eine sehr geringe Löslichkeit auf. Um diese Probleme zu untersuchen wurden verschiedene Strategien verfolgt, welche sowohl ein SSP-fähiges Monomer als auch geeignete Löslichkeit des Polymers gewährleisten sollten. Ein Trithiophen System, bestehend aus einem funktionalisierbaren Thiophen-Kern gebunden an zwei SSP-fähige Thiophen-Systeme wurde entwickelt.

Acknowledgements

At this point I would like to thank my supervisor Prof. Miriam M. Unterlass, who helped me throughout my whole thesis. Miriam always pushed me to come up with my own ideas and even allowed me to design projects on my own. I especially value this opportunity, as it helped me to grow significantly and allowed me to see the bigger picture.

I furthermore want to thank Elias Bumbaris for keeping an eye on me during my first weeks in the lab and for being an excellent lab partner and friend. I want to thank Marianne Lahnsteiner and Mohamed Musthafa Iqbal for the many delightful discussions on COFs and the great time we had during conferences. I would also like to thank all my other colleagues and friends in the Unterlass group. All of which have supported me throughout the various stages of this thesis. No matter what question I had, or problem had to be solved, they were there for me and I am forever grateful to have experienced such an incredible group. Miriam, Alonso, Tobia, Michael, Fabián, Hipassia, Marwan, Elias, Musthafa, Marianne, Lukas L., Olivier, Miriam Z., Eleonora and Simon – Thank you!

I also want to thank Werner Artner for his help in the area of X-ray analytics. His invaluable expertise and kindness never failed to impress me.

Gratitude is owed to Berthold Stöger for the SCXRD measurements he conducted.

I want to thank Stefan Weber who made it possible for me to use their H₂ autoclave setup.

I furthermore want to thank all the people outside of the university, who have helped me throughout the course of my life. My highest gratitude is owed to my parents, Andrea and Walter, for supporting me financially but most of all for raising me to be the person I am today. I would also like to thank my grandparents and my sisters for supporting me throughout many phone calls and for making every single moment spent at home special.

I also want to thank my girlfriend Teresa for her support during the last 2 years. Thank you for keeping me sane, forcing me to take breaks and for making these last 2 years a true pleasure.

I want to thank my dear friends Alwin, Andreas, Barbara, Eleonora, Michael, Nick, Simon, Stefan and all the others who endured me during difficult times and made my time in Vienna a true pleasure.

“For my partens who have supported me throughout my entire live”

Contents

Abstract	III
Kurzfassung	IV
Acknowledgements	V
1 Introduction	1
I Polyimides	3
2 General Background	4
2.1 Covalent Organic Frameworks	4
2.2 Reticular Chemistry	4
2.3 COF Structures	7
2.3.1 2D Topologies	7
2.3.2 3D Topologies	8
2.4 Dynamical Linkages	8
2.4.1 B-O Linkages	10
2.4.2 C-N Linkages	10
2.4.3 Imide Linkages	11
2.4.4 C-C Linkages	11
2.5 Synthetic Methods in COF Synthesis	12
2.5.1 Solvothermal Synthesis	12
2.5.2 Ionothermal Synthesis	12
2.5.3 Microwave Synthesis	12
2.5.4 Mechanochemical Synthesis	12
2.6 Hydrothermal Synthesis	13
2.6.1 Hydrothermal Synthesis of Polyimides	13
2.6.2 Water under Hydrothermal Conditions	14
3 Aims and Motivation	16
4 Results and Discussion	17
4.1 PI-based Frameworks <i>via</i> Hydrothermal Polymerization	17
4.1.1 Preparation of TAPM	17
4.1.2 TAPM and TrisAPM as Precursors	18
4.1.3 TAPM under HT Conditions	18

4.1.4	Polymerization and Characterization of TAPM:PMDA	18
4.1.5	Evaluation of Reaction Time and Temperature	19
4.1.6	TrisAPM-Carbocation from HT Synthesis	20
4.1.7	Implications of the TrisAPM-Cation Species on Framework Synthesis	20
4.1.8	Polymerization and Characterization of TAPM:PMA	21
4.1.9	Evaluation of Reaction Yield	24
4.1.10	Comparison with Simulated TAPM:PMA COFs	26
4.1.11	TAPM:PMA Monomer Salt	28
4.1.12	Polymerization and Characterization of the TAPM:PMA Monomer Salt	28
4.1.13	Evaluation of SEM Micrographs	31
4.1.14	Polymerization and Characterization of TrisAPM:PMDA	33
4.1.15	Polymerization and Characterization of TrisAPM:Mella	35
4.1.16	Conclusion and Outlook	36
4.2	Triazines in COFs and Materials Science	37
4.2.1	State of the Art	37
4.2.2	2,4-Diamino-1,3,5-triazines as COF Precursors	37
4.2.3	BATB – A Versatile DATz Precursor	39
4.2.4	Attempted Polymerization of BATB and Derivatives	39
4.2.5	Conventional Synthesis of Imine-based BATB-COFs	40
4.2.6	Polymerization of BATB and Derivatives towards Amino-linked Systems	41
4.2.7	Crystallography of BATB and its Derivatives	43
4.2.8	Conclusion and Outlook	44
II	Polythiophenes	45
5	General Background	46
5.1	Conductive Polymers	46
5.2	Polythiophenes	47
5.3	Poly(3,4-ethylenedioxythiophene)	48
6	Aims and Motivation	49
7	Results and Discussion	50
7.1	Initial Tests	50
7.1.1	Solid-State Polymerization	50
7.1.2	Hydrothermal Polymerization	52
7.1.3	Evaluation of the Initial Results	52
7.2	Preparation of Functionalized DBEDOT Systems	53
7.2.1	WUDL's Procedure – Optimizing Conditions	53
7.2.2	Evaluating the Effect of Substitution	55
7.2.3	Preparation of Tri-thiophenes Featuring Terminal EDOT Moieties	55
7.3	Conclusion and Outlook	57
8	Conclusion	58

9	Experimental Part	60
9.1	General Methods	60
9.2	Polyimides	61
9.2.1	Chemicals	61
9.2.2	Synthesis of TAPM	61
9.2.3	Synthesis of TAPM– based Organic Polymers	64
9.3	Diaminotriazines	69
9.3.1	Chemicals	69
9.3.2	General Synthesis of diaminotriazines <i>via</i> cyclotrimerization	69
9.3.3	Synthesis of Dimorpholinotriazines	75
9.3.4	Polymerizations of DATz's	77
9.4	Polythiophenes	80
9.4.1	Chemicals	80
9.4.2	Preparation of DBEDOT, BEDOT and PEDOT	80
9.4.3	Preparation of 2-Substituted-EDOT systems	84
9.4.4	Perparation of Trithiophene Systems	86
A	List of Structures	88
B	Polyimides	92
C	Crystallization	104

List of abbreviations and symbols

3MBDT	2,5-Dibromo-3-methylthiophene	n	amount of substance
Ac ₂ O	acetic anhydride	NBS	<i>N</i> -bromosuccinimide
AcOH	acetic acid	NMP	<i>N</i> -methylpyrrolidone
ATR	attenuated total reflectance	NMR	nucleus magnetic resonance
BATB	2,4-Bisamino-1,3,5-triazine-benzene	NSTR	non-stirred steel reactor
BEDOT	2-Bromo-3,4-ethyldioxythiophene	OLED	organic light-emitting diode
CCDC	cambridge crystallography data center	OPV	organic photovoltaics
COF	covalent organic framework	p	extent of reaction
CTF	covalent triazine framework	<i>p</i>	pressure
DATz	diaminotriazine	PEDOT	poly-3,4-ethylenedioxythiophene
DBBT	5,5'-Dibromo-2,2'-bithiophene	PI	polyimide
DBEDOT	2,5-Dibromo-3,4-ethyldioxythiophene	PMA	pyromellitic acid
DBT	2,5-Dibromothiophene	PMDA	pyromellitic dianhydride
DCB	dynamic covalent bond	POP	porous organic polymer
DMF	dimethylformamid	PSS	poly styrene sulfonate
EDOT	3,4-Ethylenedioxythiophene	PT	polythiophene
ETE	EDOT-thiophene-EDOT trithiophene	SC-XRD	single-crystal X-ray diffraction
EtOH	ethanol	SEM	scanning electron microscopy
FT-IR	FOURIER transformation infrared	sql	square lattice
GCMS	gaschromatography-mass spectroscopy	SSP	solid-state polymerization
HAE	heteroatom effect	<i>T</i>	temperature
hcb	honeycomb	<i>t</i>	time
HPP	high-performance polymer	TAPM	tetra-(4-aminophenyl)methane
HT	hydrothermal	<i>T_d</i>	decomposition temperature
HTP	hydrothermal polymerization	TGA	thermogravimetric analysis
HTS	hydrothermal synthesis	THF	tetrahydrofurane
hxl	hexagonal hexatopic	TNPM	tetra-(4-nitrophenyl)methane
kdg	Kagomé dual	TPM	tetraphenylmethane
kgm	Kagomé	TrisAPM	tris-(4-aminophenyl)methane
MellA	mellitic acid	Tz	triazine
MeOH	methanol	UV	ultraviolet
MOF	metal-organic framework	XRD	X-ray diffraction

List of Figures

2.1	First COF Syntheses	5
2.2	Reticular Chemistry	6
2.3	2D COF Topologies	7
2.4	3D COF Topologies	8
2.5	COF Linkers	9
2.6	Imine COFs	10
2.7	Imide Formation Pathways	11
2.8	Phase Diagram of Water	13
2.9	Hydrothermal Synthesis of Zeolites	13
2.10	Hydrothermal PI Synthesis <i>via</i> the Monomer Salt Route	14
2.11	Perinone Dye	14
2.12	HTW – Effect on Polarity	14
2.13	High-Temperature Water	15
4.1	Preparation of TAPM	17
4.2	Structure of TAPM and TrisAPM	18
4.3	Polymerization of TAPM with PMDA	19
4.4	Crystal Violet Dyes and the TrisAPM-carbocation	20
4.5	TrisAPM-cation and its Implications	21
4.6	TAPM:PMA XRD	22
4.7	TAPM:PMA IR	23
4.8	TAPM:PMA 2:5 XRD	24
4.9	TAPM:PMA XRD – Conc.-Screen	25
4.10	Hypothetical COF Incorporating the TrisAPM-carbocation	26
4.11	TAPM:PMA XRD Simulation	27
4.12	TAPM:PMA Monomer Salt NMR	28
4.13	XRD of the MonSalt and its SSPs	30
4.14	SEM of the MonSalt and Short Polymerizations	31
4.15	SEM of 120 hour Polymerizates	32
4.16	TrisAPM and Theoretical Framework Structure	33
4.17	TrisAPM:PMDA XRD	34
4.18	TrisAPM:MellA Theoretical Structure	35
4.19	Applications of CTFs	37
4.20	Synthesis of Triazines	38
4.21	Diaminotriazines	38
4.22	DATz and Theoretical Polymer	39

4.23	Aminal-linked Polymers	42
4.24	Crystal Structures and Micrographs of BATB and 4-NO ₂ PhMTz	43
5.1	Examples of Conductive Polymers	46
5.2	Conventional Polythiophene Synthesis	47
5.3	3-Substituted Polythiophenes	47
5.4	Doping of Polythiophenes	48
5.5	Synthesis of EDOT	48
6.1	Synthesis of PEDOT	49
6.2	Synthesis of Functionalized Polythiophenes <i>via</i> SSP	49
7.1	Dibromothiophenes	50
7.2	SSP and HTP of DBBT	51
7.3	DBBT NMR Pre and Post SSP	52
7.4	Proposed Mechanism for the SSP of DBEDOT	53
7.5	Polymerization of DBEDOT	54
7.6	Synthesis of BEDOT	55
7.7	Preparation of Substituted EDOT	56
7.8	Preparation of EDOT Terminally Functionalized Thiophenes	56
9.1	Synthesis of TPM	61
9.2	Synthesis of TNPM	62
9.3	Synthesis of TNPM	63
9.4	TAPM:PMDA Polymerization	64
9.5	TAPM:PMA Polymerization	64
9.6	Synthesis of the TrisAPM-carbocation	65
9.7	Synthesis of the TAPM:PMA MonSalt	65
9.8	Solid-State Polymerization of MonSalts	66
9.9	Hydrothermal Polymerization of TrisAPM:PMDA	67
9.10	Hydrothermal Polymerization of TrisAPM:MeLA	68
9.11	General DATz synthesis	69
9.12	BATB Synthesis	69
9.13	Synthesis of NO ₂ PhTz	70
9.14	Synthesis of NH ₂ PhTz	71
9.15	Synthesis of 4COOHPhTz	71
9.16	Synthesis of 4COHPhTz	72
9.17	Synthesis of 4PyrPhTz	73
9.18	Synthesis of DAAQ	73
9.19	Synthesis of 4-NO ₂ PhMTz	75
9.20	Synthesis of 4-NH ₂ PhMTz	76
9.21	Polymerization of DATz's	77
9.22	Attempted polyimine synthesis	78
9.23	Synthesis of Aminal-linked polymers	79
9.24	Synthesis of DBEDOT	80
9.25	SSP of DBEDOT	81
9.26	Synthesis of BEDOT Method A	81

9.27 Synthesis of BEDOT Method B	82
9.28 Synthesis of BEDOT Method C	82
9.29 Preparation of 2-substituted thiophenes	84
9.30 Synthesis of 2-Bromo-5-(chlorothieryl)-3,4-ethylenedioxythiophene	84
9.31 Synthesis of 2-Bromo-5-(nitrophenyl)-3,4-ethylenedioxythiophene Method A	84
9.32 Synthesis of 2-Bromo-5-(aminophenyl)-3,4-ethylenedioxythiophene Method B	85
9.33 Synthesis of 2,5-di(3,4-ethylenedioxythienyl)thiophene Method A	86
9.34 Bromination of the terthiophene ETE	87
B.1 TGA of TAPM:PMDA	92
B.2 IR of TAPM:PMDA A	93
B.3 IR of TAPM:PMDA B	93
B.4 TGA of the TAPM:PMA monomer salt A	94
B.5 TGA of the TAPM:PMA monomer salt B	95
B.6 IR of the TAPM:PMA monomer salt	96
B.7 PXRD of TrisAPM:PMDA	97
B.8 TGA of TriAPM:PMDA	98
B.9 TGA of TrisAPM:PMDA – conc. screen	99
B.10 PXRD of TrisAPM:Mella	100
B.11 TGA of TrisAPM:Mella	101
B.12 UV/VIS measurements of DATz systems	102
B.13 TGA of BATB	103

List of Tables

4.1	IR modes	23
4.2	TAPM:PMA Monomer Salt TGA	29
4.3	Conditions Used in the Conventional Polymerization of DATzs Towards Imides	40
4.4	Conditions Used in the Conventional Polymerization of DATz	41

Chapter 1

Introduction

Organic chemistry revolves around building molecules and materials instead of taking a top-down approach that focusses on creating a material by breaking/altering it to fit their desired use (e.g. scotch-taping graphite to obtain graphene). Hence, organic chemistry is concerned with finding new means and methods to produce materials by using known and developing new reaction pathways.

Organic chemistry and especially organic materials chemistry might be amongst the major tools enabling human advancement in the last two centuries. Understanding how molecules behave, how they react and form new compounds and how to use these findings for synthesizing new materials have been the main focus during the early days of organic chemistry in the 19th century. Chemists such as Kekulé [1], who developed the theory of chemical structure, or Friedrich Wöhler [2], the first chemist to obtain an organic molecule from an inorganic precursor, were the pioneers of the field.

In the late 19th century and especially with the beginning of the 20th century, this focus changed. The discovery of how to use petroleum to obtain a plethora of useful molecules accelerated the pace at which new materials, pharmaceuticals and especially organic polymers were discovered. Adolf von Baeyer was one of the first to discover the untapped potential of using petroleum-derived organic compounds in the synthesis of new materials. Phenolphthalein [3], a now standard pH indicator, as well as an industrially applicable synthetic route towards indigo [4], are only a few examples of his achievements.

Even though the first organic polymers were discovered during the early 20th century, a deeper understanding of how such materials formed and how they are linked was only established in 1922. Hermann Staudinger, who was later awarded a Nobel prize, realized, that organic polymers are built from small molecules, so-called monomers and are linked by covalent bonds [5]. During the second world war, polymers such as Nylon, a polymer based on the polycondensation of a dicarboxylic acid with a diamine, were mass-produced, because the derived fibers showed higher strength and durability, while being lighter in weight than conventional plant-based fibers.

To date, a plethora of organic polymers tailored to their desired use have been developed and are a crucial part of modern life. However, this diversity and hence, the prosperity of humanity has come at a cost. Firstly, a majority of these polymers can be classified as single-use materials, as they are often employed as polymer blends and separation and recycling of such blends are uneconomic. Secondly, the synthesis of these polymers often requires the use of environmentally harmful solvents or precious metal catalysts [6]. Especially polymers featuring high-performance properties, such as high chemical and thermal stability, require harsh conditions in their syntheses. Polyimides (PIs) belong to this class of HPPs and are often used as insulating materials on e.g. circuit boards. However, conventional synthesis of such materials requires $T > 300\text{ °C}$ and toxic solvents (e.g. DMF or NMP), as well as catalysts (e.g. isoquinoline).

Hydrothermal polymerization (HTP), a technique that uses exclusively water as a solvent and solid-state

polymerization (SSP) are amongst the only known methods to produce high-performance materials without the need for toxic solvents [7].

In recent years, it became apparent that our society is steering towards a tipping point. Decades of scavenging resources and mass-producing new devices to fit humanity's needs has led to an environmental crisis. Especially gases such as CO₂ or methane are amongst the major driving forces at climate change. Hence, developing materials that can capture and separate these gases from exhaust air gained interest in recent years. Porous materials of organic, inorganic and even metal-organic nature are potential candidates for solving this problem. Covalent organic frameworks (COFs), crystalline network polymers featuring high porosity, are amongst the most promising materials to tackle this task. However, only a few examples of eco-friendly syntheses have been reported [8]. Another essential question lies in the production of green and renewable energy. Solar power is usually produced using photovoltaic systems based on silicon. However, the production of single-crystalline silicon requires an immense amount of energy. Hence, alternative approaches using hybrid-materials and even fully organic systems have been developed. Entirely organic photovoltaics (PVs) are of interest due to their facile processability, *e.g.* spin-coating, which allows the production of large-area PVs in relatively short time compared to conventional systems. Organic photovoltaics (OPVs) are generally based on organic polymers such as polythiophenes. However, during the synthesis and processing of these materials, harmful conditions have to be employed.

The motivation for this work was to synthesize highly functional materials using environmentally friendly methods such as HTS and SSP.

The first part of the thesis deals with the synthesis and characterization of monomers and their polymerization towards PI-based COFs.

The second part focusses on the development of thiophene-based monomers suitable for solid-state polymerization. Both parts feature an introduction to the topic that should provide the necessary background before discussing the results and formulating conclusions.

Part I

Polyimides

Chapter 2

General Background

2.1 Covalent Organic Frameworks

Covalent organic frameworks (COFs) are extended crystalline solids, made of light elements (*e.g.* H, B, C, N, O, Si) held together by covalent bonds. COFs show vastly different challenges in synthesis than their semi-organic counterpart metal-organic frameworks (MOFs). Whereas MOF chemistry is challenged by synthesizing and controlling the metrics of building units, to open up their structures in a rational way to make crystalline and porous extended solids, the initial challenges in synthesizing COFs were more extensive, as no naturally occurring fully-organic, crystalline, extended 2D or 3D structures were known to humankind [9]. Even though organic chemistry has mastered the task of synthesizing increasingly elaborate molecules leading to the art and science of total synthesis, these tools have not, until recently, been extended to the synthesis of organic 2D and 3D structures. In 2005, YAGHI and coworkers reported the first extended organic frameworks COF-1 and COF-5 [10]. These frameworks, based on the reversible boroxine and boronate ester formation, resulted in highly porous boroxine/boronate frameworks (Fig. 2.1). In general, two challenges have to be overcome in the synthesis of such COFs. Firstly, the reaction of formation has to be slowed down enough to allow for proper crystallization, and secondly, water has to remain in the system to allow for full reversibility of the bond formation hence enabling error correction. This indicates that COF chemistry is of highly dynamic manner which has to be controlled accordingly [9][11].

2.2 Reticular Chemistry

Reticular chemistry describes the designed synthesis of extended structures featuring a specific topology, which is of utmost importance in the synthesis of COFs and MOFs. For organic systems, reticular chemistry is unique to COFs as there are no other extended organic materials with periodicity and long-range order [12]. In general, a reticular synthesis can be broken down into five steps (Fig. 2.2).

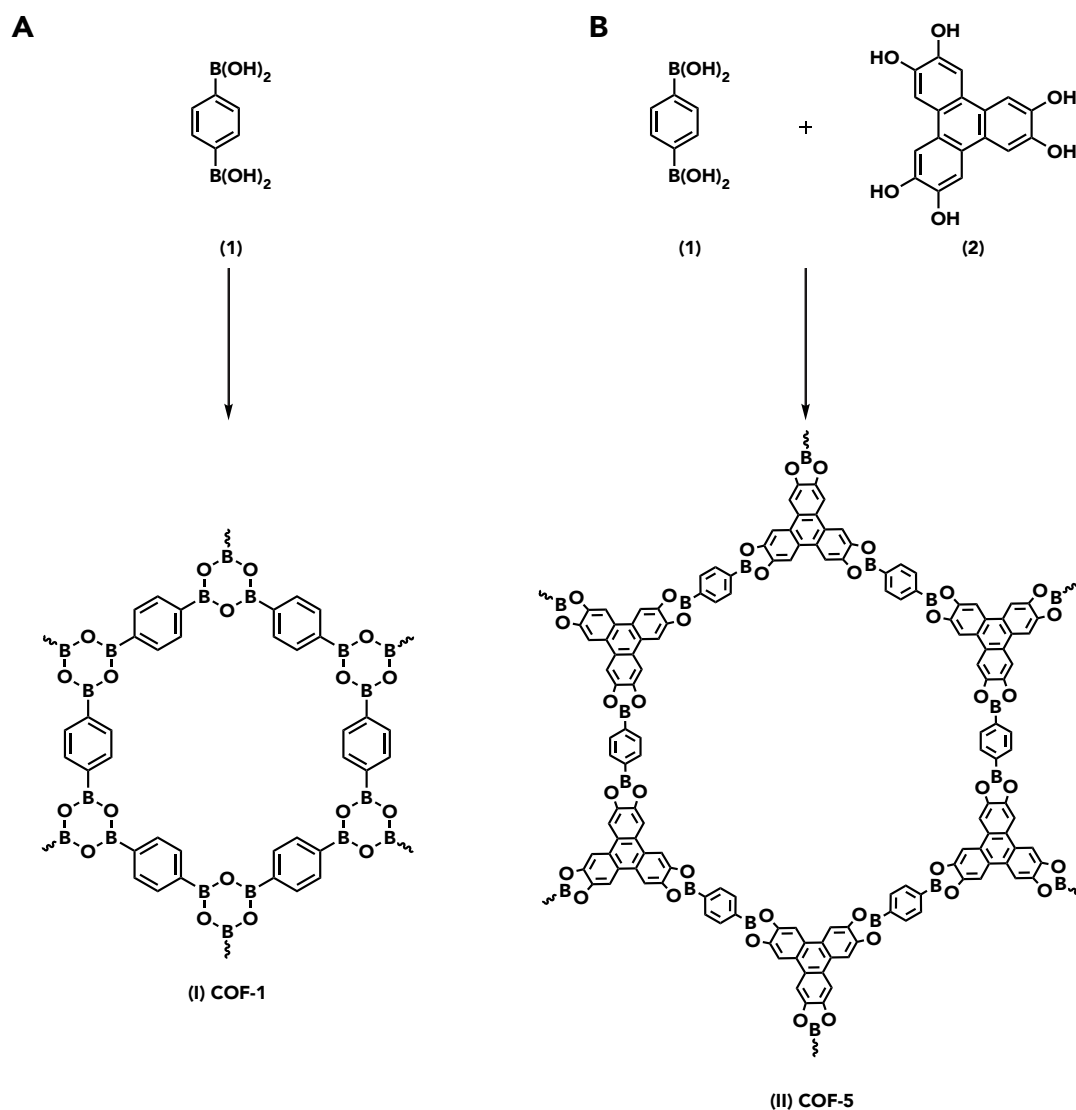


Figure 2.1: First COF Syntheses: Synthetic scheme for COF-1 (I) and COF-5 (II). **A)** shows the self-condensation of benzenediboric acid (1) resulting in boroxine linkages. **B)** shows the condensation of benzenediboric acid (1) with hexahydroxytriphenylene (2) resulting in boronate esters.

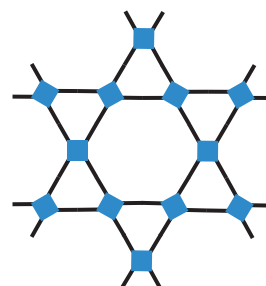
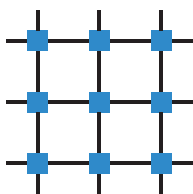
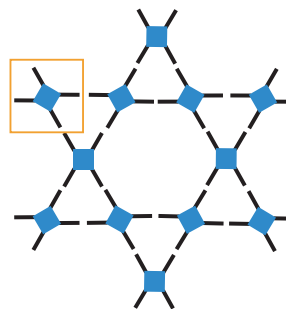
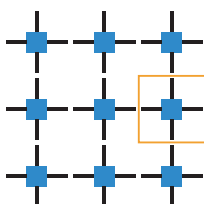
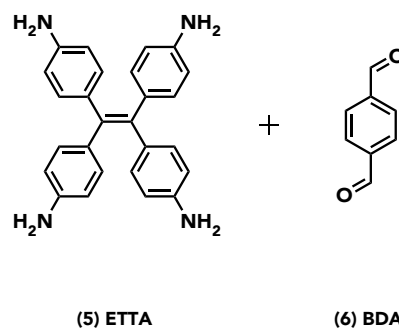
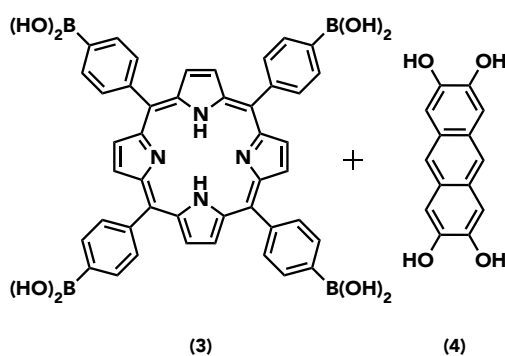
Step 1: Choosing a topology**Step 2: Breaking at the highest geometry****Step 3: Identifying molecular building-blocks****Step 4: Synthesis****Step 5: Characterization**

Figure 2.2: Reticular Chemistry: General pathway used in reticular chemistry to determine molecular building blocks from the desired topology. COF-66 a boronate-ester based and an imine based COF were chosen to show how different tetravalent precursors can lead to vastly different topologies. Adaptation from "Introduction to Reticular Chemistry" – YAGHI.

- Step 1: A target framework topology has to be chosen. Based on that, the highest symmetry embedding part of the topology is dissected into vertices by breaking them up at their edges.
- Step 2: The vertices are evaluated on their number of points of extension, their geometry and their idealized angles. This information is crucial because if just connectivity was considered, a large number of possible topologies exist.
- Step 3: Molecular equivalents that correspond to the previously determined geometries are identified, which often leads to large, poly-aromatic building blocks.
- Step 4: The COF is synthesized by stitching together the molecular building blocks through covalent bonds *via* linkages discussed in the next chapter.
- Step 5: Characterization of the obtained frameworks *via* powder X-ray diffraction (PXRD), scanning electron microscopy (SEM), transmission electron microscopy (TEM), *et cetera* [9].

In conclusion, reticular chemistry is a tool to design monomers to fit a chosen topology. However, in the case of 2D frameworks, only single layers are designed. Hence, differences can even occur for frameworks featuring the same topology design due to *e.g.* stacking effects.

2.3 COF Structures

To date, nine different topologies for COFs have been reported of which five are layered 2D structures, and four are 3D nets. In this chapter, 2D and 3D COF structures will be discussed with particular interest put on the diamond topology.

2.3.1 2D Topologies

Structures of COFs are commonly built from aromatic building blocks that endow the framework with both mechanical and architectural stability [9] [11] [13]. As a majority of COF-linkages and monomers feature sp^2 -hybridization, a vast degree of aromaticity is maintained throughout a majority of the framework, which often results in a layered structure due to the strong $\pi - \pi$ -interactions.

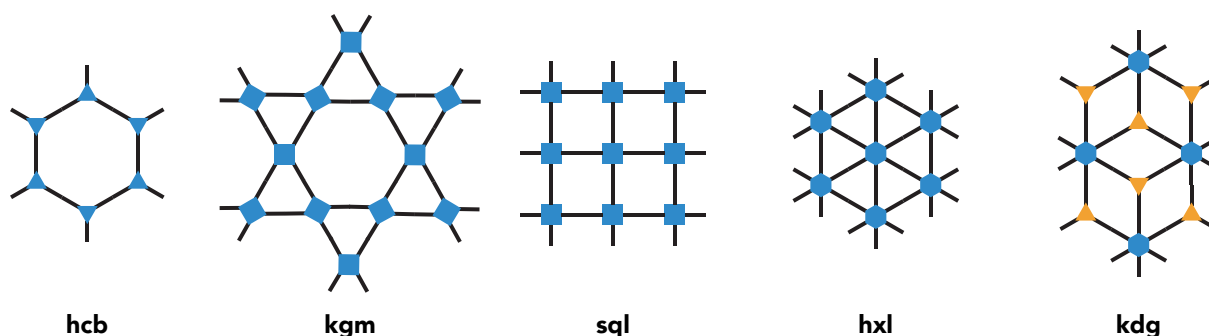


Figure 2.3: 2D COF Topologies: The most common 2D COF topologies.

Figure 2.3 shows reported 2D COF topologies. Hexagonal structures (hcb= honeycomb) are among the most prominent representatives in COF-chemistry. However, two different types of hexagonal COFs can be obtained featuring either a staggered (*e.g.* COF-1) or an eclipsed conformation (*e.g.* COF-5) [10]. In many cases, simple aromatic precursors can be used, which are often readily available or can be tuned to desire. Square-shaped precursors allow the preparation of sql- topology (square lattice) COFs. In this

case, precursor design is more demanding and often requires the preparation of functionalized porphyrins or phthalocyanines. The design of a kdg- topology (Kagomé dual) is even more demanding, as it requires the preparation of a hexagonal and a trigonal precursor. The challenge lies in designing both bond angles, as well as linker length. Both have to align perfectly to allow the formation of such a framework [10] [14]. YAGHI further expanded the range of possible 2D COF topologies after reporting the synthesis non-edge transitive nets (these are nets where not always the same links, in terms of linkage type and angle, between the molecules are used). A set of multinary COFs were designed and synthesized featuring three precursors – a hexagonal, a trigonal and a quaternary [15].

2.3.2 3D Topologies

Even though theoretically there are far more 3D topologies than 2D, only a few have been reported to date. As mentioned before, the synthesis of COFs is generally based on rigid aromatic building blocks, which are usually not available for the polyhedral precursors required in 3D COF synthesis. Most notably, the use of tetrahedral units in combination with linear building blocks resulted in the majority of literature to date. Using such systems facilitates the preparation of products featuring a diamond topology as shown in 2.4.

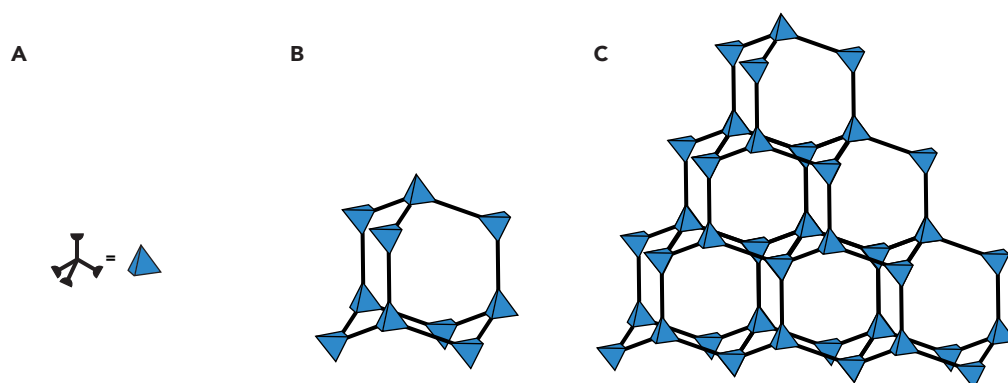


Figure 2.4: 3D COF Topologies: Schematic representation of A) a single tetrahedral building block and its representation in the following schemes, B) a single diamond unit cell and C) a 3D network comprised of these building blocks.

COF-300, a framework based on tetra(4-aminophenyl)methane and terephthalic aldehyde, was the first 3D framework and was reported by URIBE-ROMO *et al.* [16]. Due to the 3D nature of these imine-based COFs, up to nine-fold interpenetration is possible. However, interpenetration can be controlled by varying building blocks – the larger the building block, the higher the degree of interpenetration [15]. To date, only one non-interpenetrating 3D COF, PI-COF-4, has been reported. The steric hindrance resulting from the imidization of tetraaminoadamantane with PMDA results in an open framework structure with large channels [17].

2.4 Dynamical Linkages

One of the main characteristics of COFs is that they are linked *via* dynamic covalent bonds (DCBs), which are generally obtained *via* reversible organic reactions. This does not only allow for covalent bonds, but also results in the error-checking capability of reversible bonds at the same time and results in the outstanding properties of COFs. Depending on the linkage, specific properties such as chemical stability, thermal stability and crystallinity can be affected – for the better or worse. In general, a tradeoff between chemical stability and crystallinity can be found when comparing different linkages (Fig. 2.5) [18] [13].

Linkage Type		Characteristics	References
B-O	<p>(7) + (8) $\xrightleftharpoons{\text{Boronate Ester}}$ (9)</p>	<p>crystallinity: excellent thermal stability <600 °C chemical stability: sensitive to water, alcohols, acid, base, atmospheric moisture</p>	a)
	<p>(7) $\xrightleftharpoons{\text{Boroxine}}$ (10)</p>	<p>crystallinity: excellent thermal stability <500 °C chemical stability: sensitive to water, alcohols, acid, base, atmospheric moisture</p>	b)
C-N	<p>(11) + (12) $\xrightleftharpoons{\text{Imine}}$ (13)</p>	<p>crystallinity: good thermal stability <500 °C chemical stability: better than boron-based systems</p>	c)
	<p>(14) + (12) $\xrightleftharpoons{\text{Imide}}$ (15)</p>	<p>crystallinity: good thermal stability 500-600 °C chemical stability: better than boron-based systems, sensitive to base</p>	d)
	<p>(16) + (17) $\xrightleftharpoons{\text{Phenazine}}$ (18)</p>	<p>crystallinity: moderate thermal stability 850 °C chemical stability: 1 day in water, 1N HCl, 1M NaOH and organic solvents</p>	e)
	<p>(19) $\xrightleftharpoons{\text{Triazine}}$ (20)</p>	<p>crystallinity: poor thermal stability <400 °C chemical stability: high</p>	f)
C-C	<p>(21) $\xrightleftharpoons{\text{C-C}}$ (22)</p>	<p>crystallinity: not reported thermal stability <250 °C chemical stability: none reported</p>	g)
	<p>(23) $\xrightleftharpoons{\text{C=C}}$ (24)</p>	<p>crystallinity: poor thermal stability <450 °C chemical stability: excellent chemical and physical stability</p>	h)

Figure 2.5: COF Linkers: COF-linkers and characteristics. Information on these systems were derived from the cited literature. a) [10] b) [19] c) [16] d) [20] e) [21] f) [22] g) [23] h) [24]

In this chapter, the most commonly used COF-linkages will be discussed, with special focus on imide-linkages. As shown in Fig. 2.5, a wide array of possible linkages can be chosen, while still retaining reversibility in the bond formation.

2.4.1 B-O Linkages

As discussed in the previous chapter, the first generation of COFs were based on boronic acid building blocks and were reported by YAGHI [10]. Based on boronic acids a variety of COFs could be synthesized ranging from *i)* self-condensed systems over *ii)* systems using catechol and other dihydroxy species as condensation partner to *iii)* borosilicates *via* condensation of boronic acids with silanols. These systems feature excellent reversibility and error-checking capability resulting in high crystallinity as well as high thermal stability (500–600 °C) [25]. On the other hand, this reversibility results in rather moisture-sensitive systems. Furthermore, acids and even alcohols can lead the deterioration of the framework. Even though, several groups attempted to solve this problem using various strategies (*e.g.* introducing alkyl chains of various length [26]), to date, boron-based COFs still lack the desired stability for industrial applications.

2.4.2 C-N Linkages

The most commonly used C-N linked systems are imine-based COFs (*e.g.* COF-300), which were designed by YAGHI [10] and coworkers and are based on an aldimine condensation of amine and aldehyde containing building blocks. Hydrazone-linked COFs, a subclass of imine-linked COFs, show improved chemical stability compared to conventional imine COFs due to the introduction of internal hydrogen-bonding interactions. Another means to improve the stability of imine-based COFs was achieved by using phloroglucin derivatives to additionally introduce hydroxy groups and hence, induce hydrogen bonding (Fig. 2.6) [27][28].

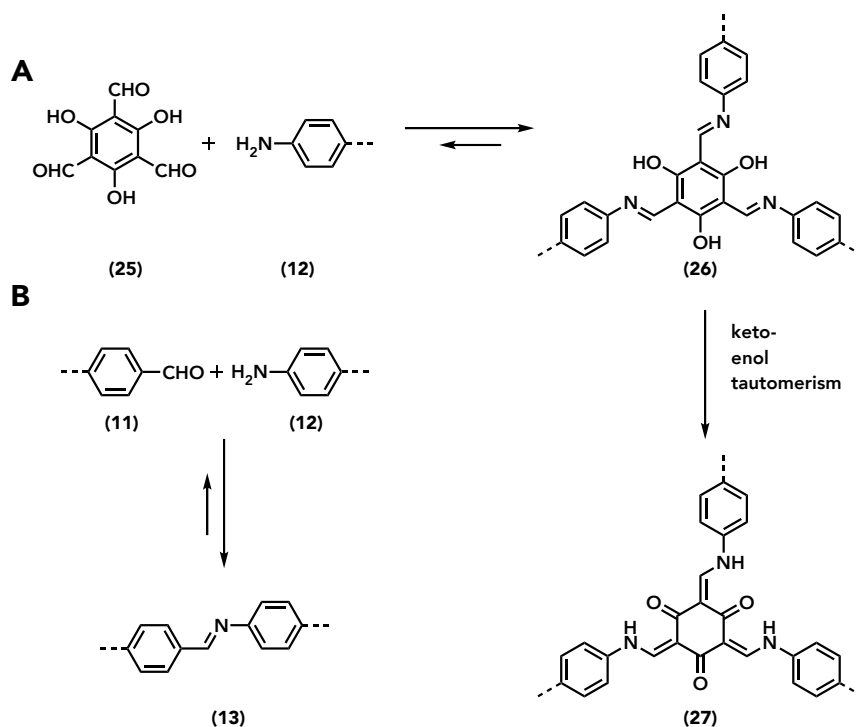


Figure 2.6: Imine COFs: Synthetic scheme for the preparation of imine COFs. **A)** COF based on a phloroglucin derivative to improve thermal and chemical stability *via* H-bonding. **B)** conventional imine-linkage.

Systems of the same type as shown in (Fig. 2.6 A) are furthermore stable due to keto-enol tautomerism,

allowing the system to be locked in the keto-form and hence, maximizing stability through hydrogen bonding [29]. Triazine-linked COFs, often referred to as covalent triazine frameworks (CTFs), are next to imine-linked COFs the most researched C-N based COF system. First introduced by THOMAS and coworkers [22], CTFs and the ease of their preparation *via* cyclotrimerization combined with high thermal and chemical stability resulted in vast interest in these systems. Another emerging class of C-N based systems are phenazine-linked COFs that are based on extended π -systems resulting in extremely thermally stable systems (up to 850 °C) [21].

2.4.3 Imide Linkages

Whereas imines are based on reversible Schiff-base chemistry, imide bonds have not been studied in dynamic covalent chemistry. However, depending on the conditions of the formation, imide formation can be carried out under reversible conditions (Fig. 2.7) [9].

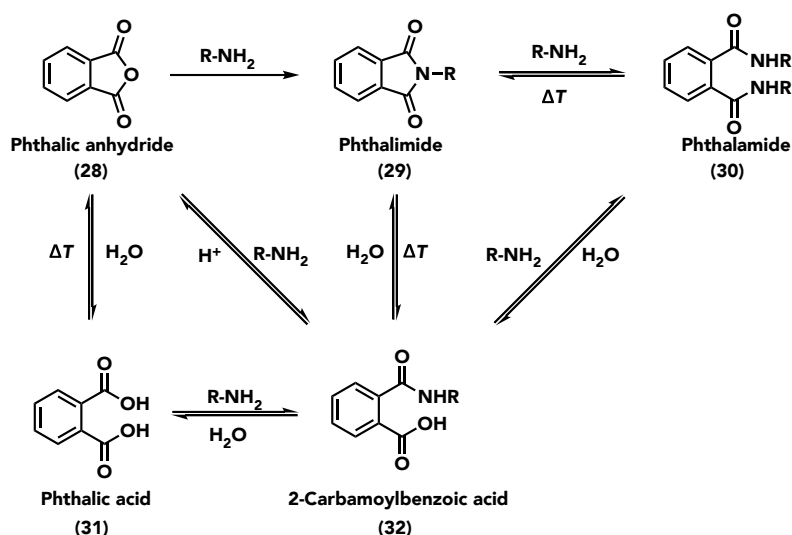


Figure 2.7: Imide Formation Pathways: Reaction of phthalic anhydride (28) in the presence of an amine. A complex equilibrium between a multitude of possible species is expected at elevated temperatures in the presence of a base. However, the absence of water favors the formation of phthalimide (29) over other products.

As shown in Fig. 2.7, the reaction of phthalic anhydride with a primary amine, a variety of intermediates are possible at elevated temperatures with phthalimide being the thermodynamically favored product. The first PI-COFs were reported using tris(4-aminophenyl)amine and PMDA (pyromellitic dianhydride) in NMP and mesitylene with isoquinoline as a basic catalyst at temperatures between $200\text{ °C} \leq T \leq 250\text{ °C}$. This combination of solvents combined with the high temperature employed in the synthesis allows for reasonable reversibility. However, PXRD studies suggest, that the formation of crystalline PI-COFs is inherently slower than for comparable imine systems, which suggests, that although error correction is possible, it proceeds much slower [17].

2.4.4 C-C Linkages

Only a few examples of C-C linked COFs exist, and most of these systems were prepared *via* ULLMANN or GLASER [24] coupling on the surface of a substrate resulting in two-dimensional nanostructures also referred to as surface COFs. A major factor in the unpopularity of these systems is the struggle to obtain highly crystalline systems as the C-C bonds are almost irreversible reducing the probability of proper rearrangement, which is imperative for the formation of highly crystalline frameworks [30].

2.5 Synthetic Methods in COF Synthesis

In this chapter, conventional synthetic methods towards the synthesis of COFs are discussed. The following techniques will be discussed: solvothermal synthesis, ionothermal synthesis, microwave-assisted synthesis and mechanochemical synthesis.

2.5.1 Solvothermal Synthesis

Solvothermal synthesis was the first method introduced by YAGHI [10], and has since been widely used for the preparation of COFs due to its suitability for the majority of linkages. In a conventional solvothermal synthesis the monomers are dispersed in a defined solvent system. After several freeze-pump-thaw cycles, the employed capillaries are sealed to ensure that the released water can't escape the vessel and hence, allowing reversibility. The system is kept at elevated temperatures for several days before the crude precipitate is filtered from the solution. The designed COFs are obtained after washing with several organic solvents, often employing soxhlet extraction. Solvents play a crucial role in the formation of the COFs as only a part of the monomers shall be dissolved at any time to ensure a slow reaction. Hence, a wide variety of solvent systems can be employed, indicating that a significant amount of experiments is needed to find the optimal system [31].

2.5.2 Ionothermal Synthesis

Ionothermal synthesis was used by THOMAS and coworkers to prepare the first reported CTFs [22]. In a typical experiment, aromatic nitriles (*e.g.* 1,4-dicyanobenzene) were dissolved in molten ZnCl_2 at 400 °C and reacted for extended periods of time. In this process, the zinc chloride acts as a solvent, as well as a catalyst to enable the cyclotrimerization to be reversible. Crystalline CTFs are obtained after washing out the salts and a purification process similar to the one employed in solvothermal synthesis. In general, CTFs prepared *via* ionothermal synthesis show poorer crystallinity than *e.g.* imine or boronate-ester based COFs [32].

2.5.3 Microwave Synthesis

Microwave-assisted synthesis of COFs was first introduced in 2009 by COOPER and coworkers [33] for the preparation of COF-5 in a solvothermal way, allowing to reduce the reaction time significantly. Interestingly, the obtained COFs showed a significantly higher BET surface area than conventionally synthesized systems. MW-assisted synthesis is interesting as it can be employed for a multitude (*e.g.* boroxine, imine, *etc.*) of systems and generally results in purer products [11].

2.5.4 Mechanochemical Synthesis

Mechanochemistry, although a traditional process on an industrial scale, is still one of the less conventional means to prepare COFs. In recent years though, pioneered by BANERJEE and coworkers, a variety of porous organic polymers (POPs) and COFs could be prepared [8]. Compared to solvothermal, ionothermal or microwave-assisted synthesis, this method is an eco-friendly alternative to produce COFs on a multigram scale by using mechanical force as the main driving force.

2.6 Hydrothermal Synthesis

Hydrothermal synthesis (HTS) is a technique inspired by the natural mineral formation and a powerful tool for obtaining highly crystalline materials. In a typical experiment, the starting compounds are dispersed in water and the mixture is heated to elevated temperatures ($>100\text{ }^{\circ}\text{C}$) under autogenous pressure in a closed vessel called autoclave. This autogenous pressure allows to move into the hydrothermal realm, indicated by the grey area in the phase diagram (Fig. 2.8).

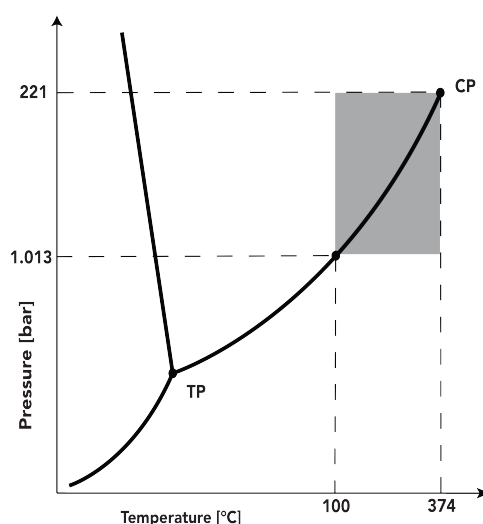


Figure 2.8: Phase Diagram of Water: The hydrothermal regime, starting $T > 100\text{ }^{\circ}\text{C}$ and $p > 1\text{ atm}$, is indicated by the gray area.

In the HT regime liquid and gaseous phase coexist. These changes enable a multitude of chemical reactions to take place including the preparation of synthetic gemstones [34] (e.g. quartz crystals), zeolites [35] and metal-organic frameworks (MOFs) [36]. Even though these materials are quite diverse, most of them, with the exception of MOFs, are formed by condensation reactions (see Fig. 2.9).

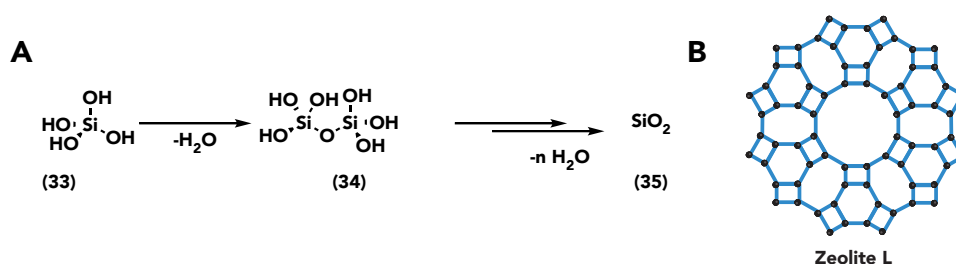


Figure 2.9: Hydrothermal Synthesis of Zeolites: A) Condensation of silicic acid to disilicic acid and further condensation to silica. B) Hydrothermal synthesis of e.g. Zeolite L is possible – Courtesy of Hipassia M. Moura

2.6.1 Hydrothermal Synthesis of Polyimides

Even though hydrothermal synthesis (HTS) has been routinely used for the synthesis of inorganic materials, its adaptation in organic synthesis was not successful until MORTON [37] reported the synthesis of low-molecular weight imide compounds in the 1990s. This proved that starting from an anhydride and an amine the formation of an imide under hydrothermal conditions was possible. Later, in 2003, HODGKIN [38]

and coworkers were able to successfully use HTS for the preparation of polyimides and hence introduced hydrothermal polymerization (HTP) (Fig. 2.10).

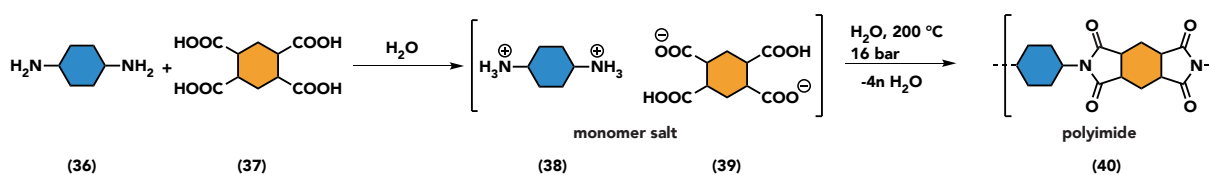


Figure 2.10: Hydrothermal PI Synthesis *via* the Monomer Salt Route: General PI synthesis employed *e.g.* for the synthesis of highly crystalline PPPI.

Recent developments by the group of UNTERLASS showed that HTS could furthermore be utilized for the synthesis of a multitude of organic small molecules (*e.g.* Fig. 2.11), polymers [7], hybrid materials [39] and even frameworks [40].

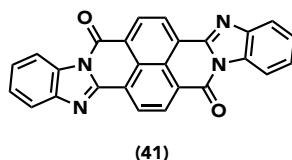


Figure 2.11: Perinone Dye: Perinone dye obtainable *via* hydrothermal synthesis in a MW procedure. Cis- and trans- perinone are obtained.

2.6.2 Water under Hydrothermal Conditions

As mentioned before, hydrothermal reactions are carried out using water at $T > 100\text{ }^\circ\text{C}$ in a pressure vessel. Hence, pressure is built up in the system as a function of T . Under these conditions, a variety of properties change. Most importantly, the ionic product is increased significantly (as shown in Fig. 2.13) and the dielectric constant [41] of the aqueous phase drops significantly. Both the liquid and the gaseous phase are influenced by HT conditions, however, the effect on the gaseous phase is diminishable compared to the influence on the liquid phase. Notably, the change of the dielectric constant in the liquid phase is of the utmost importance, as it moves into the range of common organic solvents (*e.g.* acetonitrile, DMF or NMP). At the same time, the static dielectric constant of the gas phase does not show significant change within this range. This decline in the ionic product [42] results in a significantly lower polarity of water – water becomes more apolar – and hence, the solubility of organic compounds is increased (see Fig. 2.13).

The change in the ionic product results in an increased amount of both H_3O^+ and OH^- ions in the solution at the same time. Hence, water under HT conditions acts as both an acid and base catalyst, which is beneficial for a variety of organic reactions (Fig. 2.12) including condensations, deprotections, *et cetera* [43].

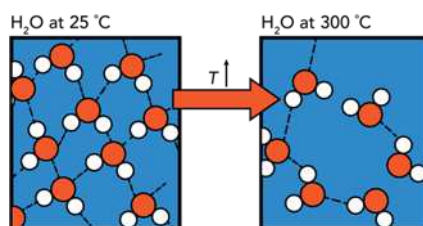


Figure 2.12: HTW – Effect on Polarity: Schematic representation of water at 300 °C. Hydrogen bonds are broken, interactions are decreased, which results in a less polar solvent. Courtesy of Miriam M. Unterlass.

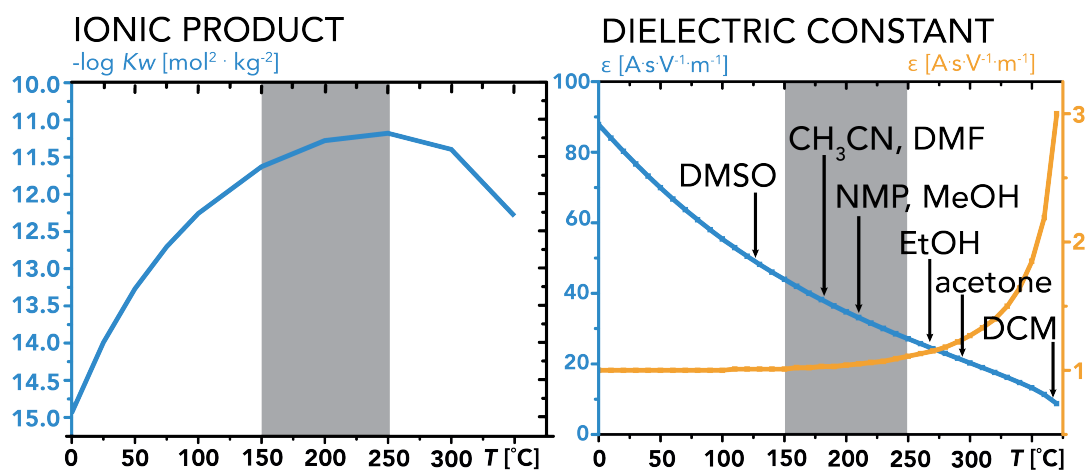


Figure 2.13: High-Temperature Water: Temperature dependence of water properties under hydrothermal conditions. Courtesy of Miriam M. Unterlass.

Chapter 3

Aims and Motivation

This project aimed to synthesize the first PI-based covalent organic frameworks *via* hydrothermal polymerization. The goal was to find a green alternative to otherwise toxic and environmental harmful techniques by using HTP. As there are only a few PI-COFs reported in the literature, two different amine-precursors were chosen for investigation. Namely, tetrakis-(4-aminophenyl)methane (TAPM) and tris-(4-aminophenyl)methane (TrisAPM) were chosen. TAPM features a tetragonal geometry, whereas TrisAPM is almost planar due to the reduced steric hindrance. Hence, different geometries should be achieved. The amine precursors were polymerized with PMDA, PMA and mellitic acid (MellA), respectively. The obtained porous organic polymers and crystalline frameworks were analyzed *via* FOURIER transform infrared spectroscopy using ATR-mode (FTR-IR-ATR), powder X-ray diffraction (PXRD) and thermogravimetric analysis (TGA). Furthermore, scanning electron microscopy (SEM) was measured to study the morphologies of the obtained networks and frameworks. The second part of this project was concerned with the synthesis of diaminotriazines (DATzs) and the evaluation of their usability as COF precursors. Using DATzs should allow the combination of two worlds - the high-performance capabilities of PI-systems with catalytic and gas-storage properties of triazines.

Chapter 4

Results and Discussion

Within this part of the thesis, a study into TAPM and TrisAPM as amine precursors in the synthesis of PI-COFs was carried out. The polymerizations were carried out using PMA, PMDA as well as Mella respectively.

4.1 PI-based Frameworks *via* Hydrothermal Polymerization

In the previous chapter, the properties of PI-based COFs were discussed. Especially, their outstanding thermal and chemical stability are of interest. The major disadvantage of PI-based frameworks lies in the harsh conditions that have to be employed in order to ensure the required reversibility. High temperatures and hence, high-boiling solvents such as DMF or NMP, as well as catalysts such as isoquinoline are required for the synthesis of such frameworks. Hydrothermal polymerization lies in stark contrast to the mentioned conventional conditions, requiring only water at elevated T as a solvent. The concept of HTS, its use, and how hydrothermal conditions are obtained was discussed in Chap. 2.

4.1.1 Preparation of TAPM

The synthesis, shown in Fig. 4.1, starts with the preparation of tetraphenylmethane (TPM) from chlorotriphenylmethane. In a first step, aniline is used at high temperatures to substitute the chlorine moiety resulting in a 4-(aminophenyl)-trisphenylmethane intermediate. The amino moiety was subsequently cleaved using isoamyl nitrite under acidic conditions and hypophosphinic acid. The resulting TPM was obtained with 90% yield and around 95% purity (according to GCMS). The remainder can be attributed to residual intermediate. This approach furthermore proved superior compared to other reported procedures (*e.g.* based on NaNO_2), as these showed lower conversion, as well as a more time-consuming workup.

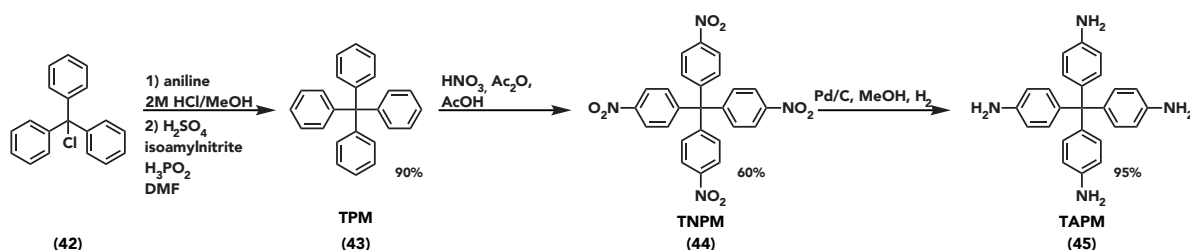


Figure 4.1: Preparation of TAPM: The first step shows the formation of TPM followed by nitration and subsequent reduction towards the desired product.

In a successive step, TPM was nitrated using fuming HNO_3 and $\text{Ac}_2\text{O}/\text{AcOH}$. Although a yield of 60% might indicate suboptimal conditions, the desired nitro species was obtained as the sole product. Hence, tedious purification could be avoided using this method. The reduction of tetra-(4-nitrophenyl)methane (TNPM) proved to be quite challenging as conventional approaches led to a mixture of products. Screened conditions included reduction with hydrazine and different Pd/C loading, reduction with tin(II)chloride-hydrate and using iron and HCl. However, using a hydrogen autoclave with MeOH as solvent resulted in almost quantitative yields (reaction NMR, GCMS) with the only losses resulting from the required filtration over Celite.

4.1.2 TAPM and TrisAPM as Precursors

TAPM was chosen as a precursor due to the possibility to get 3D networks as a result of the sp^3 hybridization of the methane carbon and hence its tetrahedral structure. TrisAPM was chosen as a neat comparison as it features more flexibility compared to TAPM (Fig. 4.2).

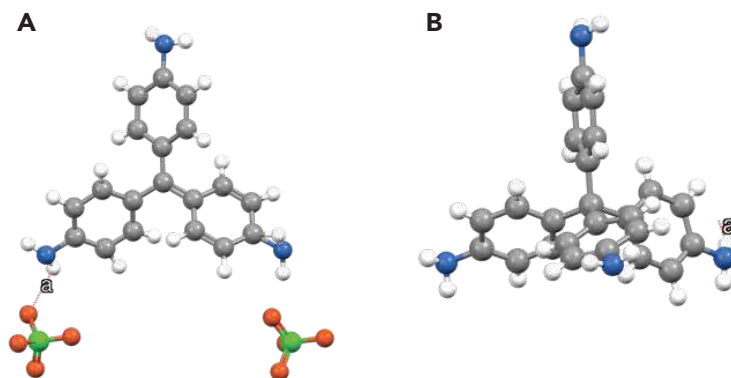


Figure 4.2: Structure of TrisAPM and TAPM: Crystal structure data from TrisAPM [45] and TAPM [44] (CCDC-identifier: RARRAE) as found on CCDC. TrisAPM could only be found as a carbocationic species with chlorate anions (CCDC-identifier: APCRBP10).

However, as can be expected from the structure of the precursors, vastly different product geometries and network structures can be expected.

4.1.3 TAPM under HT Conditions

TAPM is a highly stable organic molecule and did not show any degradation upon subjecting it to prolonged hydrothermal conditions of up to 250 °C. However, experiments at 300 °C resulted in carbonization of the precursor within a few hours. T of up to 250 °C could be used to recrystallize the precursor to obtain a purer product. However, drying TAPM after the treatment proved to be time-consuming and in the worst case resulted in a minor degree of oxidation.

4.1.4 Polymerization and Characterization of TAPM:PMDA

As discussed previously, TAPM is a highly stable precursor featuring a sp^3 hybridized carbon centre that shows little flexibility. To further reduce the flexibility and to obtain a rigid and stable network PMDA was

chosen as an initial precursor. HTP was usually conducted between $180 \leq T \leq 250$ °C using an autoclave or a stirred MW reactor at 230 °C.

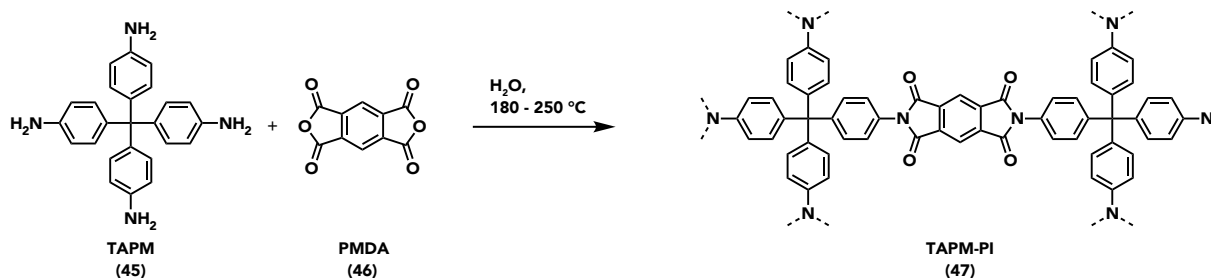


Figure 4.3: Polymerization of TAPM with PMDA: HTP of TAPM with PMDA. Autoclaves and MW-reactors were used for the polymerization.

Polymerization in the autoclaves were carried out over prolonged periods of time of up to 9 days, whereas the MW reactions were limited to a maximum of 24 hours. Due to the stirred nature of the MW reactor, reactions were able to complete faster. Yet, we found that this increased reaction speed hindered reversibility, crucial to the formation of regular networks. This can easily be seen when comparing PXRD diffractograms of the microwave products with the autoclave products, as the MW reaction products are entirely amorphous.

4.1.5 Evaluation of Reaction Time and Temperature

TAPM and PMDA are highly stable precursors. However, under HT conditions, the precursors are exposed to not only high T , but also to an extremely basic and acidic environment. Hence, the precursors are under immense stress. This could easily be observed, when moving to $T > 250$ °C. Especially, at 300 °C carbonization occurred within an hour of reaching reaction temperature T_R . Long-time exposure (5 days and more) at 250 °C also resulted in partial carbonization. Therefore, 200 °C was chosen as a general reaction temperature. Previously, the importance of reversibility and the variety of possible byproducts in the synthesis of PI-networks and frameworks were discussed. Due to this, it is not surprising that long reaction times are required to generate highly crystalline PI systems – regardless whether conventional or HT conditions are used. Nonetheless, a study into the reaction time required for full PI formation was conducted to evaluate the ease of PI formation. As 200 °C in an autoclave was chosen as the general reaction conditions for the PI synthesis, these conditions were also used to determine the reaction speed. Hence, precursors were heated to 200 °C for 2-24 hours (selected spectra can be found in the appendix B.2 and B.3). A variety of interesting phenomena could be observed. Firstly, full conversion as observed *via* ATR-IR can already be achieved after only 4 hours. Yet a deep purple solution and precipitate were obtained in the process indicating the occurrence of a side reaction that is further discussed in the following chapter. These findings are furthermore interesting as it takes around 2 hours for the autoclave to reach the desired temperature, indicating, that polymerization already begins at lower T . This so-called sub-hydrothermal polymerization (sHTP) was previously described by BAUMGARTNER *et al.* [46]. Moving to $t_R > 10$ hours resulted in the color of the solution to change to yellow and the products to be obtained as brown powders. As a change in color of the liquid phase could be observed, they were collected to investigate further. The purple solution resulted in a black precipitate. IR revealed that the precipitate corresponded to a mixture of imide and monomer salt indicated by ammonium modes.

4.1.6 TrisAPM-Carbocation from HT Synthesis

The purple color of both the solution as well as the precipitate at low reaction times indicates the formation of an intermediate or by-product. The color itself is reminiscent of methanarylamine dyes (Fig. 4.4, A) such as crystal violet. However, crystal violet dyes are in general more closely related to TrisAPM – they only have three 4-aminophenyl moieties compared of the four that TAPM has. In advance to this work, the hydrothermal polymerization of TAPM was attempted and the same phenomenon was observed. Under certain conditions, green crystals could be obtained which were found to be a TrisAPM cation according to single-crystal XRD analysis (Fig. 4.4 B and C).

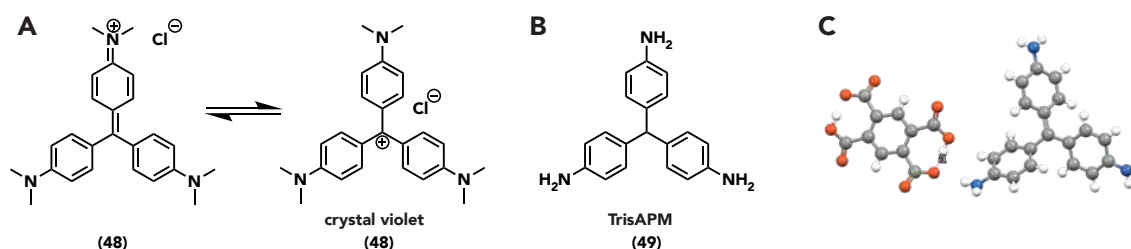


Figure 4.4: Crystal Violet Dyes and the TrisAPM-carbocation: **A)** shows commercial crystal violet dyes. **B)** shows tris(4-aminophenyl)methane. **C)** shows the TrisAPM-carbocation as obtained from hydrothermal synthesis as green crystals.

However, the conditions of the formation of said crystals were not appropriately documented. Hence, to prove our hypothesis of the formation of this intermediate under certain conditions, the experiments had to be repeated. Hydrothermal polymerizations in the same fashion as previously reported were conducted at 160, 170, 180, 190 and 200 °C for reaction times ranging from 2 to 24 hours. It was possible to obtain the desired crystals again. However, the crystals were only obtained as a by-product in low yields (<10 %). Catalytic cleavage of an aniline moiety from TAPM has been reported in 1898 by GOMBERG [47]. However, Gomberg's procedure utilizes HCl and Pt to enable the acid catalyzed elimination of aniline. As the cleavage was possible under HT conditions without a reagent present, experiments were conducted in which of 2N HCl was added to the reaction. The desired cationic species could be obtained according to NMR. Assuming that the carbocation is able to form under the reaction conditions used for HTP has severe implications on the HTS of TAPM-based frameworks.

4.1.7 Implications of the TrisAPM-Cation Species on Framework Synthesis

As it could be proven that a carbocationic intermediate can be formed during the reaction at lower temperatures the implications on the synthesis of frameworks based on TAPM have to be discussed. Since the HTS towards PIs is a polycondensation, a change in stoichiometry resulting from the cleavage of an aniline moiety would greatly impact CAROTHERS equation (Eq. 4.1). Generally speaking, the equation is only applicable for linear polymers. However, estimates for network polymers can be made.

$$\chi_n = \frac{1 + q}{1 + q - 2qp} \quad (4.1)$$

$$p = \frac{N_0 - N}{N_0} \quad (4.2)$$

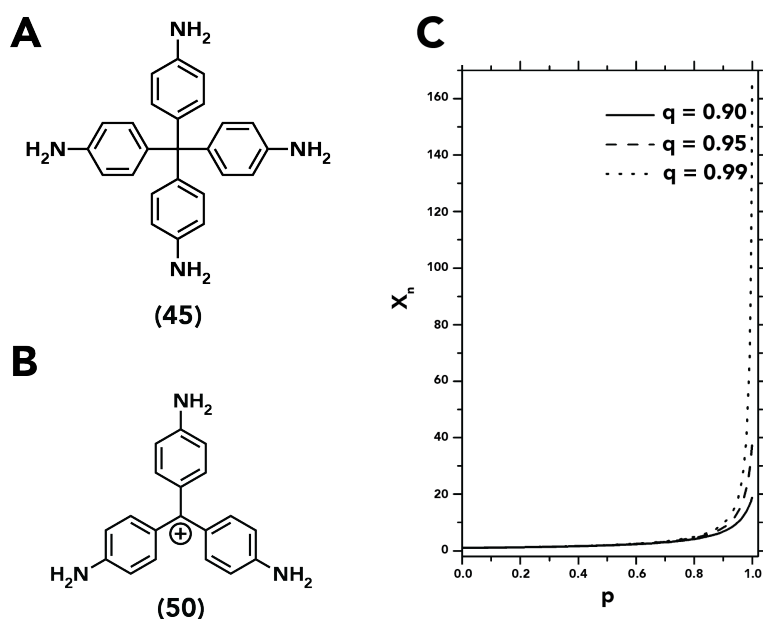


Figure 4.5: TrisAPM-cation and its Implications: Schemes of **A** TAPM and **B** TrisAPM-carbocation. **C**) Diagram derived from Carothers equation. X_n ... degree of polymerization. p ... extent of reaction. q ... molar ratio of the monomers.

Looking at Fig. 4.5 C one can easily see, that moving from an optimal stoichiometry for TAPM:PMDA (1:2) to a mixed stoichiometry of TAPM:TrisAPM-cation:PMDA has a great impact as TrisAPM:PMDA would require a 2:3 stoichiometry. Hence, the fact that while using these precursors in most cases only amorphous or partially crystalline networks were obtained, can be explained through this phenomenon. As the formation of the carbocation seems to be depending on slowing down the initial reaction speed by lowering the T and hence reducing the heating rate, it seems feasible to try to increase the initial reaction speed. Performing the reaction in a stirred flask at 80 °C on the other hand, doesn't lead to the desired product either. However, using PMA instead of PMDA increases the reaction speed as the dianhydride does not have to be opened in the process. Furthermore, using PMA reduces the risk of having a partially hydrolyzed precursor in the first place.

4.1.8 Polymerization and Characterization of TAPM:PMA

To avoid the formation of the TrisAPM-carbocation or at least to minimize its formation PMA was used instead of PMDA to enhance the reaction speed. HT experiments in the same fashion as for TAPM:PMDA were conducted.

As a first result, the formation of a purple solution and polymer at low reaction times $t_R = 2$ hours was significantly reduced but could not be avoided altogether. Hence, further experiments were conducted to obtain the carbocationic species but again, only a mixture of the PI with the carbocationic species could be obtained at certain conditions ($T = 160$ °C, $t_R = 2$ hours and $T = 170$ °C, $t_R = 2$ hours).

More extended reactions resulted in brown polymers, as was the case for TAPM:PMDA. However, PXRD (Fig. 4.6) revealed, that crystalline polymers were obtained.

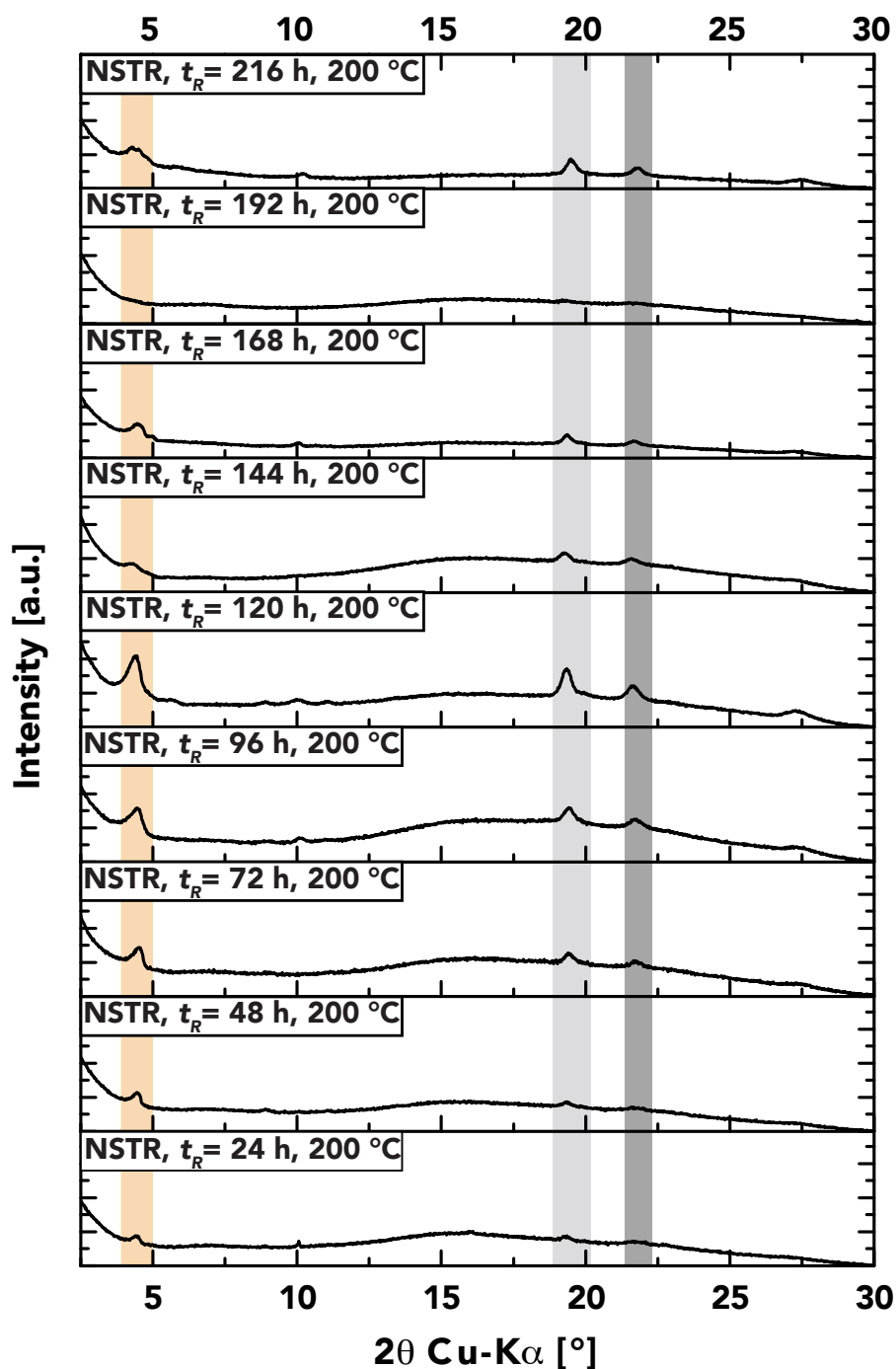


Figure 4.6: TAPM:PMA XRD: PXRD of TAPM:PMA polymerization products recorded after 1-9 days. Lowest reflection (orange) at $\sim 4.4^\circ$ (2θ , Cu- $K\alpha$, $d_{hkl} = 19.9$ Å), gray reflection at $\sim 19.3^\circ$ (2θ , Cu- $K\alpha$, $d_{hkl} = 4.6$ Å) and black reflection $\sim 21.6^\circ$ (2θ , Cu- $K\alpha$, $d_{hkl} = 4.1$ Å).

Crystallinity of the system seems to increase with t_R , as was expected. However, after $t_R = 120$ h crystallinity behaves more inconsistently. This was apparent as at $t_R > 120$ h many samples were obtained with an amorphous background, indicating that the reverse reaction might be more favored at a certain point. Furthermore, the diffractograms, in general, show the same reflections with the lowest reflection being

around 4.4° (2θ , Cu- K_α), well within the realm of 3D covalent organic frameworks.

ATR-IR spectra of the products showed little to no difference between one another with all expected modes being present, most importantly the imide-carbonyl and the C-N modes (Fig. 4.7). The spectra were furthermore compared to a model compound, (Fig. 4.7) obtained after HTS of TAPM with phthalic anhydride (autoclave, 200°C , $t_R = 72$ hour reaction). A comparison between PI-polymers at different t_R is shown in 4.1.

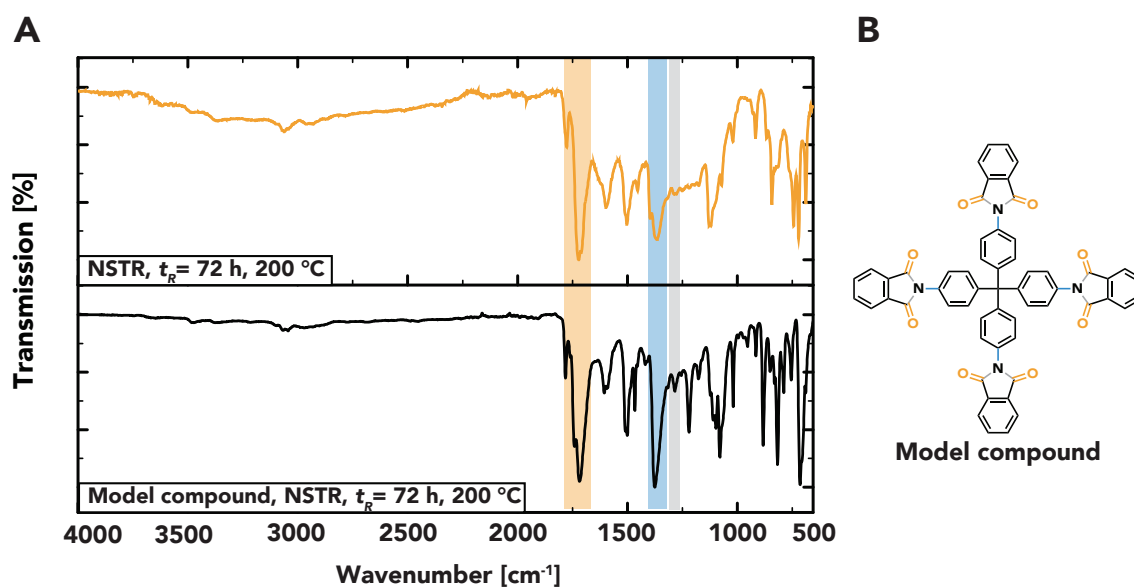


Figure 4.7: TAPM:PMA IR: A) ATR-IR spectrum of TAPM:PMA polymerization. The indicative imide-carbonyl modes at 1780 and 1714 cm^{-1} respectively are present with no other mode indicating by-products. B) Model compound obtained *via* HTS of phthalic anhydride with TAPM. Characteristic imide modes are highlighted in the molecule and in the spectrum.

Table 4.1: IR modes: Characteristic imide-IR modes as shown in Fig. 4.7 B. Especially the C = O at 1780 and 1714 cm^{-1} modes are indicative of imides.

Sample	C = O mode [cm^{-1}]	C - N mode ₁ [cm^{-1}]	C - N mode ₂ [cm^{-1}]
NSTR $t_R = 120$ h	1774 and 1720	1366	1278
NSTR $t_R = 24$ h	1774 and 1721	1366	1285

To further investigate whether the formation of the carbocation could be taken into account, TAPM:PMA polymerizations with a 2:5 stoichiometry were conducted. This stoichiometry should, in theory, take into account the PMA moiety needed to stabilize both the carbocation of the TrisAPM moiety as well as the aniline moiety, hence resulting in a remaining 2:3 stoichiometry needed for the polymerization of TrisAPM:PMA. The polymerization proceeded similar to the 1:2 polymerization of TAPM:PMA resulting in brownish powders. However, upon evaluating PXRD changes in the diffractogram were immediately visible (Fig. 4.8). Again, the lowest reflection around 4.5° (2θ , Cu- K_α) is well within the realm of 3D COF systems and the reflections in general are more pronounced compared to the signals of the 1:2 polymerization. This allows the hypothesis, that a pH-effect is enhancing the reaction speed in the early phase of the polymerization and then leads to faster crystallization.

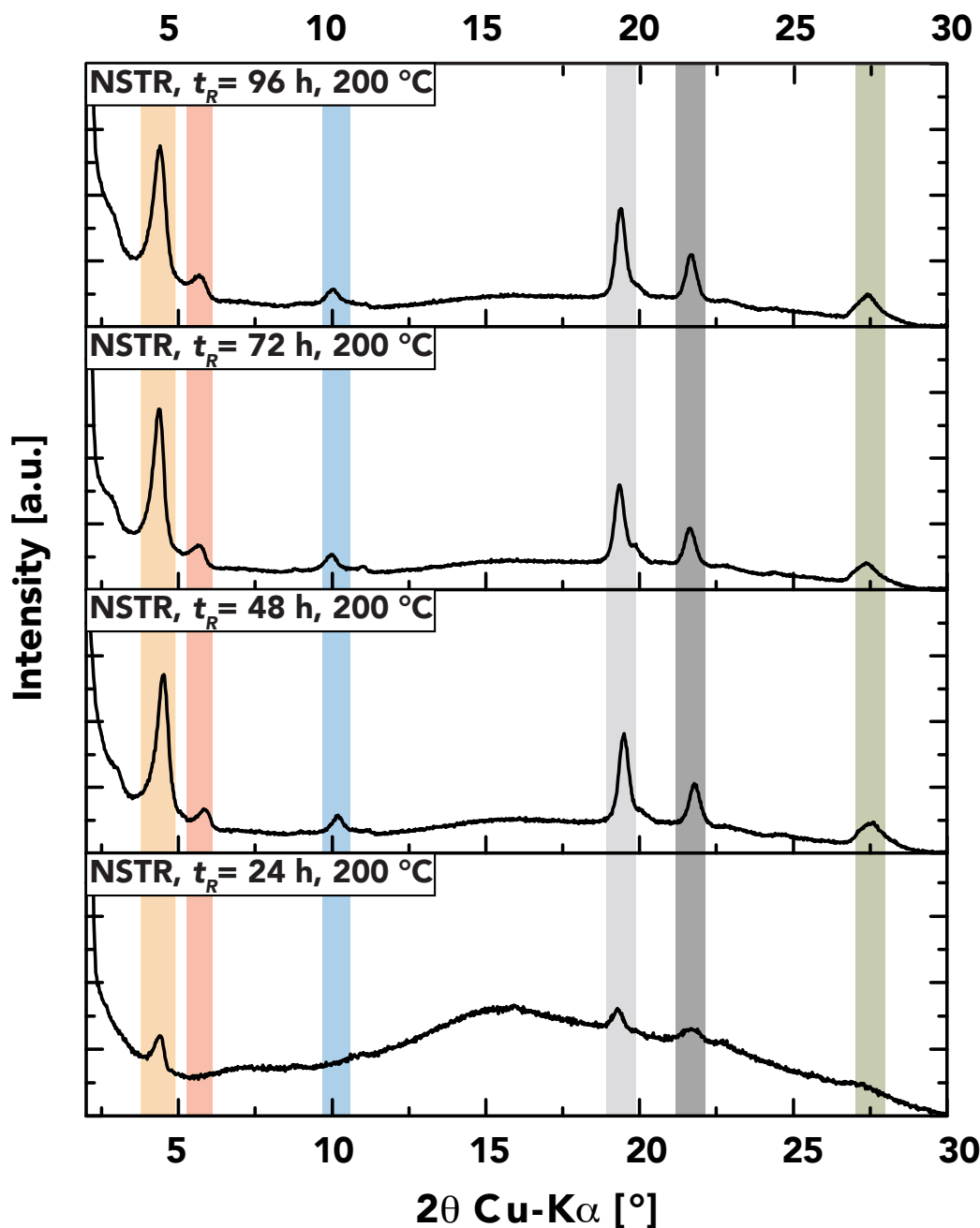


Figure 4.8: TAPM:PMA 2:5 XRD: PXRD diffractogram of TAPM:PMA after HTP for $t_R = 1-4$ days. Lowest reflection (orange) $\sim 4.5^\circ$ (2θ , Cu- $K\alpha$, $d_{hkl} = 19.6$ Å), red reflection $\sim 5.5^\circ$ (2θ , Cu- $K\alpha$, $d_{hkl} = 15.8$ Å), blue reflection $\sim 10.0^\circ$ (2θ , Cu- $K\alpha$, $d_{hkl} = 8.8$ Å), gray reflection $\sim 19.4^\circ$ (2θ , Cu- $K\alpha$, $d_{hkl} = 9.5$ Å), black reflection $\sim 21.8^\circ$ (2θ , Cu- $K\alpha$, $d_{hkl} = 4.1$ Å) and green reflection $\sim 27.5^\circ$ (2θ , Cu- $K\alpha$, $d_{hkl} = 3.2$ Å).

Interestingly, the reflections perfectly align with the ones found in the 1:2 polymerization diffractograms.

4.1.9 Evaluation of Reaction Yield

HTP is usually carried out in low concentrations – between 10 to 50 mmol/L. As conventional experiments were carried out with 10 mL of solvent in an autoclave, only small amounts of product were obtained. To ensure homogeneity of the samples at different concentrations, a c screening was conducted with c ranging from 10 to 30 mmol/L. An autoclave at $T_R = 200$ °C and $t_R = 120$ h were chosen as reaction parameters. As shown in Fig. 4.9 reflections stay the same with the lowest reflection still being around 4.38° (2θ , Cu- $K\alpha$).

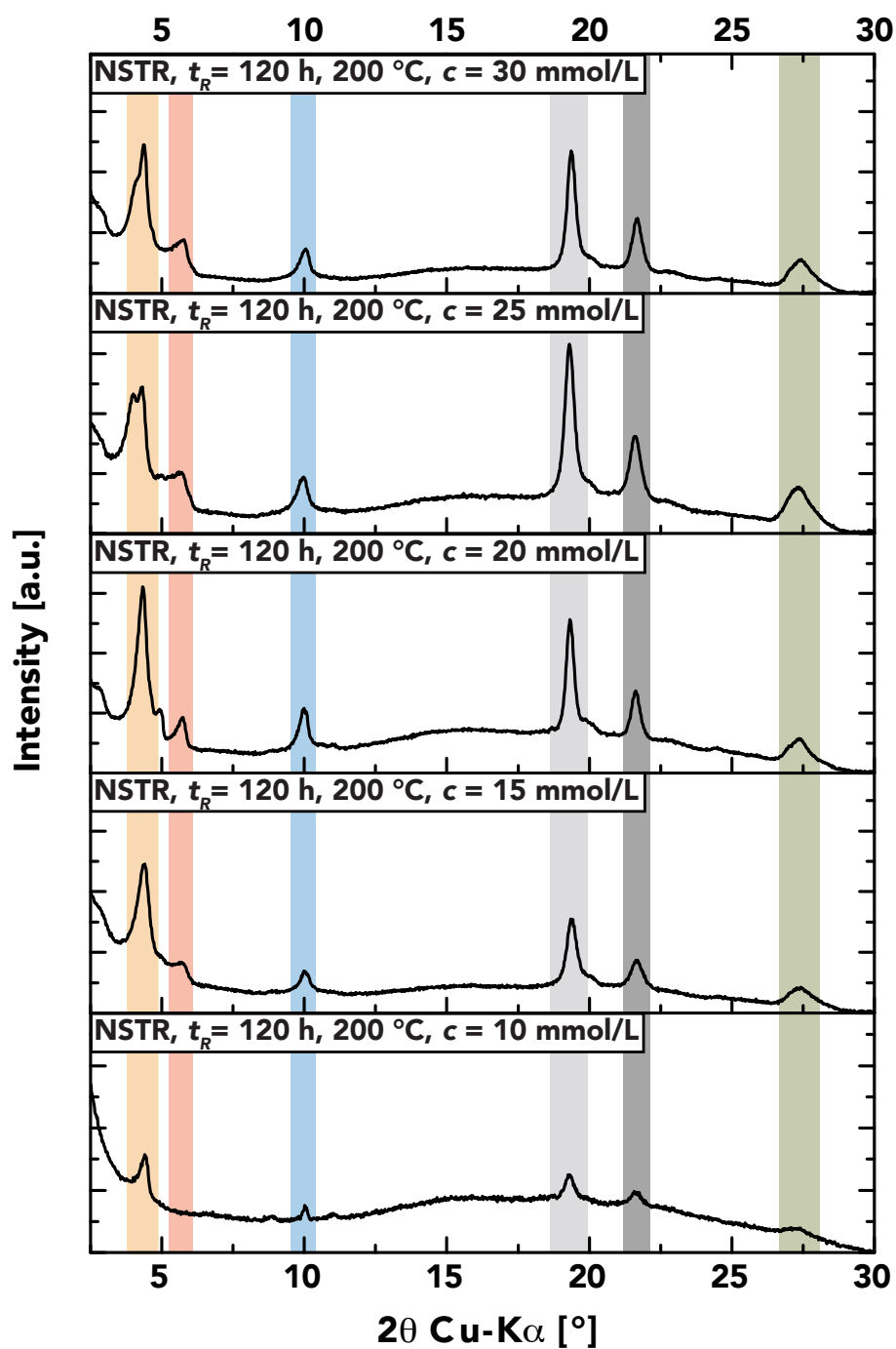


Figure 4.9: TAPM:PMA XRD - Conc.-Screen: PRXD of the concentration screening TAPM:PMA obtained after HTP with 1:2 stoichiometry at 200 °C and $t_R = 120$ h in an autoclave. Lowest reflection (orange) $\sim 4.4^\circ$ (2θ , Cu-K α , $d_{hkl} = 20.6$ Å), red reflection $\sim 5.7^\circ$ (2θ , Cu-K α , $d_{hkl} = 15.5$ Å), blue reflection $\sim 10.1^\circ$ (2θ , Cu-K α , $d_{hkl} = 8.7$ Å), gray reflection $\sim 19.0^\circ$ (2θ , Cu-K α , $d_{hkl} = 4.6$ Å), black reflection $\sim 21.7^\circ$ (2θ , Cu-K α , $d_{hkl} = 4.1$ Å) and green reflection $\sim 27.4^\circ$ (2θ , Cu-K α , $d_{hkl} = 3.2$ Å).

Comparing the diffractograms, there is no major difference between either long-time reactions of up to 120 h and the different concentrations indicating, that the concentration limit has not been reached yet. However, the overall yield of the reactions increased significantly after increasing the concentrations from

44% at 10 mmol/L to 81% at 30 mmol/L. Increased yields while up-scaling have been observed before. In this case, the assumption can be made, that due to the increased amount of starting material, the pH of the initial solution was altered and resulted in an overall better reaction.

4.1.10 Comparison with Simulated TAPM:PMA COFs

As shown in the previous chapters all TAPM:PMA polymerizations seem to yield the same product according to PXRD measurements. Theoretical simulations were conducted in our group by Musthafa Mohamed Iqbal to generate PXRDs of optimal systems. A pristine diamond system and three interpenetrated systems were simulated based on the expected diamond unit cell. However, as shown in Fig. 4.11 the simulations do not align with the experimental data. The lowest reflection lies between the lowest reflections of the pristine framework and the two-fold interpenetrated system indicating that the unit cell size should be between the two of them. It was found, that the TrisAPM-cation species can be formed under any conditions tested, which suggests, that this was also the case in the syntheses that resulted in the crystalline products. Moreover, it is impossible to quantify the amount of TrisAPM formed and hence, it is almost impossible to postulate the structure of the system correctly. However, our current hypothesis is that, the formed TrisAPM species are incorporated in the system in a semi-regular fashion resulting in a smaller unit cell than expected, which would explain the shift of the lowest reflection to higher angles. In Fig. 4.10 an idealized diamond structure, a theoretical TAPM:PMA model and a model that shows how the TrisAPM-carbocation could be incorporated is shown. As shown in 4.10, most of the structure could be retained while still incorporating the TrisAPM species.

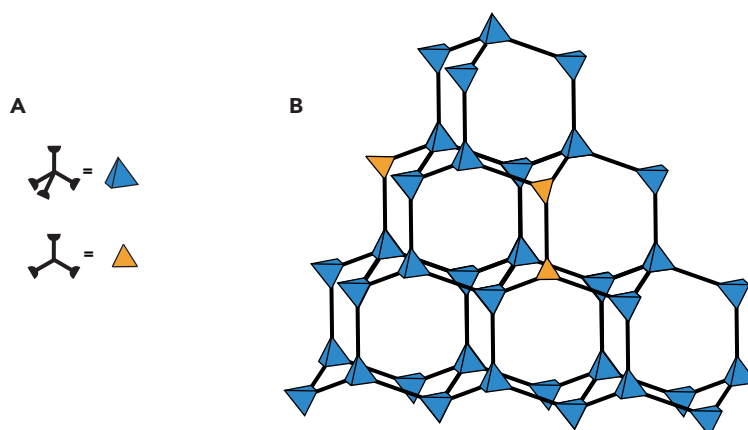


Figure 4.10: Hypothetical COF Incorporating the TrisAPM-carbocation: **A)** Representation of a tetragonal building block (e.g. TAPM (blue)) and a trigonal building block (e.g. TrisAPM-salt (orange)) in the following schemes. **B)** shows a hypothetical model that incorporates TrisAPM (orange) in the unit cell, resulting in some degree of disorder while retaining overall diamondoid structure.

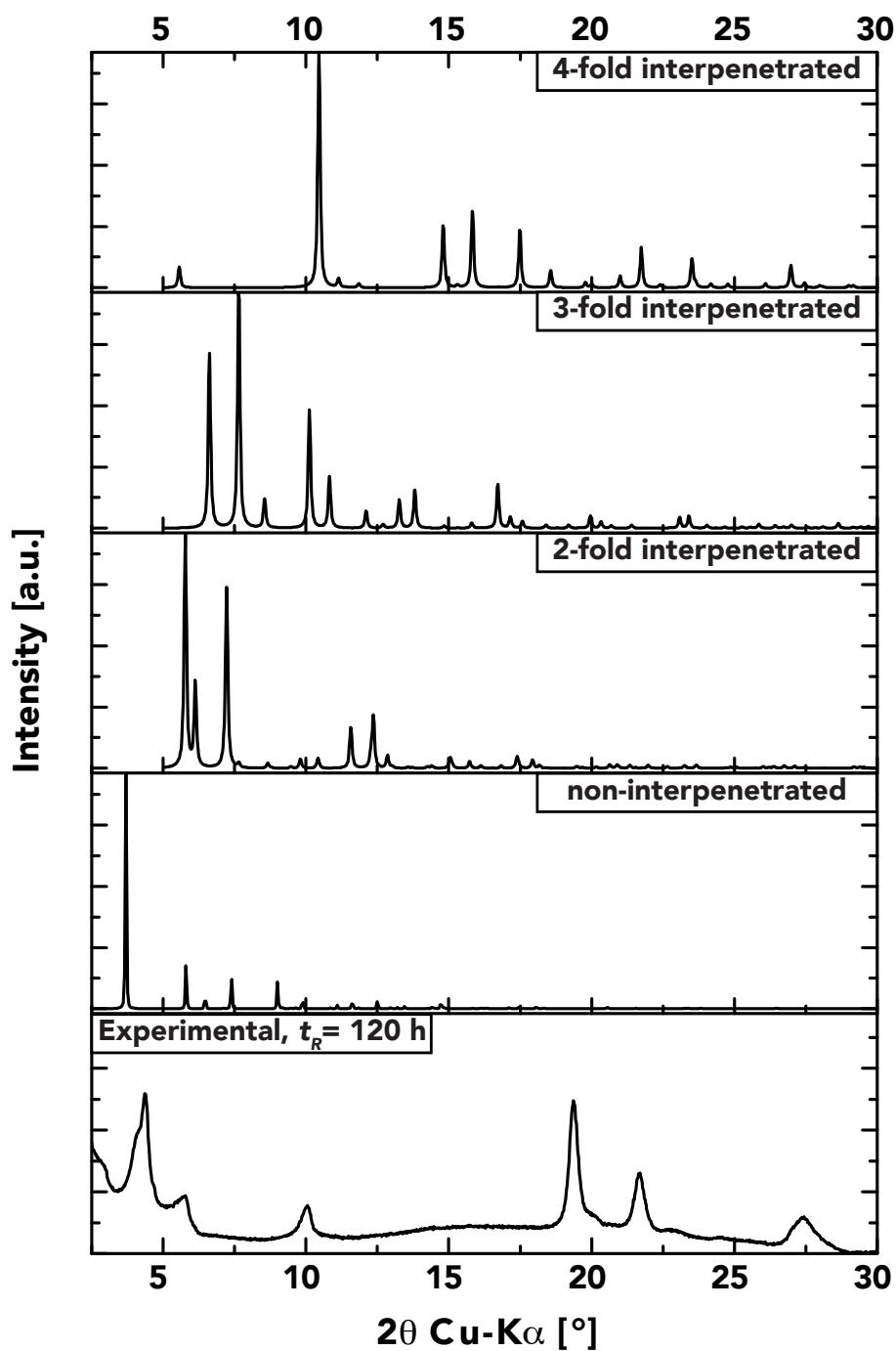


Figure 4.11: TAPM:PMA XRD Simulation: Experimental PXRD spectrum of TAPM:PMA compared to theoretical models of a pristine diamond-like structure and twice, triple and quadruple interpenetrated structures. Simulated using Materials Studio 2017.

4.1.11 TAPM:PMA Monomer Salt

Monomer salts were previously used within our group in the synthesis and polymerization of linear PIs [7]. In theory, generating a monomer salt is, as simple as combining the desired monomers in the required stoichiometry in a flask and stirring them overnight. Indeed, this was the case for the TAPM:PMA system as well and ^1H -NMR of the obtained salts confirmed the 1:2 stoichiometry. The monomer salt was characterized *via* ^1H -NMR (Fig. 4.12), PXRD (Fig. 4.13) and TGA (Appx. B.4 and Appx. B.5).

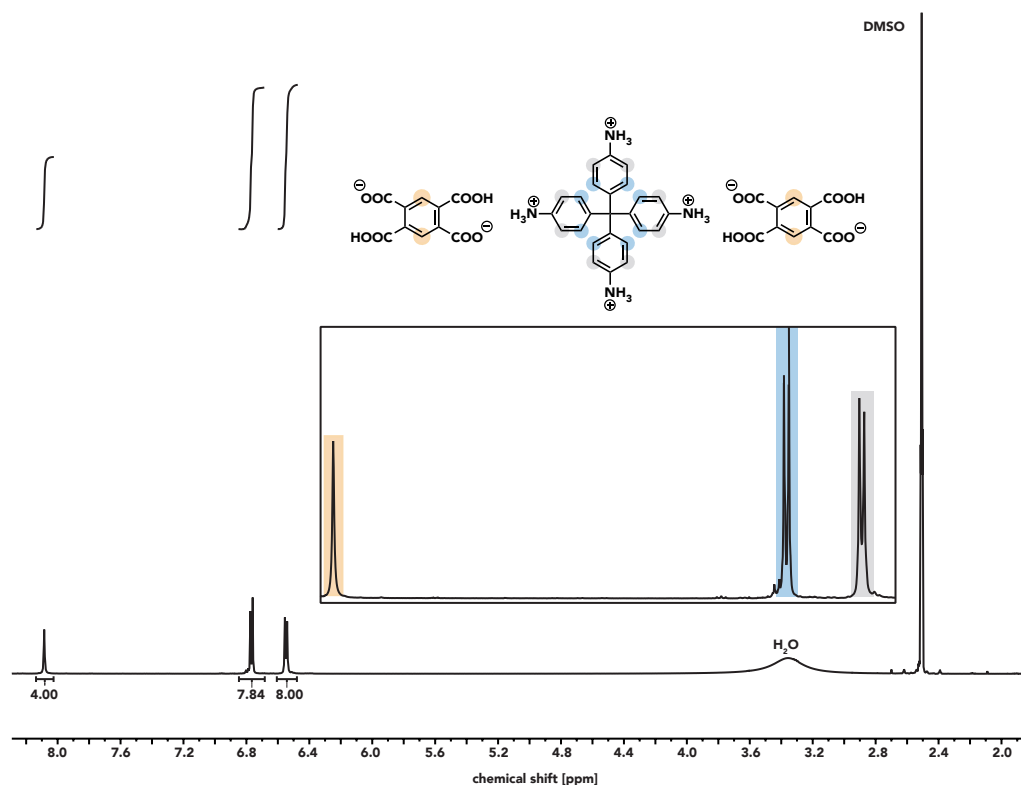


Figure 4.12: TAPM:PMA Monomer Salt NMR: ^1H -NMR of the TAPM:PMA monomer salt. The signals integrate towards a 1:2 stoichiometry. The broad water peak can be accounted to the fact that the monomer salt can not be dried in an oven or high vacuum as this would result in polymerization.

ATR-IR of the monomer salts shows the expected ammonium modes and carbonyl modes. Furthermore, amine modes are entirely absent (Appx. B.6). In many cases, the preparation of monomer salts can be accelerated by heating the suspension while stirring. However, when heating to temperatures between 40 – 80 °C partial polymerization occurred within hours, indicated by a change in color of both the solution and the precipitate to purple.

4.1.12 Polymerization and Characterization of the TAPM:PMA Monomer Salt

Polymerization of the monomer salts was performed, although the stoichiometry was off, using a simple SSP setup. A Schlenk flask was charged with the monomer salts and heated to temperatures between 80 and 200 °C for 24 or 72 hours under reduced pressure. Upon heating the monomer independent of the used temperature, the same transition in color could be observed. Color initially changed from off-white to purple followed by a change towards gray-ish after several hours, depending on T . The change in color occurred faster at higher T or slower at lower T . Quality of the vacuum used in the reaction did not affect the SSP or its speed in any way. No matter whether high-vacuum (10^{-3} mbar) or conventional membrane pump vacuum was used, the reaction proceeded in the same fashion. To optimize the SSP temperature, TGA analysis

was conducted, which revealed that SSP occurs at around 170 °C (Appx. B.4 and App. B.5). Both the products obtained *via* HTP and SSP showed the same thermal stability at $T_D \approx 530$ °C. Results of the TGA measurements are compiled in Table 4.2.

Table 4.2: TAPM:PMA Monomer Salt TGA: Polymerization temperature of the monomer salts and degradation temperature of the resulting polymerizates, solid-state polymerizates and a hydrothermal polymerizations ascomparison.

Sample type	T_{SSP} [°C]	T_D [°C]
Monomer salt 10 mol/L	172	531
Monomer salt 30 mol/L	172	527
NSTR, 200 °C, $t_R = 48$ h	-	535
SSP, 150 °C, $t_R = 72$ h	-	526
SSP, 200 °C, $t_R = 48$ h	-	532

PXRD of the polymerizates was measured and revealed that at low T_R and t_R ($t_R = 20$ h, $T = 100$ °C) full polymerization is not possible as the optimal T_{SSP} is not yet reached. However, at $t_R = 20$ h, $T = 100$ °C the amorphous background is slightly increased compared to the pristine monomer salt indicating that polymerization has started. At elevated T of 170 - 200 °C, polymerization proceeds fast and quantitatively resulting in full conversion within 20 hours with no further changes to the polymer even if kept for a total of 65 hours. As mentioned above, SSP at T beyond the T_{SSP} results in a fast and quantitative conversion towards the desired polymer. Immediately after submerging the Schlenk flask in the oil bath, a color change from off-white to purple can be observed. Crystallinity of the monomer salt is not retained during the SSP. A mostly amorphous background with small reflections at 11.4° (2θ , Cu- K_α), 17.1° (2θ , Cu- K_α) and 22.4° (2θ , Cu- K_α) is obtained after SSP (Fig. 4.13).

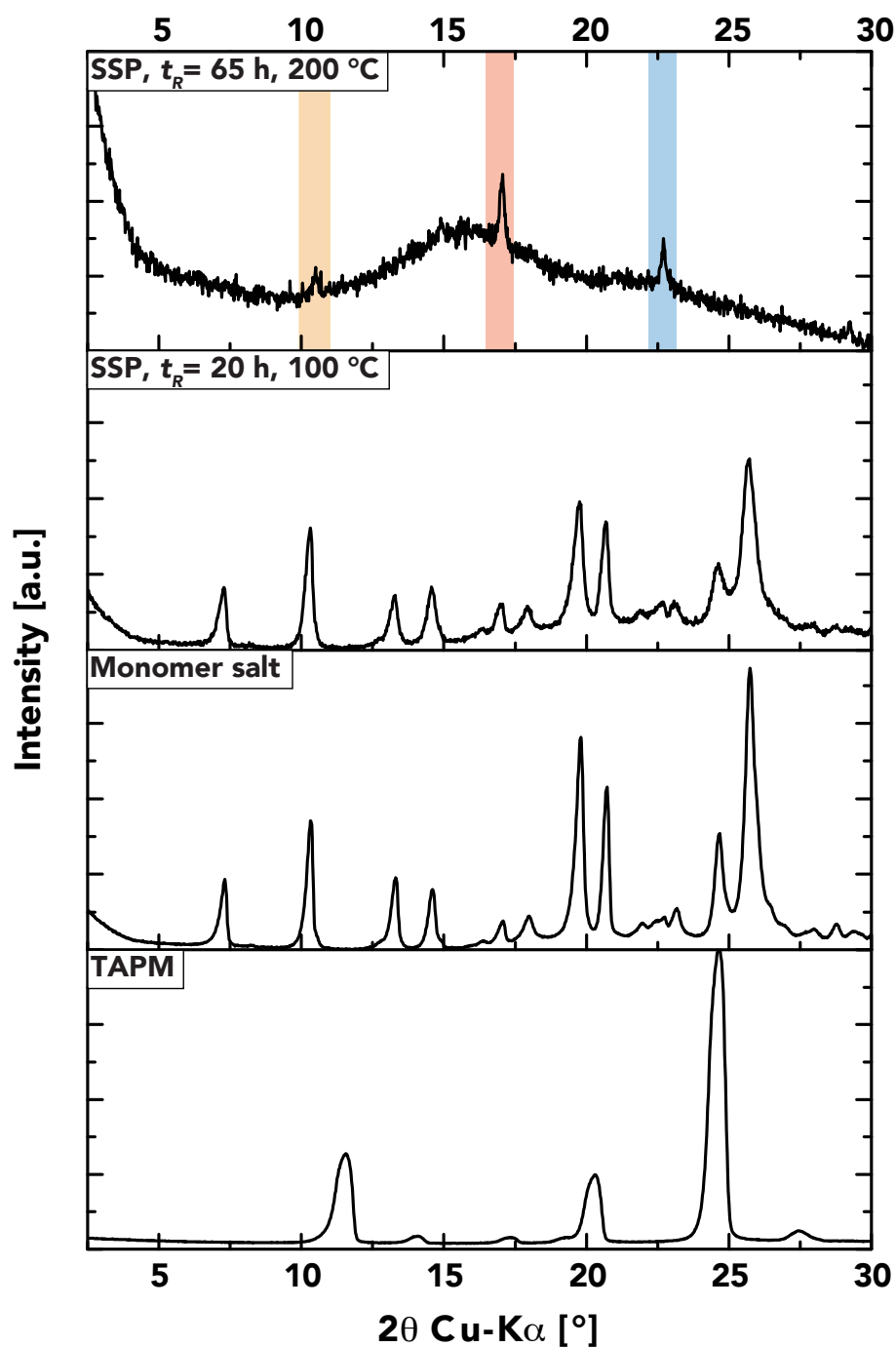


Figure 4.13: XRD of the MonSalt and its SSPs: PXRD measurement of the precursor TAPM, the pristine monomer salt, a SSP below the optimal T_{SSP} and a SSP at 200 °C. Lowest reflection (orange) $\sim 10.6^\circ$ (2θ , Cu-K α , $d_{hkl} = 8.3$ Å), red reflection $\sim 17.1^\circ$ (2θ , Cu-K α , $d_{hkl} = 5.2$ Å) and blue reflection $\sim 22.7^\circ$ (2θ , Cu-K α , $d_{hkl} = 3.9$ Å).

4.1.13 Evaluation of SEM Micrographs

As it stands, HTP of TAPM:PMA leads to the formation of several products. Firstly, the desired PI is formed and is able to form amorphous networks, which are able to transform to crystalline frameworks if given sufficient time. Secondly, a side reaction leads to the formation of a TrisAPM-carbocation species, which is formed during the initial heating process and is polymerized in the later stages of the polymerization. Thirdly, it was shown, that a monomer salt, although with the wrong stoichiometry, can be formed and polymerizes at $T \approx 170$ °C, well below our HTP temperature. However, as T above T_{SSP} are employed, SSP can occur for samples, where the concentration is too high for the monomers to be dissolved at all time. SSP can also occur later stages of the polymerization when oligomers and polymers are not soluble anymore. This effect has previously been reported by BAUMGARTNER *et al.* during a study focussing on the effects of sub-hydrothermal polymerization, hydrothermal polymerization and SSP on morphology [46].

The combination of these three phenomena leads to interesting findings with respect to the morphology obtained *via* SEM. The monomer salt (Fig. 4.14 A and B) consists of tiny agglomerated particles without any significant features. However, the product after 2 h at 200 °C NSTR reaction shows two major morphologies. Firstly, a crystalline phase consisting of large rod-like, rhombohedral particles originating from the TrisAPM-cation. Secondly, amorphous spheres are visible, which can be accounted to the polymerization, hence the formation of the PI. These initial findings perfectly align with what could be expected, as the TrisAPM-salt can be observed without using a microscope due to the size of the crystals formed and their optical properties.

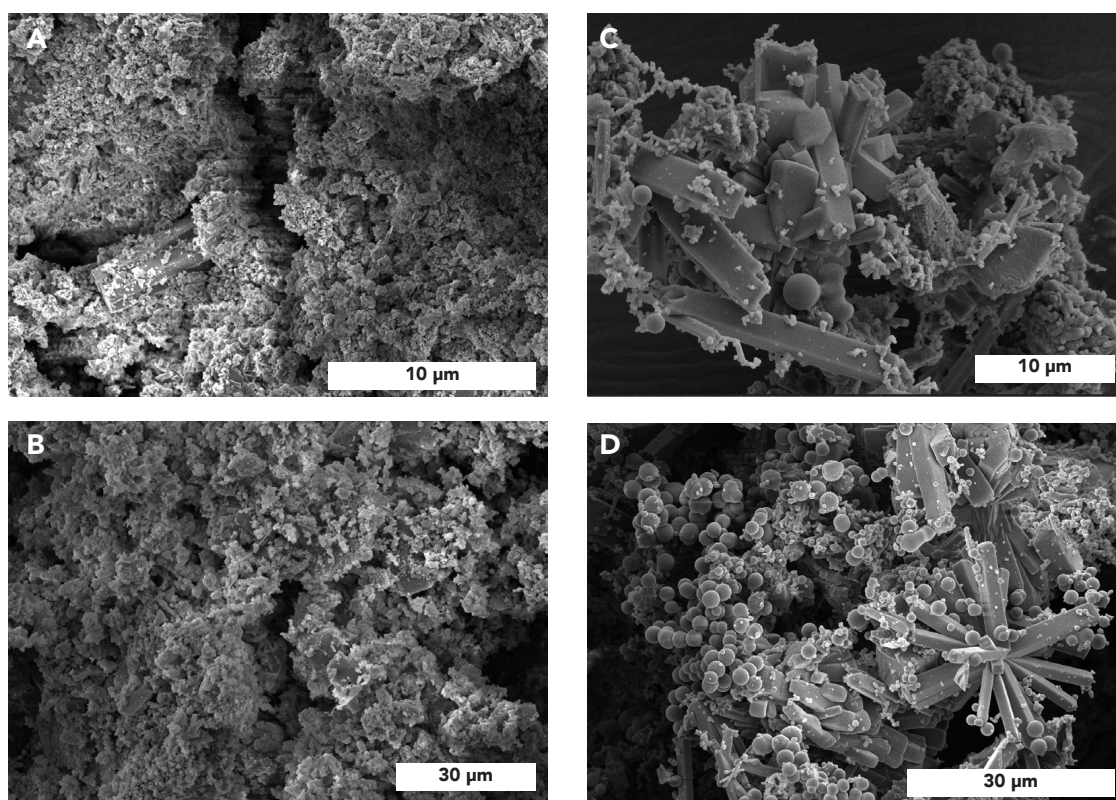


Figure 4.14: SEM of the MonSalt and Short Polymerizations: A) and B): SEM micrograph of the TAPM:PMA monomer salt. The monomer salt consists of tiny, agglomerated particles. C) and D): SEM micrograph of the 2 h TAPM:PMA polymerization at 200 °C. The sample shows both crystalline parts originating from the TrisAPM-salt and amorphous spheres from the polymerization.

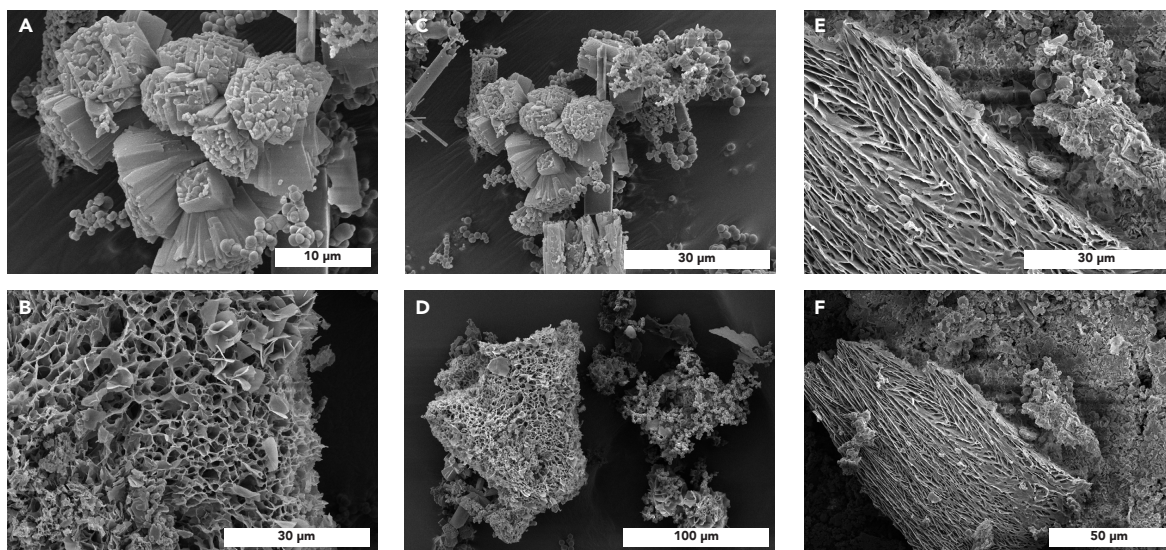


Figure 4.15: SEM of 120 hour Polymerizates: SEM micrograph of TAPM:PMA at $c = 10$ mmol/L (A-D) and $c = 30$ mmol/L (E and F).

SEM micrographs of the products obtained after HTP are depicted in Fig. 4.15. Micrographs (A-D) belong to the 120 h, 200 °C NSTR reaction with $c = 10$ mmol/L, whereas (E and F) account to the sample obtained by using $c = 30$ mmol/L at the same conditions. Two major phases can be found in the micrographs (A-D). Firstly, a bulky phase (A and C) consisting of large intergrown angular particles. Secondly, a random network of thin-walled sheets can be found. Both of these major phases co-exist with amorphous spheres reassembling the spheres found in the micrographs of the short reaction time experiment. At higher c , the micrographs change significantly. Again, a network-like morphology can be found, however, compared to the lower c sample the network is more condensed. Furthermore, a similar bulky morphology of condensed particles can be found. The latter might have formed due to SSP as a higher c was used and solubility might have been an issue. Even though, different morphologies could not only be found in a single sample but also between samples, they amount to the same PXRD diffractogram. This allows for the hypothesis that different polymorphs of the same polymer were obtained. As a variety of different phenomena occur during HTP of TAPM:PMA the variety of morphologies is not surprising.

4.1.14 Polymerization and Characterization of TrisAPM:PMDA

Tris(4-aminophenyl)methane (TrisAPM) was chosen as the second amine based precursor of interest, as it might allow for assumptions into the structure of a possible TrisAPM-cation polymerizate possible. TrisAPM features an almost planar structure which in combination with a very stiff co-monomer such as PMDA should result in a hexagonal unit cell (Fig. 4.16, B).

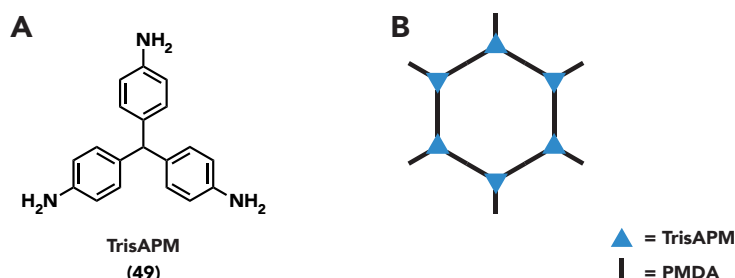


Figure 4.16: TrisAPM and Theoretical Framework Structure: A) structure of TrisAPM. B) theoretical hexagonal unit cell obtained after TrisAPM:PMDA polymerization.

TrisAPM, although featuring more flexibility, is just as stable under HT conditions as TAPM. Hence, the same conditions – NSTR, $T_R = 200\text{ }^\circ\text{C}$, $t_R = 1\text{--}9\text{ days}$ – were used in the polymerization of TAPM:PMDA. Fig. 4.17 shows the PXRD of the TrisAPM:PMDA polymerizates at different reaction times. All diffractograms show the same reflection at 8.9° (2θ , Cu- K_α) and 20.5° (2θ , Cu- K_α). However, with increasing t_R , the amorphous background increases and the reflections at higher angles become slightly more pronounced. Considering that a hexagonal unit cell should be formed, the lowest reflection is way too high in angle, indicating that the polymerization, although yielding a crystalline solid, didn't result in a covalent organic framework and presumably in a linear polymer. A concentration screening was conducted to evaluate whether similar effects as for TAPM – higher crystallinity and better yields – could be obtained. However, the results (B.7) are very inconsistent. At some concentrations, the reflection at 8.9° (2θ , Cu- K_α) is retained, whereas at some it is not present. On the other hand, all samples besides the lowest concentration ($c = 1\text{ mmol/L}$) show an additional lower angle reflection at 6.7° (2θ , Cu- K_α) as an amorphous halo. Even though this additional reflection is interesting, the fact that it occurs as an amorphous halo, as well as that it is still too high for a hexagonal unit cell indicates that further improvements are needed to obtain a crystalline framework.

TGA measurements (B.8 and B.9) shows a thermal decomposition temperature of around $T_D = 530\text{ }^\circ\text{C}$, which aligns with the thermal decomposition temperature of the TAPM:PMA system. T_D didn't change with either reaction time or with the concentration used in the reaction.

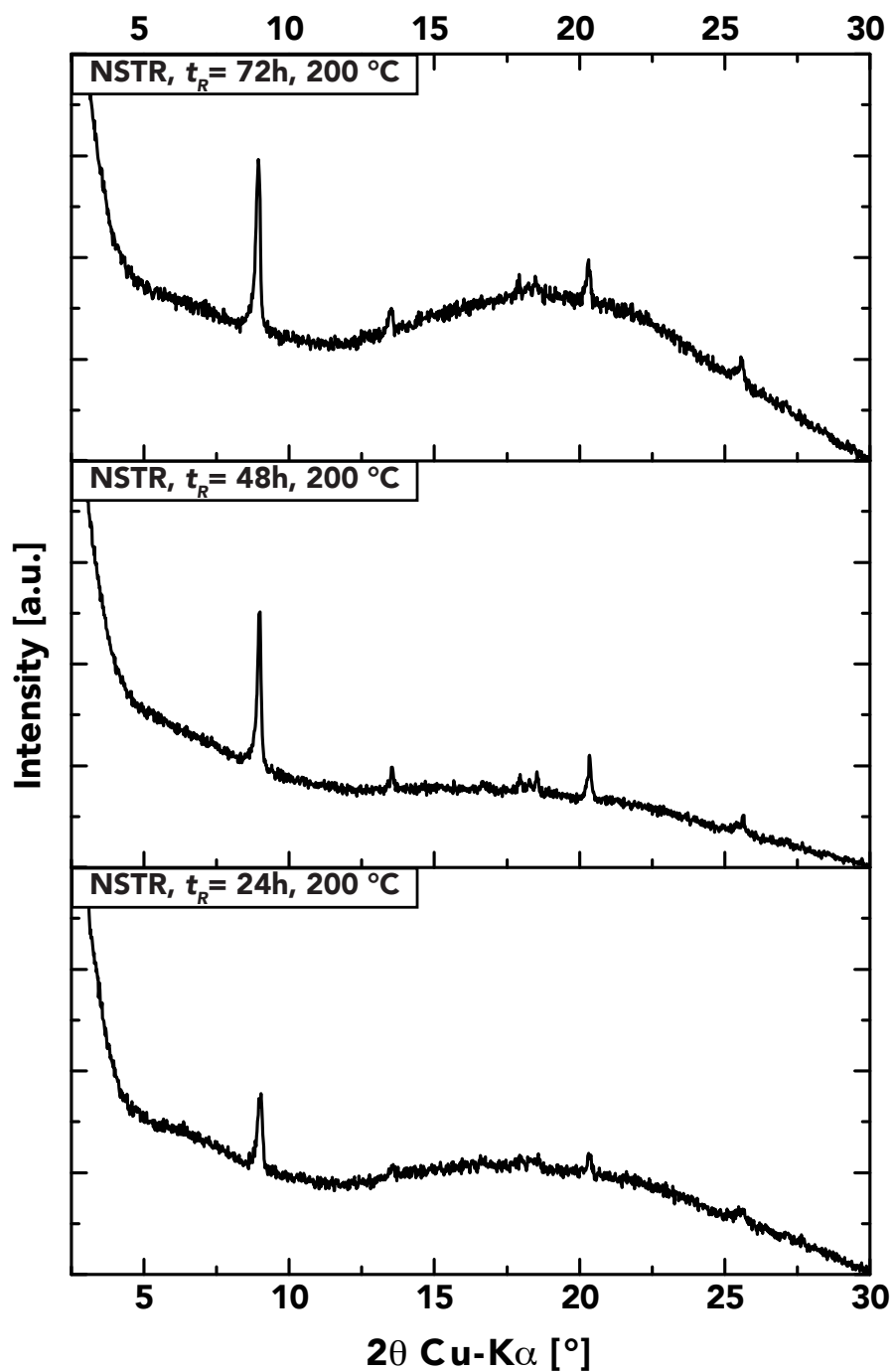


Figure 4.17: PRXD of the TrisAPM: PMDA system at different reaction times. Crystallinity seems to increase with reaction time, however the amorphous halo at higher angles increases as well.

4.1.15 Polymerization and Characterization of TrisAPM:MellA

As mentioned in the previous chapter, TrisAPM is a highly stable precursor. On paper, mellitic acid (MellA) (Fig. 4.18) is a sturdier and more planar molecule compared to PMDA and also features already opened anhydride moieties. However, thermal stability of mellitic acid is lower than the thermal stability of PMDA resulting in carbonization if $T > 220\text{ }^{\circ}\text{C}$ is used or if $t_R > 3$ days at $200\text{ }^{\circ}\text{C}$.

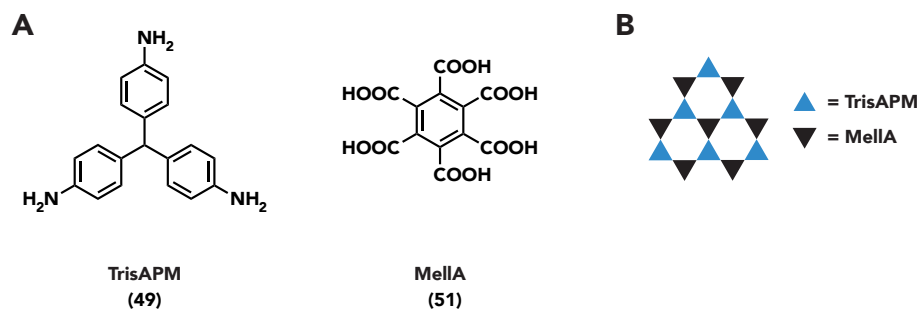


Figure 4.18: TrisAPM:MellA Theoretical Structure: **A)** structure of TrisAPM and mellitic acid. **B)** theoretical hexagonal unit cell after polymerization.

TrisAPM:MellA should also result in a hexagonal unit cell. However, in the TrisAPM:PMDA system PMDA acts as a linker resulting in a larger unit cell whereas, in the TrisAPM:MellA system the mellitic acid acts as a core system itself which should in theory yield a very small unit cell. PXRD of the system shows only an amorphous halo around 20° (2θ , Cu- K_{α}) indicating that reversibility of the system is too low or that the optimal reaction conditions were not met (Appx. B.10). TGA data shows a rather low decomposition temperature of $T_D = 480\text{ }^{\circ}\text{C}$, as well as a static mass loss between 200 and $400\text{ }^{\circ}\text{C}$ (Appx. B.11). This static mass loss together with the amorphous nature of the PXRD could indicate that the polymerization was not completely successful resulting in an unknown degree of decarbonylation. The thermal stability of MellA seems to be quite low and decarbonylation could have already started in the autoclave, which could in theory result in a mixture of imide and amide linkages during the polymerization.

4.1.16 Conclusion and Outlook

In summary, within this part of the project four different aminophenylmethane based systems with PMDA, PMA or Mella as co-monomer were investigated. A variety of porous organic polymers were synthesized *via* hydrothermal polymerization and characterized using ATR-IR, PXRD and TGA. The first part of the project was focussed on the polymerization of TAPM. We were able to synthesize TAPM:PMA based PI polymers. Thermal stability, as well as ATR-IR indicate that indeed a polyimide network was formed. However, PXRD showed only partial to no crystallinity. Upon investigating reaction speed an interesting phenomenon was found. For very low reaction times ($t_R < 10$ hours) a purple solution and precipitate was obtained. Further investigation revealed that under certain conditions small amount of green crystals could be obtained, which were found to be a TrisAPM-carbocationic species that seemingly formed through cleavage of an aniline moiety from TAPM. To date, optimal conditions to obtain this species as the sole product were not found. However, it seems that the formation of the carbocationic species is dependent on the initial reaction speed of the reaction. Slower reactions due to lower reaction temperatures and using PMDA instead of the open anhydride species PMA seem to favor the formation of the carbocation species. The carbocation can furthermore be produced *via* acid catalyzed elimination of aniline under hydrothermal conditions. The product (pararosaniline), featuring a chlorine counterion, could be confirmed *via* NMR. As a result, PMA was used in further investigations. The impact of changing to the open system was immediately obvious when crystalline reflections were found in the PXRD. The reaction was upscaled by a factor of three to see whether homogeneous results could be obtained. Indeed, this was the case, and it was even possible to obtain systems with higher crystallinity compared to lower concentration systems at the same reaction conditions. The investigation also revealed that up-scaling the reaction has a positive effect on the overall yield of the reaction, which could be increased from 40% for the lowest to 80% for the highest concentration. However, the formation of the carbocation species could not be avoided. As a crystalline system was obtained, the X-ray diffractograms were compared to simulated systems. Comparing the obtained diffractograms to the expected diamond-like systems and a variety of interpenetrated systems revealed that no fit could be found. As in all cases the TrisAPM-carbocation was formed, the assumption can be made that it was incorporated in the system and hence resulted in an altered unit cell. However, proving this hypothesis seems impossible as the amount of TrisAPM-carbocation formed during the reaction can't be measured. Furthermore, it was found that a monomer salt with a 1:2 stoichiometry could be obtained by stirring a suspension of TAPM:PMA overnight at room temperature. SSP was performed and the polymerization products were found not to reproduce the crystal structure of the monomer salt and are of amorphous to semi-crystalline nature. The products obtained after SSP showed the same thermal stability as the ones obtained *via* HTP with $T_D \approx 530$ °C. SEM micrographs of the monomer salt, as well as polymers at different t_R and c show a variety of different morphologies as a result of the polymerization. A combination of the formation of the TrisAPM-carbocation, sub-hydrothermal polymerization, hydrothermal polymerization and SSP can be seen as the origin of these morphologies. As a TrisAPM-carbocation was obtained under certain conditions TrisAPM was investigated as another amine precursor. Polymerization of TrisAPM with PMDA resulted in semi-crystalline polymers with almost the same thermal stability as TAPM:PMA. However, the lowest reflection at $8,9^\circ$ is too high for a framework that should feature a hexagonal unit cell. A concentration screening furthermore revealed, that a lower angle reflection can be obtained as an amorphous halo. Nonetheless, even if the halo would be considered a proper reflection it would still be too high to consider it a proper framework. TrisAPM:Mella polymerizates were found to be of purely amorphous nature as Mella shows lower thermal stability than PMDA and could decarbonylate under reaction conditions. Future investigation should be focused on the TAPM:PMA system, as it shows the most promising preliminary results in regards to crystallinity.

4.2 Triazines in COFs and Materials Science

In this chapter, CTFs and especially the use of 2,5-diamino-1,3,5-triazines as COF precursors will be discussed. CTFs are a family of rather well-known COFs and are of particular interest due to their high thermal and chemical stability. Furthermore, a wide array of syntheses (Chapter 2) are known which allow for decent reversibility, which is imperative in the synthesis of COFs (Chapter 2).

4.2.1 State of the Art

CTFs are attractive for a wide range of applications including separation and storage of gases, energy storage (e.g. for hydrogen storage [48] or as electrode materials [49]), photocatalysis [50] and even heterogeneous catalysis [51] (see Fig. 4.19). Of special interest is the high nitrogen content of CTFs, which is often associated with a strong hetero atom effect (HAE). N-doping can, for example, affect the electron distribution inside a carbon material, which changes the wettability of the system or e.g. the electroactive surface of electrode material. Furthermore, there are indicators that high heteroatom content can enhance the ability of a material to store gases [48] [52][53]. Due to these properties, CTFs are a fascinating material as they feature high porosity and stability while their syntheses that can be industrially scaled-up. Usually, CTFs are synthesized directly from cyanide precursors and only few non-direct methods to incorporate triazines are known as they require special precursor design.

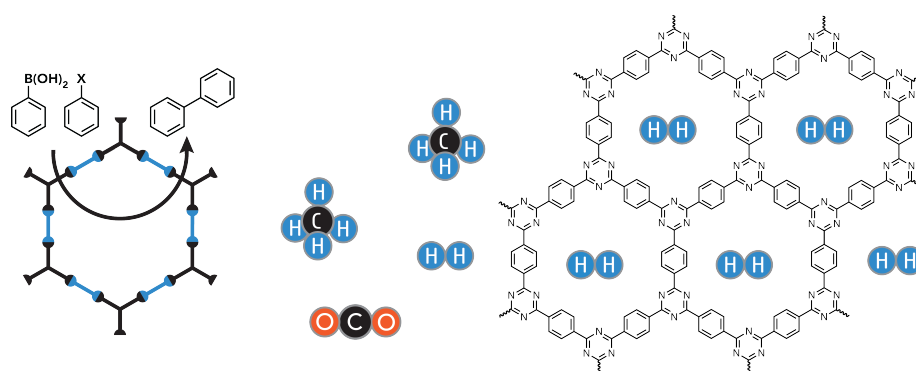


Figure 4.19: Applications for CTFs: Both catalysis and hydrogen storage are upon the most researched use-cases for CTFs due to their high heteroatom content.

4.2.2 2,4-Diamino-1,3,5-triazines as COF Precursors

Diaminotriazines (DATs) were chosen for investigation for the synthesis of PI-Tz-COFs as they feature two key building blocks of interest. Firstly, a highly stable and fully aromatic triazine precursor with the required functionality for polymerization towards PIs or polyimines is given. Secondly, tunability is retained *via* the para position of the benzene moiety. Hence, this approach would allow the combination of two worlds. Namely, triazine based COFs and the potential use cases associated while incorporating imide linkers that would improve the thermal and chemical performance even further.

Trimerization - a Strong Driving Force in Organic Synthesis

Conventionally, CTFs are synthesized with cyanides, usually of aromatic nature, as precursors. The nitrile functionality undergoes a trimerization reaction with two other nitriles to yield the desired triazine product (Fig. 4.20 A). The synthesis of DATs follows the same basic principle. Aromatic nitriles (e.g. benzonitrile or 1,4-dicyanobenzene) are combined with dicyandiamide under basic conditions to yield the desired di-

aminotriazine. In this case, the trimerization was carried out using a quick and straightforward microwave procedure (adapted from Ruiz-Osés [54]), to ensure high yields and short reaction times (Fig. 4.20 B).

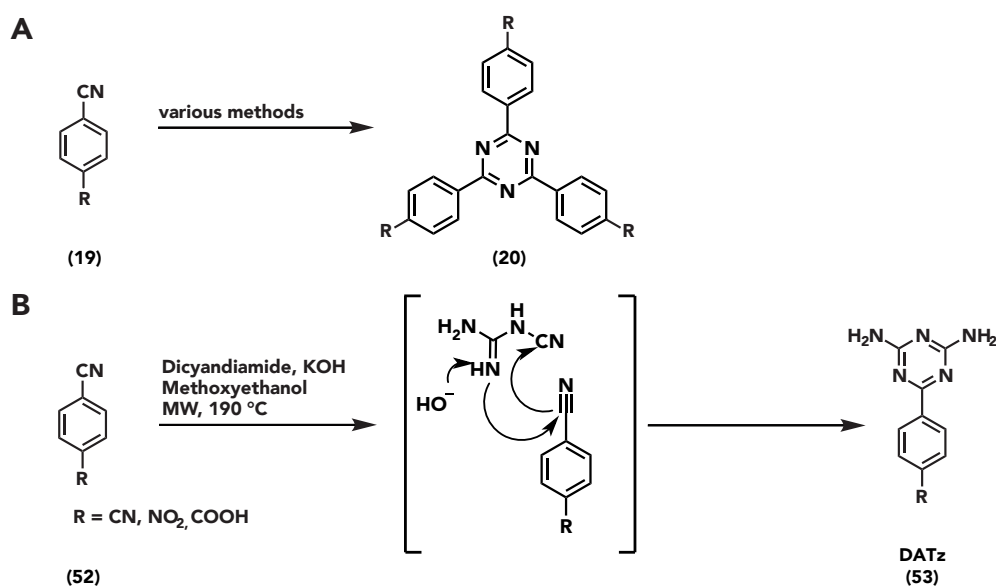


Figure 4.20: Synthesis of Triazines: Synthetic scheme for the synthesis of triazines. **A)** Trimerization of nitriles possible *via* various methods. **B)** Synthesis of diaminotriazines using cyanides and dicyandiamide in a MW procedure.

The interesting part about the synthesis shown in Fig. 4.20 B lies in the wide range of possible substrates that can be used which results in a wide range of possible products (Fig. 4.21). Hence, DATzs can be tuned towards their desired use cases. For example, UV/VIS properties of the precursors can easily be changed by using different residuals in the para position of the benzene corresponding to the triazine core, which could be interesting for application in medicine (Appx. B.12). The degree of functionality can furthermore be tuned by using specific precursors. Mono-, di-, tri- or even tetracyanobenzenes are readily available *via* different chemical vendors which may all lead to the corresponding diaminotriazines.

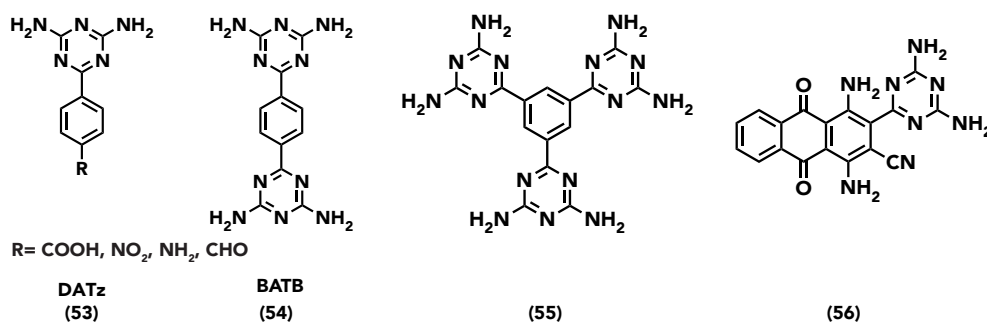


Figure 4.21: Diaminotriazines: Scheme of a variety of different DATzs many of which are obtainable *via* a 10-minute microwave procedure. Synthesis of all structures besides the tri-DATz (55) species were conducted as part of this thesis.

However, there is a limitation in the case of certain ortho dicyano-systems, as only one cyanide moiety reacted towards the DATz. To further testing the limits of the synthesis using a microwave, in the case of BATB, the synthesis was scaled up by a factor of 10, to yield 8.9 g of product in a 30-minute procedure. Four reactions of that scale were run in parallel and all resulted in an overall yield between 78 and 85% after purification. Reaction time was increased, as the heating of the larger MW system is slower and required a larger amount of solvent (1.5x compared to the conventional approach) as the reactor had to be filled up to an absolute minimum.

4.2.3 BATB – A Versatile DATz Precursor

BATB – Bis-(2,4-diamino-1,3,5-triazine)-benzene – features two triazine cores connected *via* a benzene spacer. Hence, the system features a push-pull system and is in general very electron deficient. It also features four amine moieties, two on each triazine, that should enable the synthesis of PIs. BATB can easily be prepared under basic conditions by a 5-minute MW reaction using dry 2-methoxyethanol as a solvent. BATB was obtained as a white crystalline powder that is thermally stable up to $T_D \approx 360$ °C. Single crystal X-ray diffraction (SC-XRD) of BATB crystals grown *via* hydrothermal recrystallization [55] revealed that BATB shows only little tilt across the axis as seen from the benzene core.

4.2.4 Attempted Polymerization of BATB and Derivatives

As mentioned above, the aim of this project was to generate a variety of DATz based precursors to use in the hydrothermal synthesis of COFs. Considering the high chemical and thermal stability these precursors offer, they should be ideal precursors. There is only a limited amount of literature available that focusses on the polymerization of DATzs or similar systems. For melamine, 2,4,6-triamino-1,3,5-triazine, on the other hand a large number of publications is available with the majority focusing on the synthesis of conventional polymers or porous organic polymers.

Hydrothermal Polymerization of BATB

HTP was attempted in the same fashion as was the case for TAPM based systems. Either an autoclave or a MW vial was charged with the precursors in stoichiometric amounts. Water was added and the system was heated to $180\text{ °C} \leq T_R \leq 230\text{ °C}$ for up to 3 days. However, no matter which DATz precursor was used or which conditions were chosen, no polymer was obtained. In fact, BATB and its derivatives could be retained under all circumstances as the solemn product after washing with water and acetone. These setbacks could be attributed to the fact that the ring nitrogens of the triazine core are more basic than the amine moieties. Hence, the ring nitrogens will be protonated before the amine moieties can react. This is a common issue when working with melamine and could in some cases be averted by generating a salt-like species of the precursor by adding certain acids (HCl or AcOH) to the reaction [56]. However, when attempting to add either excess 2 N or conc. HCl or 6 N AcOH to the system no reaction progress could be observed. Furthermore, no reaction could be observed upon adding either excess PMDA (up to 10 eq.) or excess phthalic anhydride (up to 7 eq.) to the reaction.

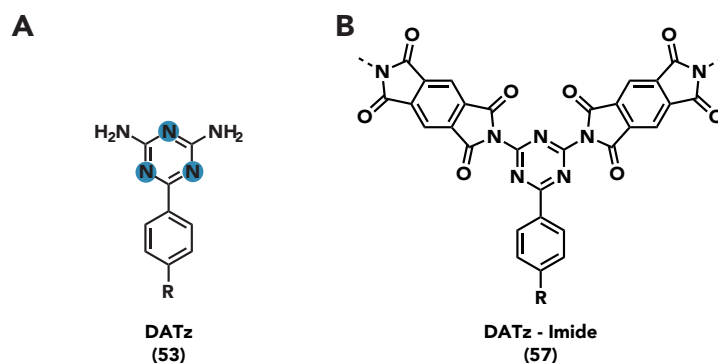


Figure 4.22: DATz and Theoretical Polymer: A) General DATz structure. Blue highlights shows the ring nitrogens that feature higher basicity than the amine moieties. B) Theoretical DATz:PMDA polymer system, which could not be obtained *via* either hydrothermal or conventional polymerization.

Conventional Polymerization of BATB and its Derivatives

As HTP did not work for any of the screened DATz systems, conventional polymerization was attempted. Conventional polyimide synthesis relies on toxic, high boiling solvents such as DMF, or NMP, as well as a reagent such as LiBr, Zn(OAc)₂ or isoquinoline. To ensure optimal conditions, all solvents and catalysts were dried before use as traces of water can severely hinder reaction progress. A total of six different solvent/catalyst systems (Tab. 4.3) were screened using literature procedures. Reaction time was varied between 24 and 96 hours depending on solvent stability and boiling point. However, the same result as previously described for the hydrothermal polymerization were obtained. Namely, BATB was retained in all cases without any reaction taking place.

Table 4.3: Conditions Used in the Conventional Polymerization of DATz towards Imides: Conventional solvent and catalyst systems used for the attempted polymerization of BATB:PMDA.

Solvent system	reagent	reaction time [h]
DMSO/ imidazole	Zn(OAc) ₂	24
NMP	-	24
NMP	LiBr	24
NMP	isoquinoline	24
DMSO/ toluene	-	24/48/72/96
imidazole	-	72

Most of these syntheses were conducted using BATB as the DATz system. However, other DATz systems such as NO₂PhTz were also screened under certain conditions but didn't show any reaction progress even though the chemical environment of the molecule is vastly different.

4.2.5 Conventional Synthesis of Imine-based BATB-COFs

Imine based COFs are amongst the most researched systems and amount to the vast majority of all published literature on COFs. A wide variety of system depending solvent mixtures have been developed that allow the preparation of small amounts of imine-COFs through a solvothermal process, as well as *via* MW-assisted synthesis. Solvent systems in solvothermal imine-COF synthesis are highly sophisticated to ensure, that at all times only a small amount of precursor is in solution and hence, only a small amount of bonds are broken to allow the reaction to be reversible. Aldehydes are generally more reactive than carboxylic acids. Hence, using aldehydes instead of anhydride species could facilitate the polymerization of DATz species. In a typical experiment, BATB and terephthalaldehyde were combined in a flask, the solvents were added, and the reaction was heated to reflux for 48 or 72 hours. Five conventional solvent systems were tested but didn't result in the formation of an imine-based COF. The experiment was also attempted under HT conditions using an autoclave at $T_R = 200$ °C and $t_R = 48$ or 72 h. However, no reaction progress could be observed and the precursors were recovered after workup.

Table 4.4: Conditions Used in the Conventional Polymerization of DATz towards Imines: Conventional and hydrothermal solvent and catalyst systems used for the attempted polymerization of BATB:terephthalaldehyde.

Solvent system	reagent	reaction time [h]
dioxane/ mesitylene	6N AcOH	48/ 72
<i>o</i> -dichlorobenzene/ <i>n</i> -propanol	6N AcOH	48/ 72
<i>o</i> -dichlorobenzene/ <i>n</i> -propanol	-	72
DMSO	-	72
DMSO/ toluene	-	72
water- hydrothermal	-	48/ 72
water- hydrothermal	6N AcOH	48/ 72

The polymerization of BATB towards imine-COFs didn't result in any polymer species. However, in the case of using pure DMSO in the polymerization, a change in morphology was observed. Nonetheless, upon filtration and washing the precipitate with acetone, the precipitate dissolved. This finding is quite interesting as BATB is not soluble in acetone, indicating that some reaction with the aldehyde occurred. The reaction was found to be the formation of an aminor-linked system as shown in Fig. 4.23. Comparable systems based on melamine and even BATB have been reported. Preparing these systems only requires 1 equivalent of *e.g.* terephthalaldehyde when polymerized together with BATB. In our initial experiments however, 2 equivalents were used, as the formation of an imine-linked system was the goal. Due to this, only low-molecular weight polymers were obtained, which explains the solubility in acetone. This approach facilitates the preparation of functionalized polymers based on DATzs. In a standard procedure, a flask was charged with the desired DATz and aldehyde precursor and was subsequently heated to reflux in DMSO for 72 hours. Functionalization is possible through both the DATz (*e.g.* R= NH₂, NO₂, COOH) and the aldehyde (*e.g.* R= CHO, NO₂, *etc.*), which allows for a high degree of tunability. Both, linear polymers as well as network systems can be synthesized.

4.2.6 Polymerization of BATB and Derivatives towards Aminor-linked Systems

The polymerization of BATB towards imine-COFs didn't result in any polymer species. However, in the case of using pure DMSO in the polymerization a change in morphology could be observed. Nonetheless, upon filtration and washing the precipitate with acetone, the precipitate was dissolved. This finding is quite interesting as BATB is not soluble in DMSO, indicating that some reaction with the aldehyde occurred. The reaction was found to be the formation of an aminor-linked system as shown in Fig. 4.23. Comparable systems based on melamine and even BATB have been reported. Preparing these systems only requires 1 equivalent of *e.g.* terephthalaldehyde when polymerized together with BATB. In our initial experiments 2 equivalents were used, as the formation of an imine-linked system was the goal. Due to this, only low-molecular weight polymers were obtained, which explains the solubility in acetone. This approach facilitates the preparation of functionalized polymers based on DATzs. In a standard procedure, a flask was charged with the desired DATz and aldehyde precursor and was subsequently heated to reflux in DMSO for 72 hours. Functionalization is possible through both the DATz (*e.g.* R= NH₂, NO₂, COOH) and the aldehyde (*e.g.* functionalized mono-aldehydes or multifunctional aldehydes), which allows for a high degree of tunability. Both, linear polymers as well as network systems can be synthesized. However, as these polymers could only be obtained under conventional conditions no further investigations were conducted.

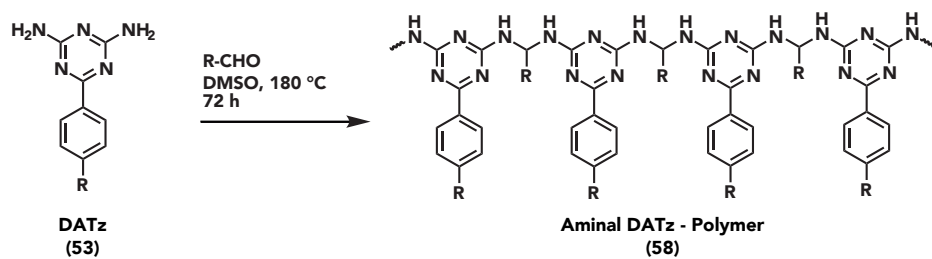


Figure 4.23: Amina-linked Polymers: Schematic synthesis of an amina-linked polymer system using DATzs with aldehydes as reaction partner.

4.2.7 Crystallography of BATB and its Derivatives

As mentioned previously BATB could be obtained as a white crystalline solid after recrystallization in water under HT conditions. In the case of 4,4'-(6-(4-nitrophenyl)-1,3,5-triazin-2,4-diyl)-dimorpholine (4-NO₂PhMTz) – a precursor specifically synthesized for a cooperation partner – orange crystals were obtained after recrystallization in DMF. SC-XRD was measured and the results are compiled in Fig. 4.24 and in the appendix (Appx. C). SC-XRD of BATB revealed that it crystallizes as a hydrate and utilizing its hydrogen bonding capabilities. BATB also shows minimal tilt across the molecule. 4-NO₂PhMTz crystallizes in an hering-bone motif and features a high crystal density of 1.4842 g/cm³.

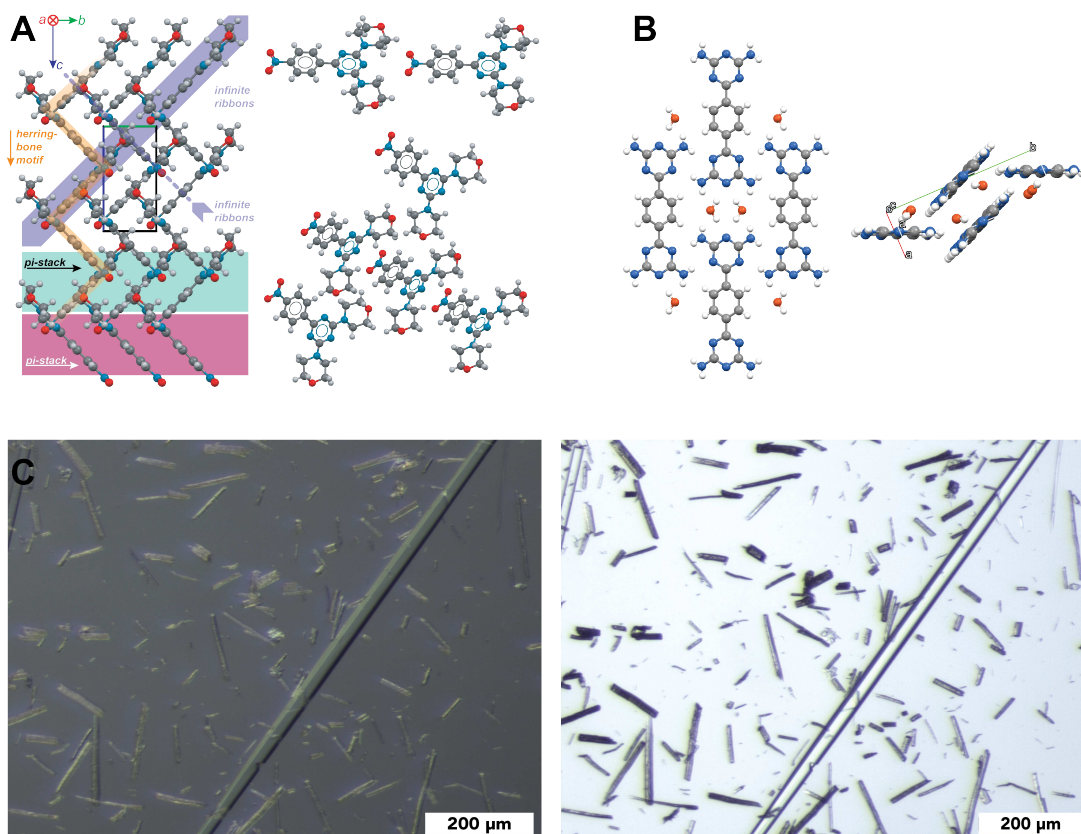


Figure 4.24: Crystal Structures and Micrographs of BATB and 4-NO₂PhMTz: **A)** Crystal structure of 4-NO₂PhMTz. **B)** Crystal structure of BATB. **C)** Micrographs of BATB crystals.

4.2.8 Conclusion and Outlook

In summary, a variety of diaminotriazines has been synthesized and their usability as precursors in polymer synthesis has been evaluated. The DATzs (with the exception of $R = \text{COOH}$) were synthesized *via* a quick and scalable MW procedure using 2-methoxyethanol as solvent. Pure products were obtained after quenching in hot water and subsequent filtration. In the case of $R = \text{COOH}$, the conventional approach (refluxing the precursors overnight) had to be used, as the MW reaction didn't result in the desired product. The initial goal of this project was to use the synthesized DATz precursors in the HTS of triazine-imide COFs, to combine the high-performance properties of the two species. However, HTP under similar conditions as previously used for the preparation of PIs was not successful. Neither HT nor conventional polymerization yielded the desired products. In both cases different additives were tested and in the case of conventional polymerization a variety of different solvent systems were used alongside the reagents. As the preparation of DATz-based PIs was not possible, polyimines were considered, as aldehydes, which feature higher reactivity than carboxylic acids, are used in their synthesis. Imines are furthermore amongst the most researched linkers in COF chemistry and hence, a wide variety of solvent/catalyst systems are reported. However, none of the tested solvent/catalyst systems resulted in the formation of the desired polymers. In the case of using DMSO without a catalyst the formation of a precipitate of different morphology than the precursors could be observed, that dissolved upon filtration a washing with acetone. It was found that this precipitate originated from the formation of an amina-linked low-molecular weight oligomer. Upon adjusting stoichiometry linear polymers as well as network polymers could be obtained featuring a high degree of tunability as both the amine and the aldehyde precursors can be tuned towards their desired use-cases.

Part II

Polythiophenes

Chapter 5

General Background

5.1 Conductive Polymers

Conductive polymers are a class of organic materials that are able to conduct electricity. Hence, these materials feature conductivity comparable to metals or semimetals. Their biggest advantage, compared to conventional, metallic systems, is the possibility to process them as solutions. The conductivity of these polymers can be explained by looking at their molecular structure. In traditional polymers such as *e.g.* polyethylenes, the valence electrons are bound in a sp^3 -hybridization, which doesn't result in electrical conductivity. In conductive polymers on the other hand, the polymer backbone features a continuous sp^2 -hybridization. To be precise, the p_z -orbitals of the carbon backbone combine to form a molecule-wide delocalized set of orbitals. These conjugated p-orbitals form a one-dimensional electronic band in which electrons can move [57]. In general, conductive polymers can be split into several groups depending on their chemical build-up. The majority of conductive polymers are based on aromatic systems with or without heteroatoms (*e.g.* N or S). Polyaniline, the first reported conductive polymer, was reported by Henry LETHEBY in the mid 19th century, as he described oxidized polyanilines to show a deep blue color, whereas their reduced form is colorless. A major gain in interest was however vacant till 1977, when SHIRAKAWA *et. al.* reported polyacetylenes, a very simple conductive polymer that could be turned into a highly conductive polymer by a redox reaction with iodine or bromine [58]. This discovery lead to a boom in the research of conductive polymers and prepared the ground for organic electronics such as, organic light-emitting diodes (OLEDs), organic field-effect transistors (OFETs), and organic photovoltaics (OPVs). Nowadays, a plethora of conductive polymers such as polyfluorenes, polyphenylenes, polypyrroles, polyanilines, polythiophenes are known and are still being heavily investigated (see Fig. 5.1).

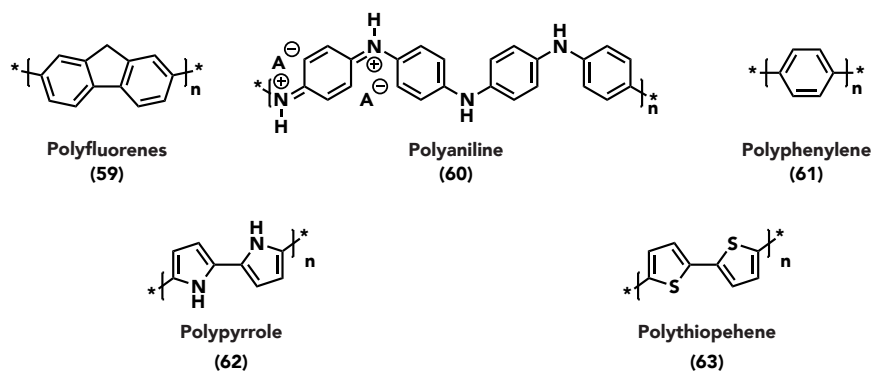


Figure 5.1: Examples of Conductive Polymers: Schematic representation of the most common classes of conductive polymers. PTs and polyanilines require to be oxidized to become conductive.

5.2 Polythiophenes

PTs are a class of polymers, that become conductive upon oxidation. PTs gained a lot of interest after the pioneers of conductive polymer research, MACDIARMID, SHIRAKAWA and HEEGER received a Nobel prize in 2000. Both, the ability to become conductive upon oxidation, as well as their optical properties and their stimuli-responsive behavior make PTs an interesting class of materials. Changes in color and conductivity of the polymers can be explained by the same mechanism and is a result of twisting the polymer backbone and disrupting conjugation. This makes PTs attractive as molecular sensors [59] [60]. Preparation of PTs can be achieved *via* electrochemical and chemical methods. However, only chemical methods are reviewed in this chapter. Conventional methods involve organometallic polycondensations between two monomers in the presence of a metal such as Zn or Mg. A variety of such methods are shown in Fig. 5.2. The methods shown below feature a halide-based precursor that is transformed into a metalorganic intermediate that is subsequently reacted towards the desired product in a homo-coupling reaction [58].

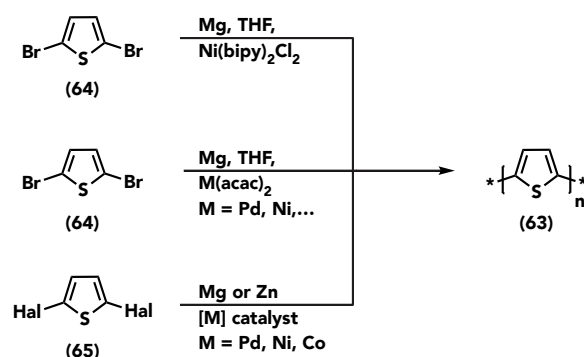


Figure 5.2: Conventional Polythiophene Synthesis: Organometallic polycondensation of 2,5-dihalo-thiophenes utilizing metal-reagents.

Simple PTs, as shown in Fig. 5.2, are almost insoluble. Hence, special PTs have to be prepared to ensure processability. This problem can easily be solved by introducing side chains in 3-position of the thiophenes as shown in Fig. 5.3. However, performance of 3-substituted PTs is vastly dependent on the regioselectivity of the side chains (*e.g.* the optical bandgap depends significantly on the amount and the regioselectivity of 3-substituted thiophenes in the system [61].)

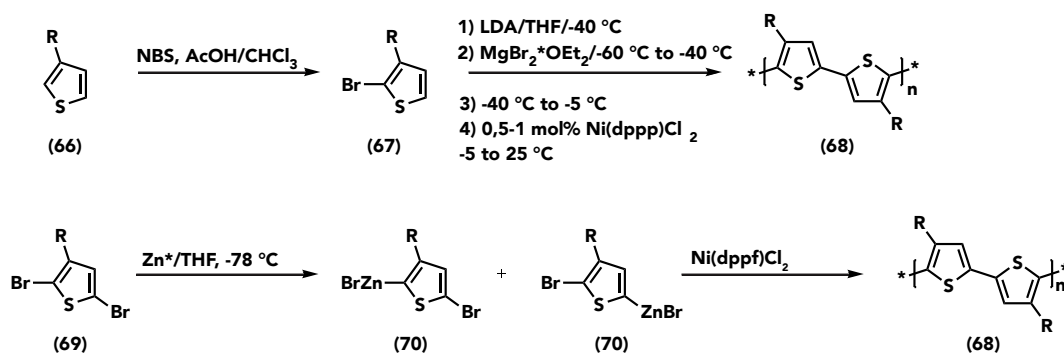


Figure 5.3: 3-Substituted Polythiophenes: Metal-assisted synthesis of polythiophenes with regioregular 3-substitutes. A) shows the KUMADA-style coupling polymerization reported by MCCULLOUGH. B) shows the zinc-based polymerization reported by RIEKE.

The syntheses featured in Fig. 5.3 facilitate the preparation of highly regioregular PTs. Regioregularity depends vastly on the type of catalyst employed in the synthesis, which is why especially Pd-based catalysts, such as Pd(PPh₃)₄, are frowned upon as they result in regiorandom PTs [62]. Side-chain functionalization of

PTs results in higher solubility and therefore better processability. However, the degree of functionalization affects the overall performance of the polymer. Furthermore, if non-aliphatic functional groups are used, the electrochemical properties of the system can be altered indicating a simple approach towards tunable systems. As mentioned earlier, PTs can be made conductive by doping with halides such as iodine or bromine which results in oxidation of the system (Fig. 5.4).

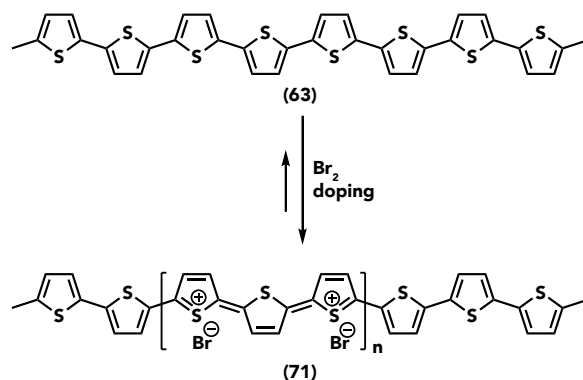


Figure 5.4: Doping of Polythiophenes: Schematic representation of halide-doping induced oxidation of polythiophenes to facilitate conductivity.

5.3 Poly(3,4-ethylenedioxythiophene)

Poly(3,4-ethylenedioxythiophene) (PEDOT) is a well-known representative of PTs, which has been heavily investigated for its use in OPVs, especially as copolymerizates with polystyrene sulfonate (PSS) (e.g. PEDOT:PSS [63]). PEDOT is especially interesting as it is completely transparent in its oxidized form. A variety of methods are reported that facilitate the preparation of PEDOT. However, all of them require the preparation of EDOT in the first place. EDOT can be prepared in a 2-step procedure shown in Fig. 5.5 starting from dimethoxybutadiene [64].

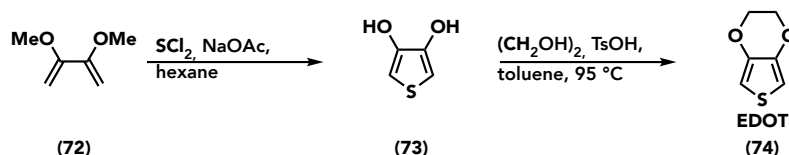


Figure 5.5: Synthesis of EDOT: Preparation of EDOT. The first step features an electrophilic introduction of the sulfur atom into a butadiene system followed by the formation of the cyclic ether through a tosyl-activated substitution.

PEDOT itself is poorly soluble. However, this problem is circumvented by the PSS matrix that is used in the preparation of e.g. OPVs. In this system, PEDOT carries the positive charge, whereas PSS carries the negative charge. Preparation of such systems can be achieved by preparing an aqueous solution of PSS with EDOT and then polymerizing it in a solution of sodium persulfate and ferric sulfate [63].

Chapter 6

Aims and Motivation

PTs are one of the most researched types of conductive polymers as precursors are often readily available and allow for extensive tunability by chemical means. However, processing of such polymers is often only possible *via* solution-processing, which requires the polymers to be highly soluble to avoid using even more toxic solvents or larger amounts of solvents. In 2003, WUDL and co-workers reported [65] the SSP of brominated ethylene-3,4-dioxythiophene (EDOT) towards its polymeric form – poly-3,4-ethylenedioxythiophene (PEDOT). Interestingly, WUDL's procedure results in crystalline PTs with higher conductivity compared to conventional, amorphous systems, making this procedure not only greener, but also results in higher performance materials.

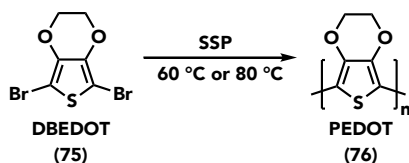


Figure 6.1: Synthesis of PEDOT: SSP of 2,5-dibromo-3,4-ethylenedioxythiophene at elevated temperatures resulting in crystalline PTs.

The aim of this project was to synthesize a variety of different thiophene precursors suitable for SSP while retaining crystallinity. In addition, a means to ensure tunability to improve solubility/processability had to be incorporated. Initially, a variety of simple dibromothiophenes were screened to see whether the procedure is applicable for any type of thiophene. As these initial tests failed, more complex systems were designed to enable SSP.

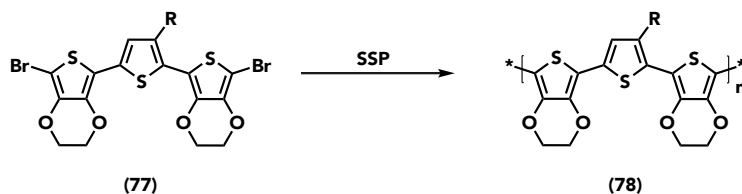


Figure 6.2: Synthesis of Functionalized Polythiophenes *via* SSP: Polymerization of functionalized polythiophenes featuring different chain length of the residuals.

Chapter 7

Results and Discussion

7.1 Initial Tests

In order to test the feasibility of WUDL's procedure for simple and readily available thiophene systems a variety of dibromothiophenes (Fig. 7.1) were chosen. Especially, 3-functionalized thiophenes are of interest, as their properties can be tuned by choosing certain functional groups. Comparing these systems to DBEDOT, a large difference in their chemical environment can be found. DBEDOT features an electron stabilizing dioxy-system, that greatly influences its overall electron density. The other systems, however, are not able to redistribute electron density with the same ease and are conventionally used to prepare precursors suitable for a SUZUKI-type or KUMADA-type polymerization. Furthermore, DBT and 3MDBT are liquids, which would of course not result in a SSP. However it still work as a proof of concept concerning the polymerization of simple dibromothiophenes in solution. Based on these precursors, both SSP and HTP was attempted to see whether polymerization was possible.

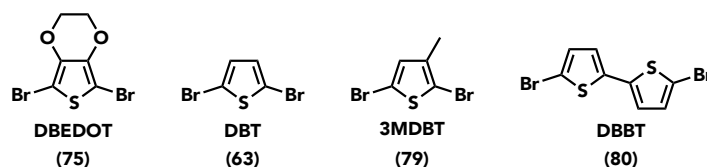


Figure 7.1: Dibromothiophenes: DBEDOT and a variety of simple and readily available 2,5-dibromothiophenes for their feasibility SSP and HTS.

7.1.1 Solid-State Polymerization

SSP was performed using a Schlenk flask attached to a gas-washing flask. The flask was charged with the precursors and then heated to temperatures between 80 and 120 °C for up to 3 days. During this time, DBBT showed an ample change in color from off-white to yellowish. Furthermore, the sodium thiosulfate solution in the gas-washing flask showed the formation of a white precipitate, indicating that bromine formed during the reaction. DBT and 3MDBT didn't show any change in appearance and ¹H-NMR revealed that no reaction occurred at all. ¹H-NMR of DBBT showed only minor changes and some signals were shifted towards higher field. PXRD of DBBT after the reaction showed little to no change. These changes can however be accounted to the fact that some amount of bromine was formed during the reaction that resulted in a change in chemical nature and crystal structure.

The sequestered bromine furthermore acted as a dopant, and oxidized some amount of the thiophene system making it conductive, resulting in a fluorescent product.

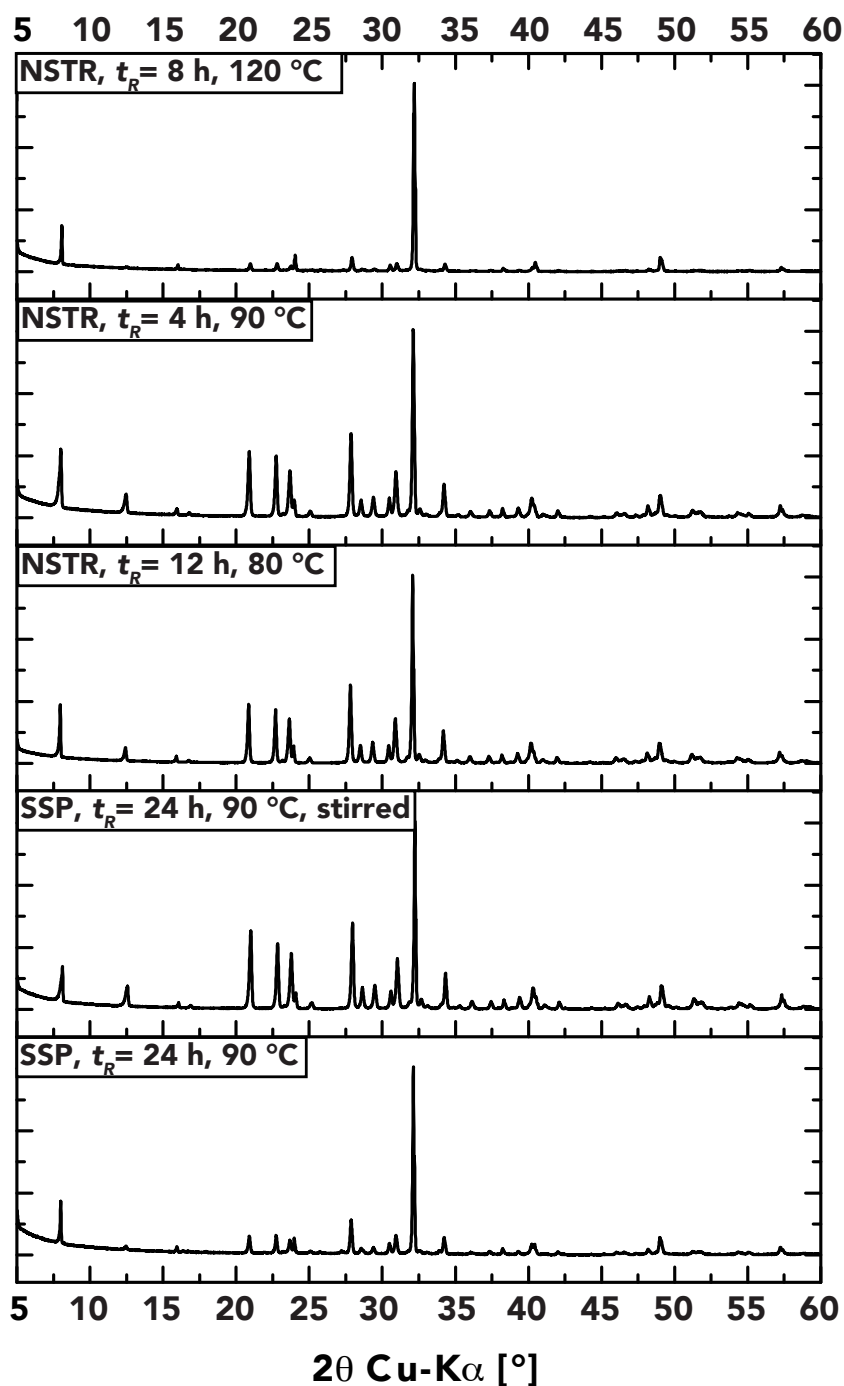


Figure 7.2: SSP and HTP of DBBT: SSP and HTP of DBBT (80). No polymerization occurred under both conditions. Elimination of bromine explains differences in the diffractograms.

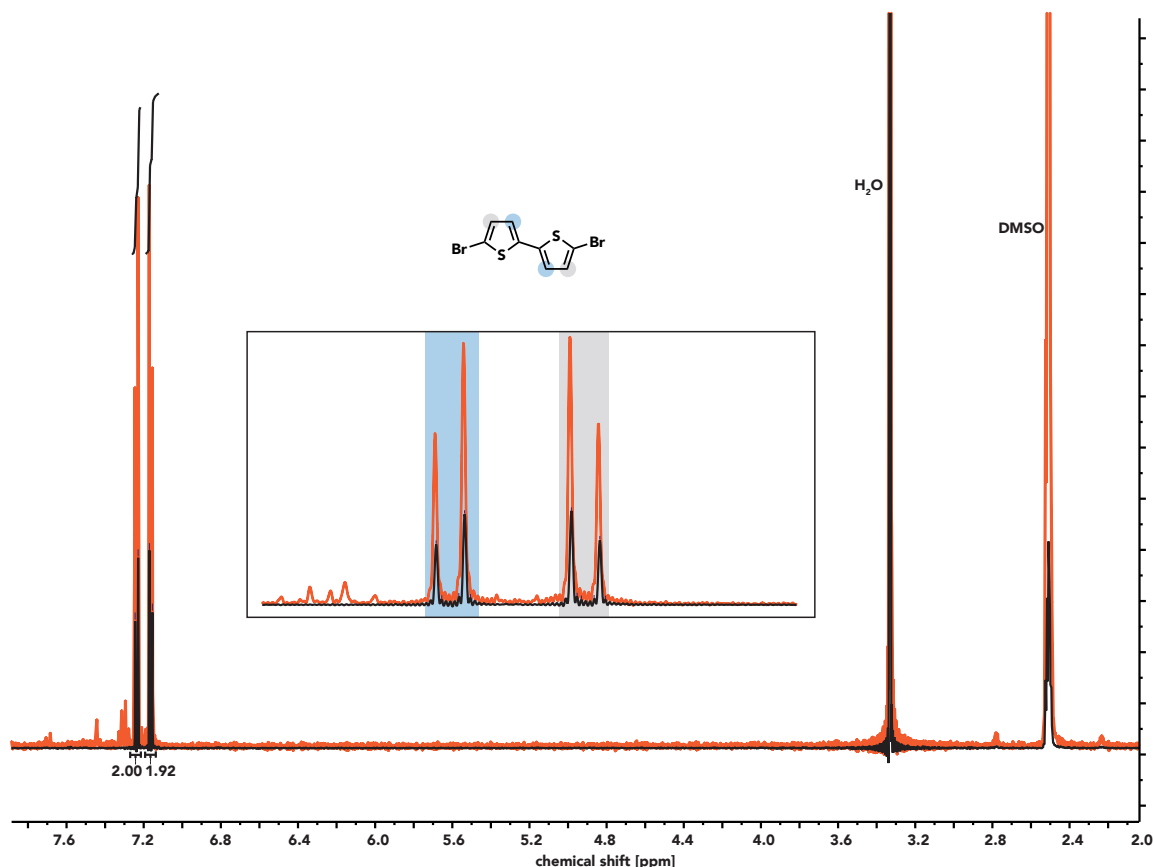


Figure 7.3: DBBT NMR Pre (black) and Post (red) the attempted SSP and HTP: ^1H NMR spectrum of 2,2'-dibromo-5,5'-bithiophene in DMSO. Solvent signal at 2.5 ppm. Water peak at 3.33 ppm. Two duplets corresponding to the CH on the thiophene backbone.

7.1.2 Hydrothermal Polymerization

HTP was attempted under the same conditions as the corresponding SSP. Furthermore, experiments at 200 °C were conducted. An autoclave was charged with the precursors and water was added. As even if no polymerization occurs, bromine can be stripped from the precursor some experiments were performed with an equimolar amount of sodiumthiosulfate (equimolar to the theoretical bromine content) present. At temperatures between 80 and 120 °C no reaction occurred. However, in the case of the 200 °C reaction a black material was obtained, indicating that carbonization instead of polymerization occurred. The aqueous phase was either yellowish or whiteish depending on whether sodiumthiosulfate was present or not, indicating that, indeed bromine was separated. Neither GCMS nor ^1H -NMR could be measured for the 200 °C samples, as the obtained product was not soluble in any conventional solvents. PXRD however, showed a very broad halo around 25–27° (2θ , Cu- K_α) indicating that rather than polymerization carbonization occurred. ^1H -NMR of the low temperature samples revealed that the same effect, as for the attempted SSP occurred. Hence, the precursor was mostly retained. PXRD of these samples (Fig. 7.2) confirm these findings.

7.1.3 Evaluation of the Initial Results

After evaluating the initial results, it was quite apparent, that the procedure proposed by Wudl was only applicable for systems featuring a certain molecular structure/functionality. Furthermore, we found, that HTP doesn't seem to be suitable for the polymerization of brominated thiophenes, as these systems seem to carbonize at temperatures above 150 °C. In addition, all experiments at temperatures above 120 °C lead to a large amount of bromine being formed in an aqueous medium.

7.2 Preparation of Functionalized DBEDOT Systems

As initial attempts to use simple thiophene precursors failed, a more sophisticated approach was tested. In this chapter, the synthesis and use of BEDOT-terminated systems for the dimerization and polymerization of functionalized thiophenes is discussed. In addition, WUDL's initial approach using DBEDOT was reproduced to verify optimal conditions.

7.2.1 WUDL's Procedure – Optimizing Conditions

To verify the procedure, a batch of DBEDOT was prepared by simple bromination of EDOT using NBS. NBS was added to a cooled solution of EDOT in THF over the course of 30 minutes. The solution was stirred at RT for 60 minutes and worked up to yield DBEDOT as a white crystalline solid. Polymerization was attempted in both an oven under air and in Schlenk flasks under Ar to verify the best conditions. Successful polymerization could quickly be verified by a change in color from white to black. The crystallite shape of the precursor was retained in the process. However, PXRD indicates that only a partially crystalline polymer was obtained. Due to the poor solubility of the polymer, NMR couldn't be measured. Interestingly, polymerization doesn't seem to be affected by the presence of air, which indicates that the radical formed in the reaction must be very stable (Fig. 7.4). Both, at 60 and 80 °C the reaction could be completed, however, at 80 °C the polymerization was significantly faster. The 80 °C SSP (shown in Fig. 7.5) shows an experiment, where the product already turned from its initial white crystalline form towards its black polymeric form. However, it seems as if only surface polymerization occurred, as the PXRD shows clear reflections of the precursors with some amount of amorphous background forming around 27° (2 θ , Cu-K α).

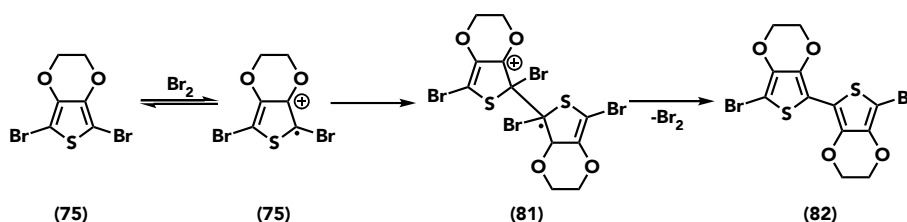


Figure 7.4: Proposed Mechanism for the SSP of DBEDOT: Scheme of WUDL's proposed mechanism of polymerization of DBEDOT. [65]

HTP as an alternative to WUDL's procedure was also tested to see, whether crystallinity could be retained under these harsh conditions. Initially only low-temperature experiments at 80 °C inside an NSTR were conducted. However, the reaction seemed to be slower compared to the SSP variant. The appearance and the PXRD of the product align perfectly with the 80 °C SSP sample. Both, the long-term SSP at 60 °C, as well as the $t_R = 15$ hours, 200 °C HT reaction show a loss of crystallinity. However, these findings are in line with "crystalline" PEDOT in literature.

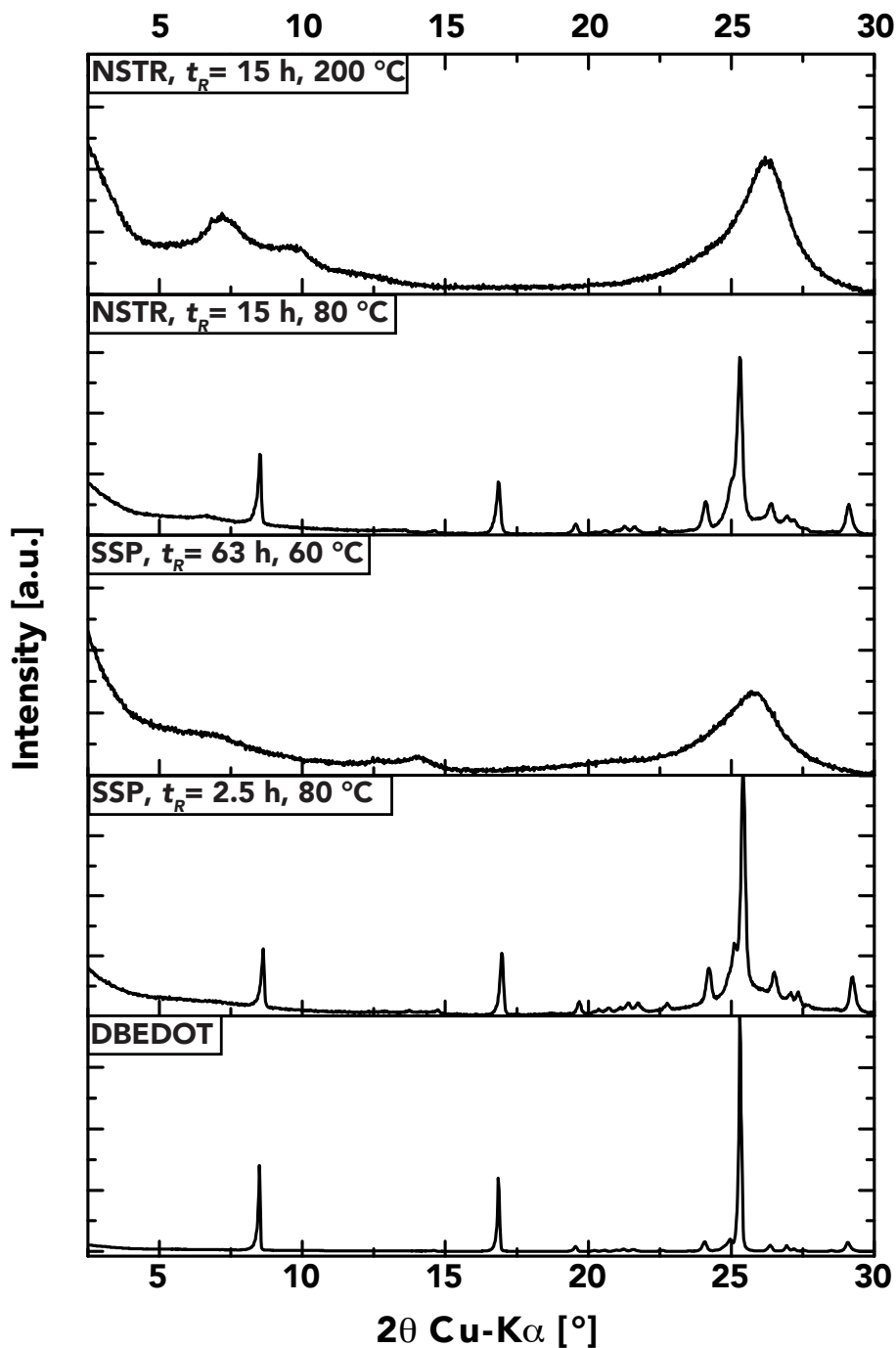


Figure 7.5: Polymerization of DBEDOT: XRD of DBEDOT, its SSP and HTP. Reaction progress could be followed by a change in appearance of the crystals from white to black.

To test the limits of this method, we first attempted to prepare mono-brominated EDOT (BEDOT) to perform controlled dimerization reactions and use the corresponding dimers for further modification. However, only method B of the three methods shown in Fig. 7.6 yielded the desired 2-bromo-EDOT. The first two methods A and B rely on the direct bromination of EDOT as reported in [66]. Method A yielded a mixture

of BEDOT and DBEDOT. However, upon column chromatography the products polymerized. Using method B it was possible to prepare BEDOT in low yields. The low yields can be explained due to the workup as even slightly acidic conditions lead to direct polymerization of the mono brominated species towards the dimer and PEDOT [66]. Due to this, purification of the colorless oil *via* column chromatography was not possible. Synthesis C relies on the elimination of bromine from DBEDOT, which can be achieved using *n*BuLi. Even though *n*BuLi is a strong base easily capable of removing the halide, the synthesis couldn't be performed properly as direct dimerization and polymerization occurred. At this point, it should also be noted, that BEDOT proved to be highly unstable, as the thermal energy of taking a flask out of the freezer was enough to fully polymerize the species within seconds.

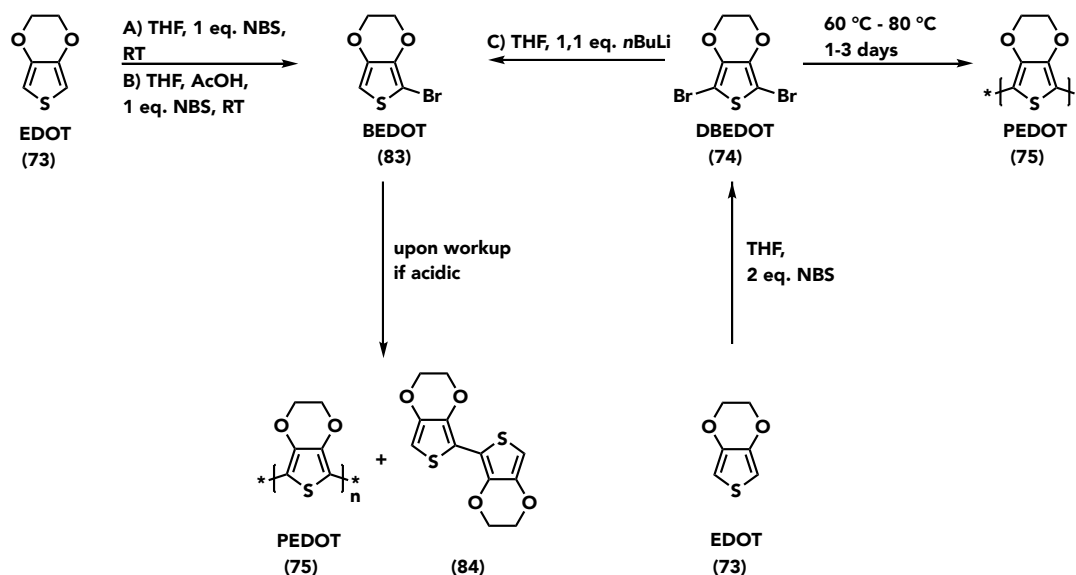


Figure 7.6: Synthesis of BEDOT: Synthetic scheme for the synthesis of BEDOT and DBEDOT starting from EDOT. Dimerization of BEDOT being the main problem.

7.2.2 Evaluating the Effect of Substitution

Due to the effort required in the preparation of BEDOT, as well as its unstable nature, another approach towards mono substituted EDOT systems was investigated. A variety of 2-substituted-5-bromo EDOT systems were prepared using Suzuki coupling reactions. The syntheses were monitored using GC-MS and product formation could be confirmed. However, upon workup and purification using a conditioned column, the substances dimerized and could only be retained as the dimers (Fig. 7.7). Column chromatography was either performed using basic aluminum oxide or silica conditioned with diethylamine, as acidic conditions can lead to polymerization of the product [66]. Interestingly, these substances showed an additional effect, which affects their dimerization. All of them showed high fluorescence, which decayed quickly, indicating a highly UV-unstable nature of the molecules. However, even under optimal conditions, dimerization occurred in all cases while purifying the products.

7.2.3 Preparation of Tri-thiophenes Featuring Terminal EDOT Moieties

As the initial attempts to prepare mono-brominated EDOT systems as well as the preparation of mono substituted BEDOT systems failed, a third approach towards functionalized EDOT systems was tested. The goal was to prepare stable tri-thiophenes that feature terminal EDOT moieties. This approach does not only allow for a high degree of tunability depending on the third moiety used in the system, but also allows for a more controlled overall synthesis. Two general procedures relying on different coupling reactions were

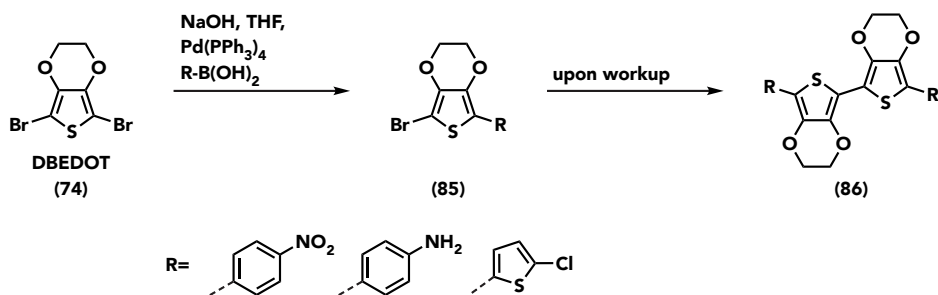


Figure 7.7: Preparation of Substituted EDOT: Preparation of substituted EDOT: Synthetic approach towards the synthesis of 2-substituted-5-bromo species.

attempted. The first, based on Suzuki coupling relied on the lithiation-borylation of EDOT and subsequent reaction with the desired 3-functionalized dibromo thiophene. However, the workup of the mono lithiation-borylation proved to be problematic. The second approach (Fig. 7.8) is based on a Kumada coupling reaction. In a first step, a Grignard reagent is prepared *via* *n*BuLi mediated metalation. The obtained reagent was directly used and coupled with the desired dibromo thiophene. The tri-thiophene could be obtained after purification. The first step was attempted using both MgBr_2 [67] and diethylether as well as using the resulting complex $\text{MgBr}_2 \cdot \text{Et}_2\text{O}$ respectively. This was done due to the highly hygroscopic nature of MgBr_2 that can affect the reaction and is not as pronounced in the etherate complex. However, using the complex directly slowed down the reaction in a fashion that makes it unsuitable.

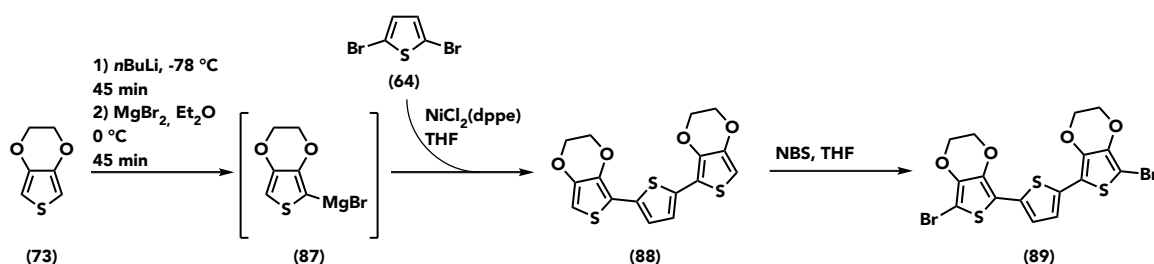


Figure 7.8: Preparation of EDOT Terminally Functionalized Thiophenes: Synthetic scheme for the preparation of functionalized tri-thiophenes.

Upon bromination of these tri-thiophene systems the high reactivity as well as the catalytic nature of their solution polymerization proved problematic. Initial attempts to brominate these systems in the same fashion as EDOT proved unsuccessful, as in all cases, a vast amount of polymer was obtained. Even after cooling to -5°C during the reaction, some amount of polymer was obtained indicating that heat resulting from the reaction has to be dissipated immediately.

7.3 Conclusion and Outlook

In summary, a variety of syntheses aimed to push the boundaries of SSP of thiophenes were carried out. Initial attempts to synthesize a variety of monosubstituted thiophenes to study the reaction were not successful, as both the unstable nature of the precursors, as well as the capability of these precursors to polymerize in solution upon UV irradiation made it impossible to get reproducible results. Taking these insights into consideration a synthetically more demanding approach was chosen. This synthetic approach ensured stability of the systems as well as allows for tunability through the middle thiophene moiety. However, upon bromination of these systems, some degree of polymerization occurred which could not be avoided to date.

Chapter 8

Conclusion

This thesis dealt with the synthesis and characterization of *N*- and *S*- heterocycle based monomers and their environmentally friendly polymerization towards functional polymers.

HTP and SSP were chosen as means of polymerization. Both are inherently green techniques, as only water is used as a solvent in the case of HTP, and SSP is an overall solvent-free method.

The first part of the thesis was focussed on the preparation and evaluation of amine-based precursors. Among these, TAPM was the most prominent precursor due to its simple preparation and its interesting tetrahedral geometry enabling the synthesis of 3D polymers. Furthermore, initial work on the TAPM:PMDA system had been conducted in the group before this thesis and an interesting phenomenon was found in the HT elimination of aniline, which resulted in a salt. The elimination, although under vastly different conditions, was previously reported by GOMBERG in 1898 and could be reproduced under HT conditions (Pt-catalyzed with HCl) by adding a small amount of HCl to the reaction and hence increasing acidity. It was furthermore found that a small amount of the salt species could form under conventional reaction conditions (autoclave, 200 °C, $t_R = 24$ -120 h), complicating polymer synthesis. However, the formation seems to be affected by the initial reaction speed of the system and the acid precursor was subsequently changed to PMA. Using PMA, although the formation of the salt couldn't be avoided altogether, crystalline polymers could be obtained according to PXRD. Crystallinity, as determined *via* PXRD, increased till $t_R = 120$ h, but behaved more inconsistently after that point - more samples were obtained with an amorphous background or were amorphous altogether. SSP of a TAPM:PMA monomer salt was performed and resulted in semicrystalline polymers with the same thermal stability $T_D \approx 530$ °C as the samples obtained *via* HTP, however featuring significantly less crystallinity than these samples. SEM micrographs of the samples revealed that several different morphologies were obtained. This can be explained by the variety of polymerization types that under the used conditions ($T_R = 200$ °C) coexist along each other. Initially sub-HTP exists before reaching the HT realm and hence HTP starting. As temperatures above T_{SSP} ($T_{SSP} \approx 170$ °C) are used, SSP can occur when oligomers and polymers precipitate. Nonetheless, the samples still show the same diffraction pattern in PXRD, indicating that the different morphologies are of the same crystal structure. The obtained diffractograms didn't align with simulated systems, which could be a result of the influence of the TrisAPM-salt. Besides aminophenylmethanes, DATzs were investigated for their suitability as amine precursors for HTP. The desired DATzs could be obtained *via* a quick and versatile MW reaction with only minimal workup required. Polymerization of these DATzs proved to be problematic as in all cases only the precursors were retained. Neither polymerization under HT or conventional conditions resulted in any type of polyimide. As a result, polymerization towards polyimines was attempted as the increased reactivity of aldehydes compared to acids was expected to solve the problem. However, neither HTP nor conventional polymerization resulted in the desired polymers. It was found, that using a 1:1 stoichiometry amination-linked polymers could be

obtained under conventional conditions. However, as the goal of this thesis was the preparation of polymers under environmentally friendly conditions no further investigation was conducted.

The second part of the thesis was concerned with the preparation of thiophene-based monomers and their SSP towards polythiophenes. EDOT-based systems were chosen for the investigation as the polymerization of brominated EDOTs was reported by WUDL. To tackle the biggest disadvantage of such systems, their low solubility, EDOT-terminated trithiophenes were synthesized featuring a tunable thiophene moiety in the middle. The synthesis of such systems could be realized *via* the preparation of GRIGNARD-EDOT reagents *via* a lithiation approach and subsequent Ni-catalyzed reaction with the desired functionalized dibromothiophene. The required bromination of these trithiophenes proved to be problematic, as the thermal energy released during bromination was enough to polymerize some amount of the precursor, making it impossible to obtain pure dibromotrithiophenes. Some degree of polymerization could be observed even when cooling to $T \approx -5\text{ }^{\circ}\text{C}$, indicating the high reactivity of these systems and hence their potential for SSP.

Overall, the goals of this thesis were met in most cases. It was shown, that HTP is a suitable method to obtain crystalline PI networks, if given sufficient t_R . It was shown that under the screened conditions a multitude of reactions occur at the same time, resulting in a variety of different morphologies. DATzs proved to be unsuitable for HTP under the screened conditions. However, a facile synthetic pathway towards a variety of different DATzs was found that could *e.g.* be used to prepare DATz-derived bioactive molecules. Lastly, the suitability of tunable thiophiophene precursors for SSP was evaluated. The ability of the designed systems for SSP couldn't be evaluated as some degree of polymerization occurred while brominating the system. However, this can be accounted to the high reactivity of the system which is promising for the ability of the systems to solid-state polymerize. The synthetic procedure should however be revised and optimized for further studies.

Chapter 9

Experimental Part

9.1 General Methods

FT-IR-ATR spectra were recorded on a Bruker Tensor 27 working in ATR MicroFocusing MVP- QL with a diamond crystal, using OPUS (version 4.0) software for data analysis. Resolution was set to 2 - 4 cm^{-1} , and spectra were recorded from 4000 to 600 cm^{-1} . ^1H and ^{13}C solution NMR spectra were recorded on a Bruker AVANCE 250 (250.13 MHz), a Bruker Avance III HD (600 MHz) and a Bruker AVANCE DPX 300 spectrometer (300.13 MHz) equipped with a 5 mm inverse-broad probe head and z-gradient unit. Optical microscopy was performed on a LEICA M 125 microscope, images were taken using the software LAS v3.7. Scanning electron microscopy (SEM) was carried out with a Quanta 200F FEI microscope. Typically the samples were measured at 5 kV or 10 kV, with a working distance of 9 - 10 mm and spot size 2.0 or 2.5. Prior to imaging, samples were loaded on carbon-coated stubs and coated by sputtering with a 17 nm thick layer of Au/Pd 60/40 alloy with a Quorum Q105T S sample preparation system. Thermogravimetric analysis (TGA) was carried out using a Netzsch TG 209 analyzer at a heating rate of 10 K/min under nitrogen atmosphere, equipped with NETZSCH Proteus (Version 4.3) software. Powder X-ray diffraction (PXRD) data was collected with a PANalytical X'Pert Pro multi- purpose diffractometer (MPD) in Bragg Brentano geometry operating with a Cu anode at 40 kV, 40 mA, and an X-Celerator multichannel detector was used. Samples were ground and mounted as loose powders on silicon single crystal sample holders. The diffraction patterns were recorded between 1° and 30° (2ϑ (Cu- $k\alpha$)), as well as 5° and 60° (2ϑ (Cu- $k\alpha$)) with 69.215 s/step and a step size of 0.0050134 Å, sample holders where rotated during the measurement with 4 s/turn. Single crystal X-ray diffraction analysis (SC-XRD) was carried out on a Bruker KAPPA APEX II diffractometer system using Saint Plus, Sadabs and Jana2006 software. GC-MS measurements were carried out on a Thermo Scientific machine (Trace 1300 gas chromatography with 30 m TR-5MS column and a ICQ LT Single Quadrupol mass spectrometer (EI)). The oven was kept at 100 °C for 4 minutes and was then heated to 300 °C at a rate of 30 °C per minute. The m/z ratio of the peak with the highest intensity was noted.

9.2 Polyimides

9.2.1 Chemicals

Isoamylnitrite (>95%), tris(4-aminophenyl)methane (>97%), mellitic acid (>98%) were purchased from TCI. Pd/C (10%) was purchased from ABCR. PMDA and PMA were purchased from Sigma Aldrich. Chlorotriphenylmethane (Aldrich, 98%), aniline, methanol, acetone, THF, hydrochloric acid (>97%), sulphuric acid (>98%), hypophosphinic acid (50%), DMF, glacial acetic acid (>99%), fuming nitric acid (>99%) and acetic anhydride were purchased from the university. Aniline and DMF were distilled before use.

9.2.2 Synthesis of TAPM

Preparation of Tetraphenylmethane

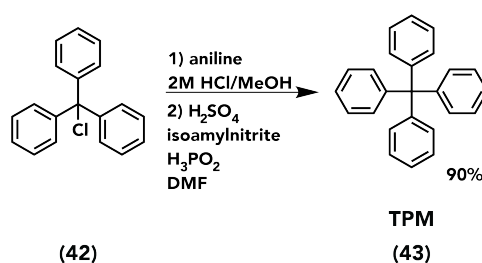


Figure 9.1

Entry	
chlorotriphenylmethane	1.00 eq.
aniline	2.50 eq.
2M HCl	-
methanol	-
conc. sulphuric acid	-
isoamyl nitrite	-
hypophosphinic acid 50%	1.75 eq.
DMF	-

Step 1: A three-neck flask equipped with a mechanic stirrer, a pressure equalizing dropping funnel, and a reflux condenser attached to an argon inlet was flushed with argon and charged with chlorotriphenylmethane and freshly distilled aniline. The flask was slowly heated to 190 °C and kept at the temperature for 15 minutes to obtain a tarnished white solid after cooling to room temperature. The solid was then removed from the flask and crushed using a mortar and pestle. Another flask equipped with a reflux condenser and a magnetic stirrer was charged with the off-white powder 2N HCl and methanol. The solution was heated to 90 °C for 1 hour after which the solution was cooled to room temperature, filtered and washed with water. The obtained off-white powder was milled with a mortar and pestle and was dried at 80 °C under reduced pressure.

Step 2: A three-neck flask equipped with a mechanic stirrer, a pressure equalizing dropping funnel, an argon inlet and a reflux condenser attached to a bubbler was flushed with argon and charged with the product of step 1 and DMF. The solution was cooled to -10 °C using an ice/salt cooling bath before adding sulfuric acid over the course of 1 hour. Isoamyl nitrite was added *via* dropping funnel at the same temperature

over the course of 30 minutes and the obtained solution as stirred for 1 hour. Hydrophosphorous acid was slowly added *via* dropping funnel and H₂ evolution could be observed. After complete addition, cooling was removed, and the suspension was heated to 50 °C till hydrogen evolution ceased. The solution was filtered and subsequently washed with DMF, water and ethanol twice. The obtained white to yellowish powder was dried at 80 °C under reduced pressure.

yield: 95 % of theory, white-yellowish powder

¹H NMR (250 MHz, Chloroform-d₃): δ 7.37 – 7.16 (m, 20H).

GCMS (70 eV): m/z (%): 320,1 (93,5) M+

Preparation of Tetra-(4-nitrophenyl)methane

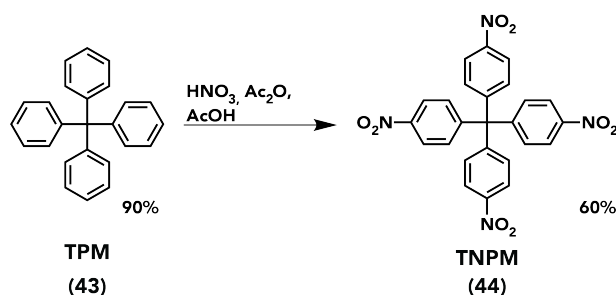


Figure 9.2

Entry

tetraphenylmethane	1.00 eq.
fuming nitric acid	40.0 eq.
glacial acetic acid	20.0 eq.
acetic anhydride	6.0 eq.

A three-neck flask equipped with a magnetic stirrer and a reflux condenser and a pressure equalizing dropping funnel was charged with fuming nitric acid and cooled to -15 °C with an ice/salt bath. After temperature was reached, tetraphenylmethane was added in small portions over the course of 1 hour to minimize NO_x formation. The solution was stirred for 1 hour before adding a solution of glacial acetic acid and acetic anhydride *via* dropping funnel. After 30 minutes, the solution was filtered and washed with glacial acetic acid, methanol and chilled THF to yield an off-white solid that was dried under vacuum at 80 °C to obtain the pure product with 60 % yield.

yield: 60 % of theory, off-yellowish powder

¹H NMR (250 MHz, DMSO-d₆): δ 8.23 (d, 8H), 7.61 (d, 8H).

Preparation of Tetra-(4-aminophenyl)methane

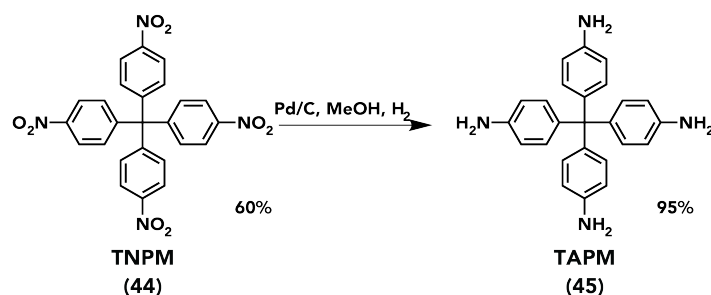


Figure 9.3

Entry

tetra-(4-nitrophenyl)methane 1.00 eq.

Pd/C 10 % 0.05 w%

methanol -

An autoclave vial equipped with a magnetic stirrer was charged with tetra-(4-nitrophenyl)methane, Pd/C and degassed methanol. The resulting suspension was degassed with argon for 5 minutes before being flushed 3 times with hydrogen. The autoclave was charged with 20–30 bar hydrogen pressure and the suspension was stirred overnight. Full conversion was checked *via* TLC and the solution was filtered over a pad of Celite with THF as supporting solvent. The solvent was removed under reduced pressure and the product was dried under reduced pressure (fine vacuum) at 80 °C to yield an off-white powder.

yield: 95 % of theory, white powder

¹H NMR (250 MHz, DMSO-d₆): δ 6.78 – 6.59 (m, 8H), 6.47 – 6.30 (m, 8H), 4.84 (s, 8H).

9.2.3 Synthesis of TAPM- based Organic Polymers

Hydrothermal TAPM:PMDA polymerization

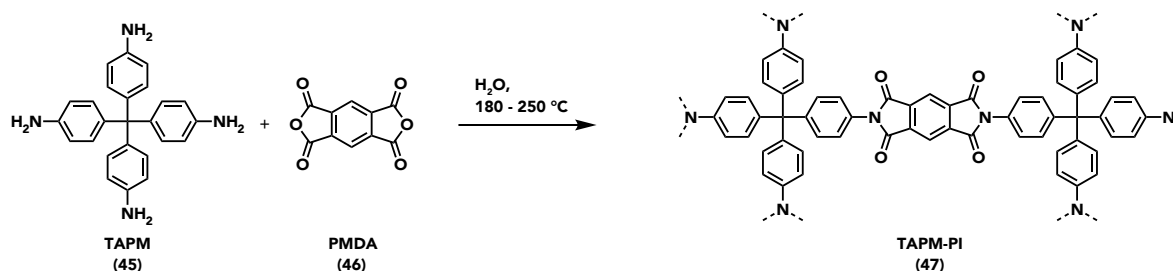


Figure 9.4

Entry

tetra-(4-aminophenyl)methane	1.00 eq.
PMDA	2.00 eq.
water	-
-	-

In a general experiment, an autoclave vial was charged with tetrakis-(4-aminophenyl)methane, a stoichiometric amount of pyromellitic dianhydride and water was added. The obtained suspension was heated to 200 °C (230 °C, 250 °C) under autogenous pressure. After a predetermined period of time, the autoclave was removed from the oven and slowly cooled to room temperature. The obtained precipitate was filtered, washed with water, acetone and THF before drying at reduced pressure at 80 °C for at least 24 hours.

Hydrothermal TAPM:PMA Polymerization

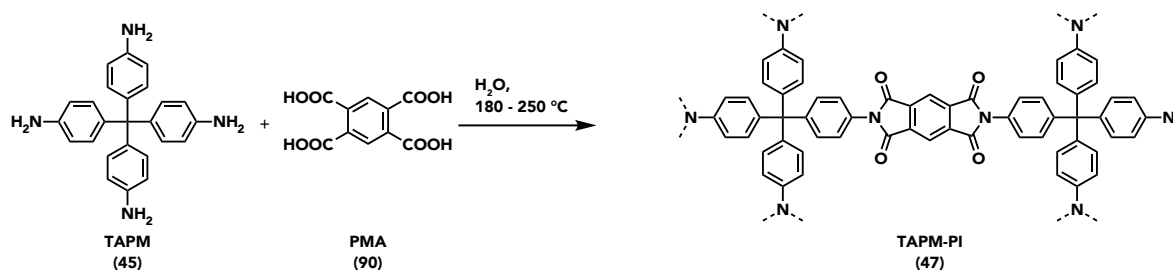


Figure 9.5

Entry

tetra-(4-aminophenyl)methane	1.00 eq.
PMA	2.00 eq.
water	-
-	-

In a general experiment, an autoclave vial was charged with tetrakis-(4-aminophenyl)methane, a stoichiometric amount of pyromellitic acid and water was added. The obtained suspension was heated to 160 – 180 °C under autogenous pressure. After a predetermined period of time, the autoclave was removed from the oven and slowly cooled to room temperature. The obtained precipitate was filtered, washed with water

before drying at reduced pressure at 80 °C for at least 24 hours. A purple precipitate resulting from the polymerization of TAPM with PMA was obtained as the main product. The desired product was obtained in small amounts as green crystalline needles. SC-XRD was measured. ^1H -NMR could not be measured as the product could not be obtained in the required amount.

Synthesis of TrisAPM-carbocation

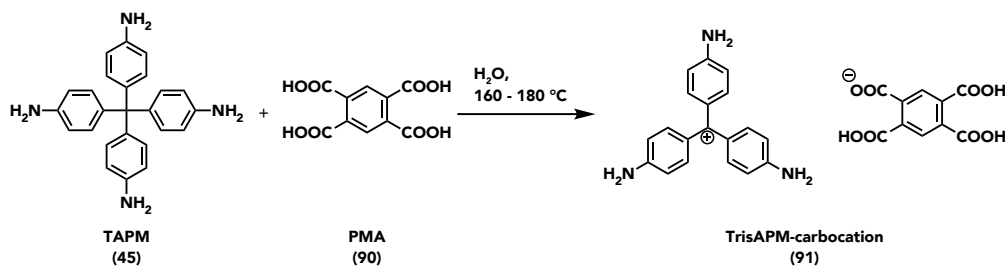


Figure 9.6

Entry

tetra-(4-aminophenyl)methane	1.00 eq.
PMA	2.00 eq.
water	-

In a general experiment, an autoclave vial was charged with tetrakis-(4-aminophenyl)-methane, a stoichiometric amount of pyromellitic acid (PMA) and water was added. The obtained suspension was heated to 200 °C (230 °C, 250 °C) under autogenous pressure. After a predetermined period of time, the autoclave was removed from the oven and slowly cooled to room temperature. The obtained precipitate was filtered, washed with water, acetone and THF before drying at reduced pressure at 80 °C for at least 24 hours.

Synthesis of the TAPM:PMA Monomer Salt

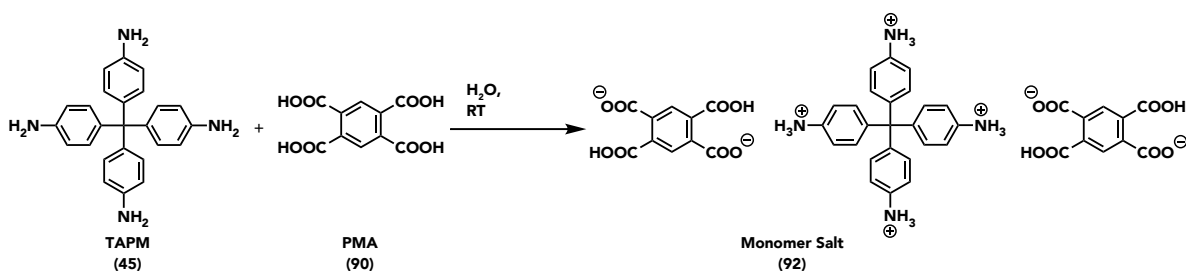


Figure 9.7

Entry

tetra-(4-aminophenyl)methane	1.00 eq.
PMA	2.00 eq.
water	-

In a general experiment, a round bottom flask was charged with tetrakis-(4-aminophenyl)methane, a stoichiometric amount of pyromellitic acid and water was added. The suspension was degassed for 15

minutes and stirred overnight at room temperature. After 1 hour, the initially brownish looking solution turned lighter. The obtained product was filtered and washed with water and small amounts of acetone before drying the samples under reduced pressure at room temperature.

yield: 95 % of theory, off-white powder

^1H NMR (600 MHz, DMSO- d_6): δ 8.09 (s, 4H), 6.78 – 6.74 (m, 8H), 6.59 – 6.51 (m, 8H).

Solid-State Polymerization of the Monomer Salt

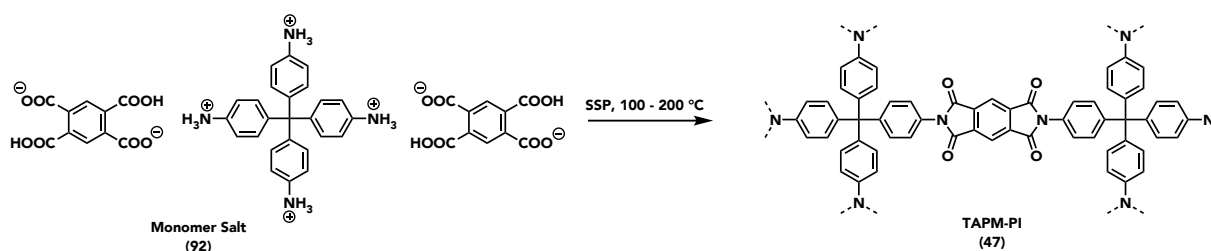


Figure 9.8

Entry

Monomer Salt 1.00 eq.

In a general experiment, a Schlenk flask was charged with the TAPM:PMA- monomer salt. Vacuum between 10 mbar and 10^{-3} mbar was applied for 10 minutes before the flask was heated to 100 – 200 °C in a preheated oil bath for at least 24 and up to 72 hours. After cooling to room temperature, the precipitate was collected.

Hydrothermal Polymerization of TrisAPM:PMDA

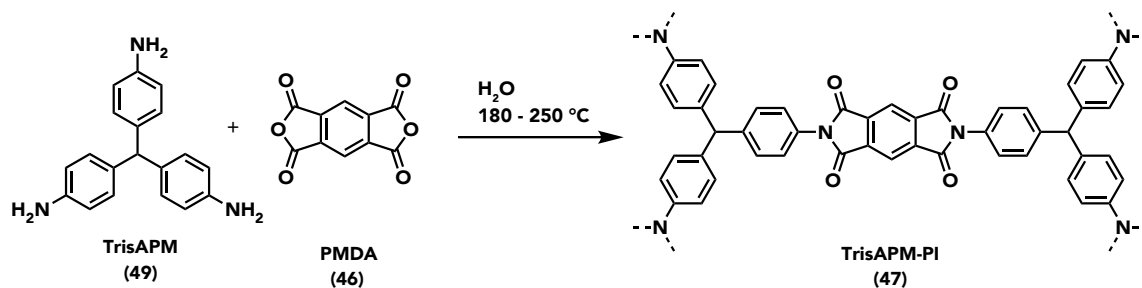


Figure 9.9

Entry

tris-(4-aminophenyl)methane 1.00 eq.

PMDA 2.00 eq.

water -

In a general experiment, an autoclave vial was charged with tris(4-aminophenyl)methane, a stoichiometric amount of pyromellitic dianhydride and water was added. The obtained suspension was heated to 200 °C (230 °C, 250 °C) under autogenous pressure. After a predetermined period of time, the autoclave was removed from the oven and slowly cooled to room temperature. The obtained precipitate was filtered, washed with water, acetone and THF before drying at reduced pressure at 80 °C for at least 24 hours.

Hydrothermal Polymerization of TrisAPM:MellA

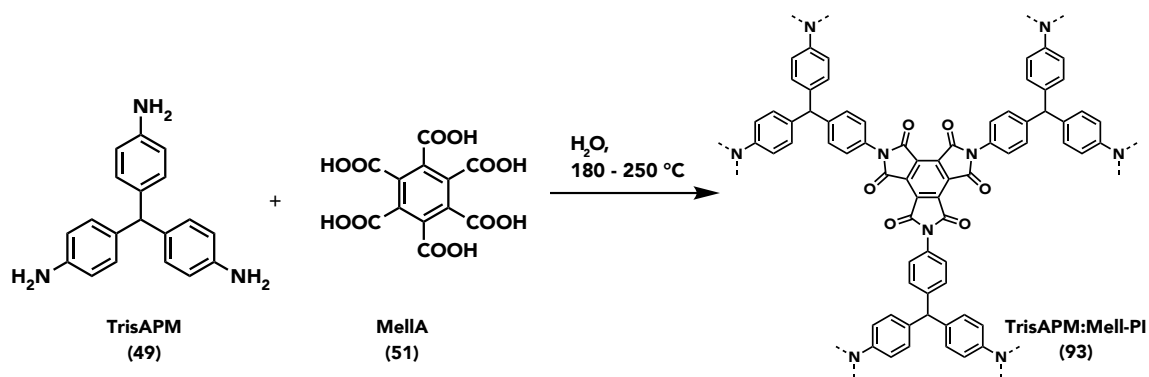


Figure 9.10

Entry

tris-(4-aminophenyl)methane	1.00 eq.
MellA	1.00 eq.
water	-

In a general experiment, an autoclave vial was charged with tris(4-aminophenyl)-methane, a stoichiometric amount of mellitic acid (MellA) and water was added. The obtained suspension was heated to 200 °C (230 °C, 250 °C) under autogenous pressure. After a predetermined period of time, the autoclave was removed from the oven and slowly cooled to room temperature. The obtained precipitate was filtered, washed with water, acetone and THF before drying at reduced pressure at 80 °C for at least 24 hours.

9.3 Diaminotriazines

9.3.1 Chemicals

Dicyandiamide (99%), 1,4-dicyanobenzene (98%) was purchased from Sigma Aldrich. 2-Methoxyethanol (stabilized with BHT, >99%) was purchased from TCI. Imidazole (99%), KOH, 4-nitrophenylbenzonitrile (>97%), 1,4-diamino-2,3-dicyano-9,10-anthraquinone (>90%), sodium hydride (60% suspension in paraffine oil), tinchloride dihydrate, dichlorodiethylether, sodium hydroxide, 4-cyanopyridine, 3-cyanobenzaldehyde (99%), 4-aminobenzonitrile, methanol, acetone, THF, DMSO, NMP, toluene, o-dichlorobenzene, ethanol, ethylacetate, n-propanol, dioxane, mesitylene and terephthalaldehyde (99%) were purchased from the university. THF, DMSO, NMP, toluene, o-dichlorobenzene, n-propanol, dioxane and mesitylene were dried and distilled before use.

9.3.2 General Synthesis of diaminotriazines *via* cyclotrimerization

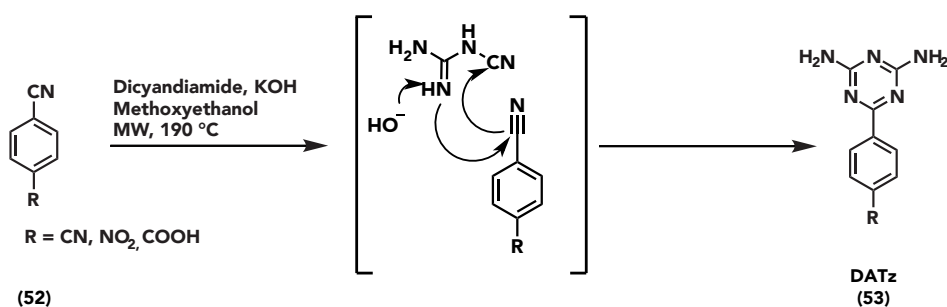


Figure 9.11

The described reaction is a cyclotrimerization of a cyanide with dicyanamide to yield the desired diaminotriazine. Conditions had to be tuned slightly according the chemical environment of the precursor and all syntheses are reported below. In a general procedure, a 20 mL microwave vial was charged with the desired precursors, potassium hydroxide and 2-methoxyethanol. The vial was flushed with argon and heated to 190 °C for 5 to 10 min in a microwave. The vial was cooled to room temperature and the obtained product purified.

Synthesis of Bis-(2,4-diamino-1,3,5-triazine)-benzene (BATB)

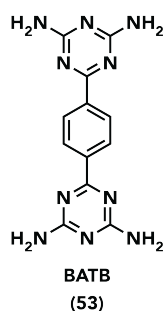


Figure 9.12

compound	eq.	n [mmol]	m [g]	V [mL]
1,4-dicyanobenzene	1.00	6.00	0.768	
dicyandiamide	2.00	12.00	1.008	
potassium hydroxide	0.18	2.00	0.112	
2-methoxyethanol				14.00

The solution was cooled to room temperature and the obtained precipitate was poured onto hot water and stirred for 10 minutes to remove remaining dicyandiamide and 1,4- dicyanobenzene. The solution was filtered, and the obtained precipitate was washed twice with methanol and acetone. The off-white product was dried under reduced pressure.

yield: 1,42 g (79,9 % of theory), off-white, crystalline solid

^1H NMR (250 MHz, DMSO- d_6): δ 8.32 (s, 4H), 6.77 (s, 8H).

Synthesis of 6-Nitrophenyl-2,4-diamino-1,3,5-triazine (4- NO_2PhTz)

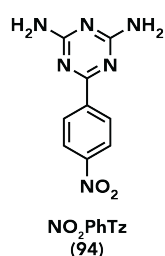


Figure 9.13

compound	eq.	n [mmol]	m [g]	V [mL]
4-nitrobenzonitrile	1.00	1.02	0.151	
dicyandiamide	1.73	1.77	0.102	
potassium hydroxide	0.34	0.34	0.019	
2-methoxyethanol				10.00

The solution was cooled to room temperature and the obtained precipitate was filtered, washed twice with methanol and acetone. The orange product was dried under reduced pressure.

yield: 0,142 g (60 % of theory), orange precipitate

^1H NMR (250 MHz, DMSO- d_6): δ 8.51 – 8.42 (m, 2H), 8.39 – 8.31 (m, 2H), 6.94 (s, 4H).

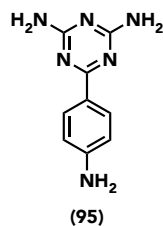
Synthesis of 6-Aminophenyl-2,4-diamino-1,3,5-triazine (4-NH₂PhTz)

Figure 9.14

compound	eq.	n [mmol]	m [g]	V [mL]
4-nitrobenzonitrile	1.00	1.00	0.118	
dicyandiamide	1.30	1.30	0.104	
potassium hydroxide	0.30	0.30	0.017	
2-methoxyethanol				6.00

After the microwave reaction, a yellow solution was obtained that didn't result in a precipitate upon quenching with water, acetone or isopropanol. The solvent was removed and revealed a mixture of mostly the precursor with little product formed.

yield: 0%

Synthesis of 4-(4,6- Diamino-1,3,5-triazin-2-yl)- benzoic acid

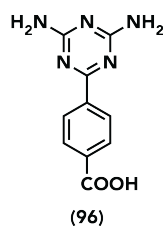


Figure 9.15

compound	eq.	n [mmol]	m [g]	V [mL]
4-nitrobenzonitrile	1.00	1.00	0.118	
dicyandiamide	1.30	1.00	0.084	
potassium hydroxide	1.05	1.05	0.059	
2-methoxyethanol				6.00

After the microwave reaction, a yellow solution was obtained that didn't result in a precipitate upon quenching with water, acetone or isopropanol. The solution was reduced to dryness and revealed a mixture of mostly the precursor with little product formed.

yield: 0%

Alternative synthesis of 4-(4,6- Diamino-1,3,5-triazin-2-yl)- benzoic acid

compound	eq.	n [mmol]	m [g]	V [mL]
4-nitrobenzonitrile	1.00	1.00	0.118	
dicyandiamide	1.30	1.00	0.084	
potassium hydroxide	1.05	1.05	0.059	
2-methoxyethanol				6.00

A three-neck flask equipped with a reflux condenser was charged with 4-cyanobenzoic acid, dicyandiamide, potassium hydroxide and methoxy ethanol. The solution was heated to reflux for 30 hours. The solution was neutralized using 2N HCl and the resulting precipitate filtered, washed with ethanol and dried to yield a white precipitate.

yield: 0,185 g (80% of theory), white precipitate

^1H NMR (250 MHz, DMSO- d_6): δ 8.20 – 8.10 (d, 2H), 7.95 – 7.84 (dd, 2H), 6.74 (s, 4H).

Synthesis of 4-(4,6- Diamino-1,3,5-triazin-2-yl)- benzoic aldehyde

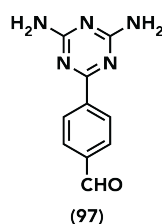


Figure 9.16

compound	eq.	n [mmol]	m [g]	V [mL]
4-nitrobenzonitrile	1.00	1.00	0.118	
dicyandiamide	1.00	1.00	0.084	
potassium hydroxide	0.15	0.15	0.008	
2-methoxyethanol				5.00

The solution was cooled to room temperature and the obtained precipitate was filtered, washed twice with methanol and acetone. The obtained off-white precipitate was not the product.

yield: 0%

Synthesis of 4-(4,6- Diamino-1,3,5-triazin-2-yl)- pyridine

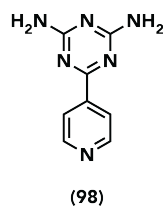


Figure 9.17

compound	eq.	n [mmol]	m [g]	V [mL]
4-nitrobenzonitrile	1.00	1.00	0.104	
dicyandiamide	1.30	1.30	0.109	
potassium hydroxide	0.30	0.30	0.019	
2-methoxyethanol				6.00

The solution was cooled to room temperature and the obtained precipitate was filtered, washed twice with methanol and acetone. After the microwave reaction, the solution was cooled to room temperature and the solvent was removed. The obtained precipitate was recrystallized from methanol. The product was subsequently recrystallized using hydrothermal recrystallization.

yield: 0,065 g (34,5 % of theory), white-yellowish crystals

Synthesis of 1,4-Diamino-2-(4,6- diamino-1,3,5-triazin-2-yl)-3-dicyano-9,10-anthraquinone

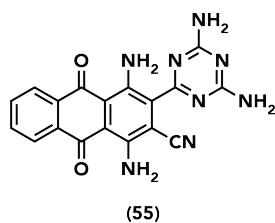


Figure 9.18

compound	eq.	n [mmol]	m [g]	V [mL]
1,4-diamino-2,3-dicyano-9,10-anthraquinone	1.00	1.00	0.288	
dicyandiamide	2.60	2.60	0.218	
potassium hydroxide	0.30	0.30	0.017	
2-methoxyethanol				6.00

After the microwave reaction the solution was cooled to room temperature and the obtained precipitate was filtered and was washed twice with methanol and acetone. The product was obtained as a mixture of the precursor and the monotriazine product.

yield: 0,072g (15,7% of theory), dark blue precipitate

Synthesis of 1,4-Diamino-2-(4,6-diamino-1,3,5-triazin-2-yl)-3-dicyano-9,10-anthraquinone

compound	eq.	n [mmol]	m [g]	V [mL]
1,4-diamino-2,3-dicyano-9,10-anthraquinone	1.00	1.00	0.288	
dicyandiamide	2.60	2.60	0.218	
potassium hydroxide	0.30	0.30	0.017	
2-methoxyethanol				6.00

A three-neck flask equipped with a reflux condenser was charged with 1,4-diamino-2,3-dicyano-9,10-anthraquinone, dicyandiamide, potassium hydroxide and methoxy ethanol. The solution was heated to reflux for 30 hours. The solution was neutralized using 2N HCl and the resulting precipitate filtered, washed with ethanol and dried to yield a white precipitate.

yield: 0.310 g (83.3% of theory), dark blue precipitate – monotriazine compound

^1H NMR (600 MHz, DMSO- d_6): 8.27 – 8.20 (m, 2H), 7.93 – 7.86 (m, 2H), 7.14 (d, $J = 11.3$ Hz, 4H).

9.3.3 Synthesis of Dimorpholinotriazines

Preparation of 4,4'-(6-(4-Nitrophenyl)-1,3,5-triazin-2,4-diyl)-dimorpholine (4-NO₂PhMTz)

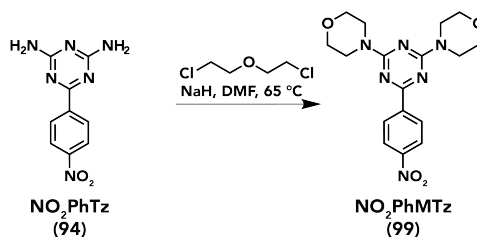


Figure 9.19

compound	eq.	n [mmol]	m [g]	V [mL]
4-NO ₂ PhTz	1.00	4.31	1.000	
dichlorodiethylether	2.10	9.04	1.293	1.06
sodiumhydroxyde 60% dispersion	4.29	18.46	0.738	
DMF				8.75

Flask A: An Ar flushed 50 mL 3-neck flask was charged with 4-NO₂PhTz, dichlorodiethylether and 5 mL dry DMF were added. The solution was stirred under Ar.

Flask B: An Ar flushed 50 mL 3-neck flask was charged with sodiumhydride and 3,75 mL DMF were added. Solution A and B were heated to 65 °C to yield suspensions in both cases. Temperature of solution A was further increased to obtain a suspension before transferring solution A into solution B using a cannula. Upon combining the solutions, color immediately changed to black. The solution was stirred at 60 °C for 90 minutes to obtain a brown solution that was subsequently poured on ice and stirred for 45 minutes to obtain a light brown precipitate. The solution was filtered and washed with EtOH. The precipitate was dried for 2 hours in a vacuum drying oven at 80 °C before being refluxed in ethanol. The precipitate was filtered and washed with cold ethanol. Single-crystals could furthermore be obtained through recrystallization in DMF.

yield: 0,80 g (77 % of theory), orange to brown powder - orange crystals after recrystallization.

¹H NMR (250 MHz, Chloroform-d): δ 8.55 (ddd, J = 9.0, 4.6, 2.0 Hz, 2H), 8.29 (dq, J = 9.2, 2.1 Hz, 2H), 4.30 – 3.48 (m, 16H).

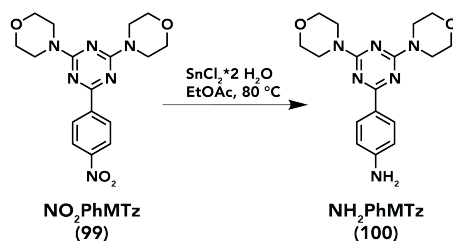
Preparation of 4,4'-(6-(4-Aminophenyl)-1,3,5-triazin-2,4-diyl)-dimorpholine (4-NH₂PhMTz)

Figure 9.20

compound	eq.	n [mmol]	m [g]	V [mL]
4-NO ₂ MPhTz	1.00	0.40	0.150	
SnCl ₂ ·2H ₂ O	5.00	2.01	0.454	
ethyl acetate				10.00

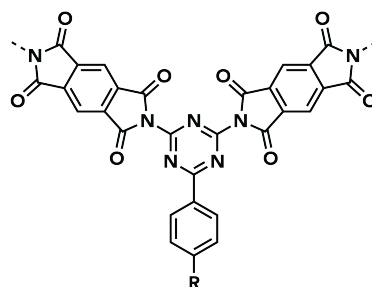
A 25 mL flask was charged with 4-NO₂PhMTz, tinchloride-dihydrate and ethylacetate. The flask was flushed with argon and heated to 80 °C. The solution was stirred overnight and after cooling down, the solution was poured onto water, and neutralized using 1 N NaOH. A precipitate formed after reaching neutral pH which was filtered, washed with ethanol and dried under high vacuum.

yield: 0,089g (70,7 %), yellow powder

¹H NMR (250 MHz, DMSO-d₆): δ 8.06 (d, J = 8.6 Hz, 2H), 6.62 – 6.51 (m, 2H), 5.71 (s, 2H), 3.92 – 3.56 (m, 16H).

9.3.4 Polymerizations of DATz's

Attempted Polymerizations Towards Polyimides



DATz - Imide
(56)

Figure 9.21

Hydrothermal polymerization

In a general procedure an autoclave or a microwave vial was charged with the desired precursors in stoichiometric amounts and water was added. The system was then heated to 180–250 °C in case of the autoclaves and 230 °C in case of the microwave. Microwave reactions were usually conducted for 30–180 minutes whereas the autoclave reactions were reacted for 24–72 hours. After cooling the reactor down, the suspensions were filtered. In all cases, a precipitate originating from the DATz precursor was obtained.

Conventional Polymerization

Solvent System	catalyst	reaction time[h]
DMSO/ imidazole	Zn(OAc) ₂	24
NMP	-	24
NMP	LiBr	24
NMP	isoquinoline	24
DMSO/ toluene	-	24/48/72/96
imidazole	-	72

In a general procedure, a 50 mL 3-neck flask was charged with the desired precursors as well as the desired solvent/catalyst system. The solution was degassed with argon and attached to a DEAN aperture. The reaction was heated to reflux for 24–96 hours before cooling down to room temperature. The solutions were filtered and washed with acetone. In all cases, a precipitate originating from the DATz precursor was obtained.

Attempted Polymerizations Towards Polyimines

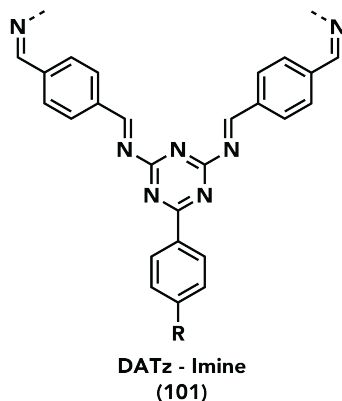


Figure 9.22

Conventional Polymerization

Solvent System	catalyst	reaction time[h]
dioxane/ mesitylene	6N AcOH	48/ 72
o-dichlorobenzene/ n-propanol	6N AcOH	48/ 72
o-dichlorobenzene/ n-propanol	-	72
DMSO	-	72
DMSO/ toluene	-	72

In a general procedure, a 10 mL single neck flask was charged with the desired precursors and the chosen solvent system. The obtained suspension was degassed and subsequently heated to reflux for 48-72 hours. After cooling to room temperature, the solutions were filtered and washed with acetone. In all cases, a precipitate originating from the DATz precursor was obtained.

Hydrothermal Polymerization

Solvent System	catalyst	reaction time[h]
water	-	48/ 72
water	6N AcOH	48/ 72

In a general procedure, an autoclave was charged with the precursors and was heated to 200 °C. After 48 – 72 hours the autoclaves were cooled to room temperature and filtered. The filtrate was washed with water and acetone. The obtained precipitate originated from the DATz precursor.

Polymerization Towards Amino-linked Polymers

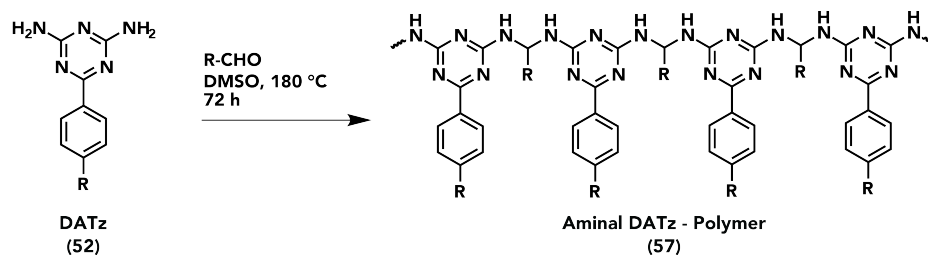


Figure 9.23

compound	eq.	n [mmol]	m [g]	V [mL]
BATB	1.00	2.00	0.593	
Terephthalaldehyde	1.00	2.00	0.268	
DMSO				20.00

A dry and argon flushed 50 mL 3-neck flask was charged with BATB and terephthalaldehyde. After flushing with argon, dry, freshly distilled DMSO was added and the solution was degassed while heating to 100 °C. Upon reaching 100 °C the precursors were dissolved, and bubbling was stopped. The solution was subsequently heated to 180 °C and the obtained yellow solution was stirred at this temperature for 72 hours. After cooling to room temperature, a white to yellow precipitate was obtained, filtered, washed with water, acetone and THF. The obtained amino-linked polymer was dried at 6 mbar and 50 °C for 2 hours.

9.4 Polythiophenes

9.4.1 Chemicals

Triisopropyl borate (98%), *N*-bromosuccinimide (98%) and 3-chlorophenylboronic acid were purchased from TCI. 1,3-Bis(diphenylphosphino)propane nickel(II)chloride and 3-bromothiophene (97%) were purchased from ABCR. 5,5'-Dibromo-2,2'-bithiophene (99%), 4-nitrophenylboronic acid (97%), 2,5-dibromo-3-methylthiophene (97%), 2,5-dibromothiophene (95%), 5-chloro-2-thienylboronic acid and *n*-butyllithium solution 2.5M in hexanes were purchased from Sigma Aldrich. Magnesium bromide (98%), magnesiumbromide etherate, 2,5-dibromo-3-*n*-butyl-thiophene (96%), potassium carbonate, THF and 2-bromothiophene (97%) were purchased from the university. THF was dried over sodium before use.

9.4.2 Preparation of DBEDOT, BEDOT and PEDOT

Synthesis of 2,5-Dibromo-3,4-ethylenedioxythiophene

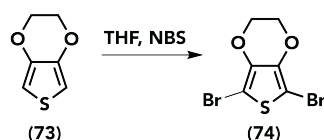


Figure 9.24

compound	eq.	n [mmol]	m [g]	V [mL]
EDOT	1.00	8.00	1.14	0.85
NBS	2.10	16.80	2.99	
THF				30.00

A three-neck flask equipped with a glass washing flask, an argon inlet and a septum and was charged with EDOT under argon flow and degassed THF. NBS was added to the solution in small portions over the course of 25 minutes. Upon adding NBS color initially changed to dark blue/purple but changed to yellow after around 1 minute. The solution was stirred for 4 hours at room temperature. The solution was poured onto 100 mL 1 M KOH and extracted three times with 50 mL THF. The combined organic layers were washed with water and brine before concentrating the solution to 10 mL. 5 mL ethanol were added and the solution was set to crystallize over night. The product was obtained after filtration as white crystalline needles which were washed with chilled methanol. This procedure was repeated three times with the mother liquor to maximize the yield.

yield: 1,537 g (64 %), white crystals

^1H NMR (250 MHz, DMSO- d_6): δ 4.30 (s, 4H).

Polymerization of 2,5-Dibromo-3,4-ethylenedioxythiophene

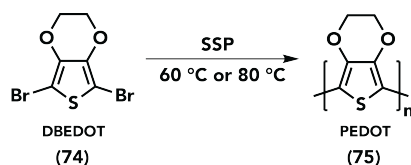


Figure 9.25

compound	eq.	n [mmol]	m [g]	V [mL]
DBEDOT	1.00	0.17	0.05	

A flask was charged with 50 mg of DBEDOT and sealed. The flask was placed in an oven at 60–80 °C and were polymerized for 2–65 hours.

yield: 0,024 g (100 %), black crystalline material

Attempted SSP of Dibromothiophenes

In a general procedure, a Schlenk flask connected to a gas washing flask with sodium thiosulphate was charged with 1 mmol of the desired dibromothiophene precursor. The flask was heated to 80 or 120 degreeCelsius and kept at the temperature for 24–72 hours. No reaction occurred for 2,5-dibromothiophene and 2,5-dibromo-3-methylthiophene. Some degree of dehalogenation occurred for 5-5'-Dibromo-2,2'- bithiophene however no polymerization occurred.

Attempted Hydrothermal Polymerization of Dibromothiophenes

In a general procedure, a NSTR was charged with 1 mmol of the desired dibromothiophene precursors and water. Some experiments were furthermore carried out using sodiumthiosulphate to minimize the risk if bromine was sequestered. Reactions were carried out at 80 and 200 °C. At 80 °C no reaction occurred. At 200 °C on the other hand, carbonization occurred for all samples.

Synthesis of 2-Bromo-3,4-ethylenedioxythiophene Method A

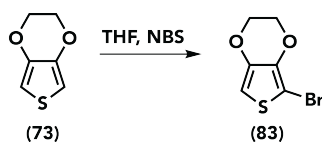


Figure 9.26

compound	eq.	n [mmol]	m [g]	V [mL]
EDOT	1.00	4.00	0.569	0.43
NBS	1.05	4.20	0.748	
THF				15.00

A three-neck flask equipped with a gas washing flask, an argon inlet and a septum was charged with EDOT under argon flow and degassed THF. NBS was added to the solution in small portions over the course of 25

minutes. Upon adding NBS color initially changed to dark blue/purple but changed to yellow after around 1 minute. The solution was stirred for 4 hours at room temperature. The solution was poured onto 25 mL of saturated sodium thiosulphate and extracted three times with 75 mL THF. The combined organic layers were washed with water and brine. The organic phase was separated, dried over MgSO_4 , filtered and the solvent was removed. Upon purification using column chromatography (PE:DCM 2:5) the product polymerized and couldn't be retained.

Synthesis of 2-Bromo-3,4-ethylenedioxythiophene Method B

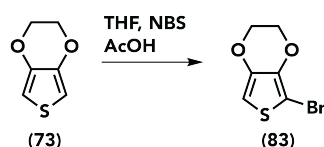


Figure 9.27

compound	eq.	n [mmol]	m [g]	V [mL]
EDOT	1.00	4.00	0.569	0.43
NBS	1.05	4.20	0.748	
glacial acetic acid				10.00
THF				15.00

A three-neck flask equipped with a glass washing flask, an argon inlet and a septum was charged with EDOT and a degassed mixture of THF and glacial acetic acid under argon flow. NBS was added to the colorless solution over the course of 20 minutes and the reaction was stirred at room temperature for 2 hours. The slightly purple solution was poured onto water and a white emulsion was obtained which was extracted with THF. Brine had to be added to obtain a phase separation. The solution was extracted two times with 50 mL THF and the combined organic layers were dried over magnesium sulphate. The solvent was reduced to 5 mL and the yellow solution was stored in the freezer. Upon taking the solution out of the freezer a phase separation could be observed and a black precipitate had formed indicating polymerization.

Synthesis of 2-Bromo-3,4-ethylenedioxythiophene Method C

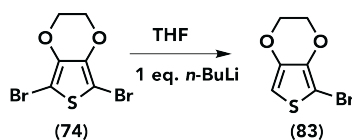


Figure 9.28

compound	eq.	n [mmol]	m [g]	V [mL]
DBEDOT	1.00	2.00	0.600	
$n\text{-BuLi}$ 2.5M	1.10	2.20		0.88
THF				15.00

A 50 mL three-neck flask with a septum and a bubbler was flushed with argon and charged with DBEDOT and dry THF. The solution was cooled to $-78\text{ }^{\circ}\text{C}$ using an acetone/liquid nitrogen bath and $n\text{-BuLi}$ was

added dropwise over 2 minutes. The solution was stirred at this temperature for 2 hours before letting it warm to room temperature and stirring for another 3 hours. The solution was quenched with 30 mL water and extracted three times with DCM. The combined organic layers were washed with brine and dried over magnesium sulphate to obtain a slightly yellow solution. The solution was concentrated to 30 mL and stored in the freezer overnight to yield a off-white precipitate. NMR of the precipitate revealed that the product was formed but was impure. Column chromatography with a basic conditioned solid phase (triethylamine was used) was conducted (PE:DCM 2:5) but a pure product was not obtained. The product was stored overnight in the freezer and upon taking it out of the freezer it polymerized immediately.

9.4.3 Preparation of 2-Substituted-EDOT systems

General Procedure for the Microwave Assisted SUZUKI coupling reactions

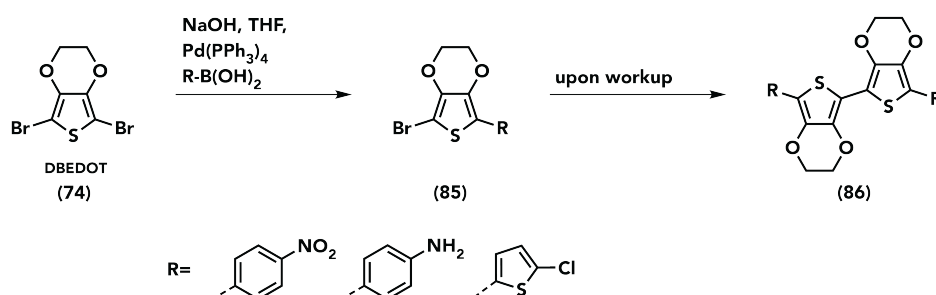


Figure 9.29

In a general procedure, a microwave vial was flushed with argon and charged with the solid precursors. The liquid precursors were degassed before being added to the vial. The suspension was stirred at room temperature for 1 minute before being heated to 130 °C for 1 hour.

Synthesis of 2-Bromo-5-(Chlorothiophenyl)-3,4-ethylenedioxythiophene

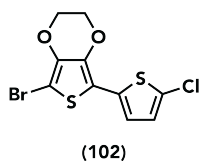


Figure 9.30

compound	eq.	n [mmol]	m [g]	V [mL]
DBEDOT	1.00	0.35	0.107	
5-Chlorothiophenylboronic acid	1.00	0.058		
Pd(PPh ₃) ₄	0.05	0.04	0.046	
potassium carbonate 2M	10.00	3.50		1.85
THF				3.75

The solution turned black upon heating. The solution was filtered over celite and the combined yellow to brown organic layers were washed with brine and dried over magnesium sulphate. The solvent was reduced to 10 mL and 5 mL ethanol was added. The product was obtained as a brown oil which was found to be a mixture of the desired product as a side product and the corresponding dimer as the main product.

yield: 0%

Synthesis of 2-Bromo-5-(nitrophenyl)-3,4-ethylenedioxythiophene

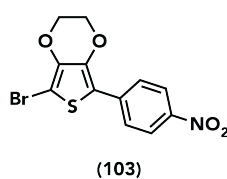


Figure 9.31

compound	eq.	n [mmol]	m [g]	V [mL]
DBEDOT	1.00	0.75	0.225	
4-nitrophenylboronic acid	1.00	0.75	0.125	
Pd(PPh ₃) ₄	0.05	0.04	0.046	
potassium carbonate 2M	10.00	3.50		3.75
DMF				7.50

Upon heating to 130 °C a phase separation could be observed that vanished after around 30 minutes. The obtained dark suspension was filtered over Celite and washed with 150 mL THF. The combined organic layers were washed with water and brine. The combined organic layers were dried over magnesium sulphate and the solvent was removed. NMR of the brown precipitate revealed that the dimer was obtained almost exclusively. Furthermore, signals originating from the PPh₃ could be observed, indicating that the conditions were too harsh for the catalyst.

yield: 0%

Synthesis of 2-Bromo-5-(aminonitrophenyl)-3,4-ethylenedioxythiophene

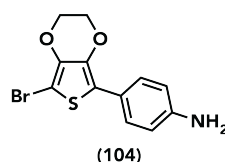


Figure 9.32

compound	eq.	n [mmol]	m [g]	V [mL]
DBEDOT	1.00	0.75	0.225	
4-aminophenylbispinacolate	1.00	0.75	0.164	
Pd(PPh ₃) ₄	0.05	0.08	0.087	
potassium carbonate	5.00	3.75	0.518	
THF				7.50

A dark yellow solution was obtained after reaching reaction temperature and the formation of a black solid could be observed. The solution was filtered over Celite, extracted with THF and washed with water and brine. The organic layers were dried over magnesium sulphate and the solvent was removed. NMR of the dark brown oil revealed that the dimer was obtained as the main product.

yield: 0%

9.4.4 Perparation of Trithiophene Systems

Synthesis of 2,5-Di(3,4-ethylenedioxythienyl)thiophene Method A

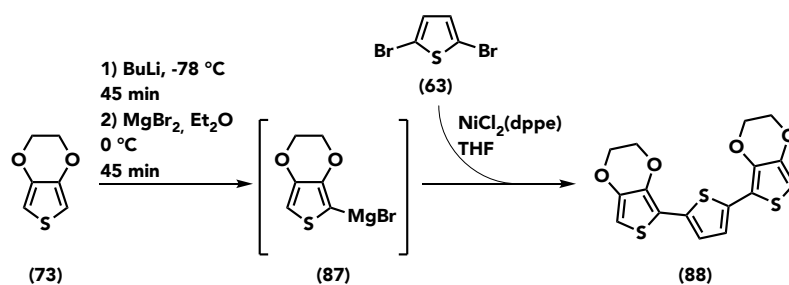


Figure 9.33

compound	eq.	n [mmol]	m [g]	V [mL]
EDOT	3.00	7.50		0.80
<i>n</i> -BuLi 2.5M	3.30	8.25		3.30
MgBr ₂	3.30	8.25	1.519	
Et ₂ O				10.00
2,5-dibromothiophene	1.00	2.50		0.28
THF				20.00
NidppfCl ₂	0.02	0.038	0.020	

A 50 mL three-neck flask with two septums and an argon inlet was charged with EDOT and 20 mL degassed THF. The solution was cooled to $-78\text{ }^{\circ}\text{C}$ using an acetone/liquid nitrogen bath and *n*-BuLi was added dropwise *via* syringe. The slightly yellow solution was stirred for 45 minutes at the temperature and then slowly warmed to room $0\text{ }^{\circ}\text{C}$ by changing to an ice bath. In a second flask, the magnesium bromide was suspended in diethylether to obtain a grey suspension. The suspension was cooled to $0\text{ }^{\circ}\text{C}$ transferred using a cannula. The solution was stirred for 45 minutes before adding 2,5-dibromothiophene and the catalyst to obtain a red suspension and a white precipitate. The solution turned clear and changed color to orange after heating to room temperature. After 3 hours, a dark red solution was obtained and the solution was stirred over night. The solution was poured on 50 mL water to obtain a yellow suspension and a brown solid. The obtained solution was extracted with THF and washed with brine before separating the phases and drying the organic phase over magnesium sulphate. After removing the solvent a brown oil was obtained. A column was prepared (PE:EA 5:1) for which the product was prepared on 5 g of silica.

yield: 0,175 g (% of theory)

^1H NMR (250 MHz, DMSO- d_6): δ 7.13 (s, 2H), 6.60 – 6.54 (m, 2H), 4.32 (dtd, $J = 26.7, 3.8, 2.5\text{ Hz}$, 8H). GCMS

Synthesis of 2,5-Di(3,4-ethylenedioxythienyl)thiophene Method B

compound	eq.	n [mmol]	m [g]	V [mL]
EDOT	3.00	7.50		0.80
<i>n</i> -BuLi 2.5M	3.30	8.25		3.30
MgBr ₂ *Et ₂ O	3.30	8.25	1.519	
Et ₂ O				10.00
2,5-dibromothiophene	1.00	2.50		0.28
THF				20.00
NidppfCl ₂	0.02	0.038	0.020	

A 50 mL three-neck flask with an argon inlet, a septum and a gas washing flask was charged with EDOT and dry degassed THF. The solution was cooled to -78 °C using an acetone/liquid nitrogen bath and *n*-BuLi was added dropwise *via* syringe. The solution was stirred at that temperature for 45 minutes before being warmed to 0 °C in an ice bath. In a second flask, MgBr₂*Et₂O was mixed with 10 mL of diethylether to obtain a white suspension. The suspension was transferred using a funnel under argon flow, as the cannula got clogged during the process. The obtained suspension was stirred for 1 hour before adding adding 2,5-dibromothiophene and the catalyst. The suspension was stirred overnight. TLC of the reaction indicated that no reaction progress was obtained. Reaction GCMS confirmed these findings.

Bromination of 2,5-Di(3,4-ethylenedioxythienyl)thiophene

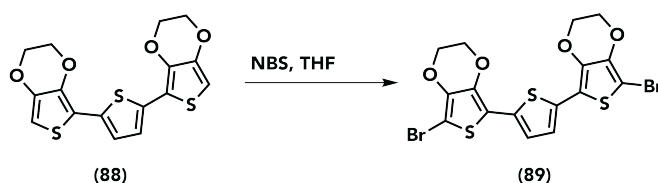


Figure 9.34

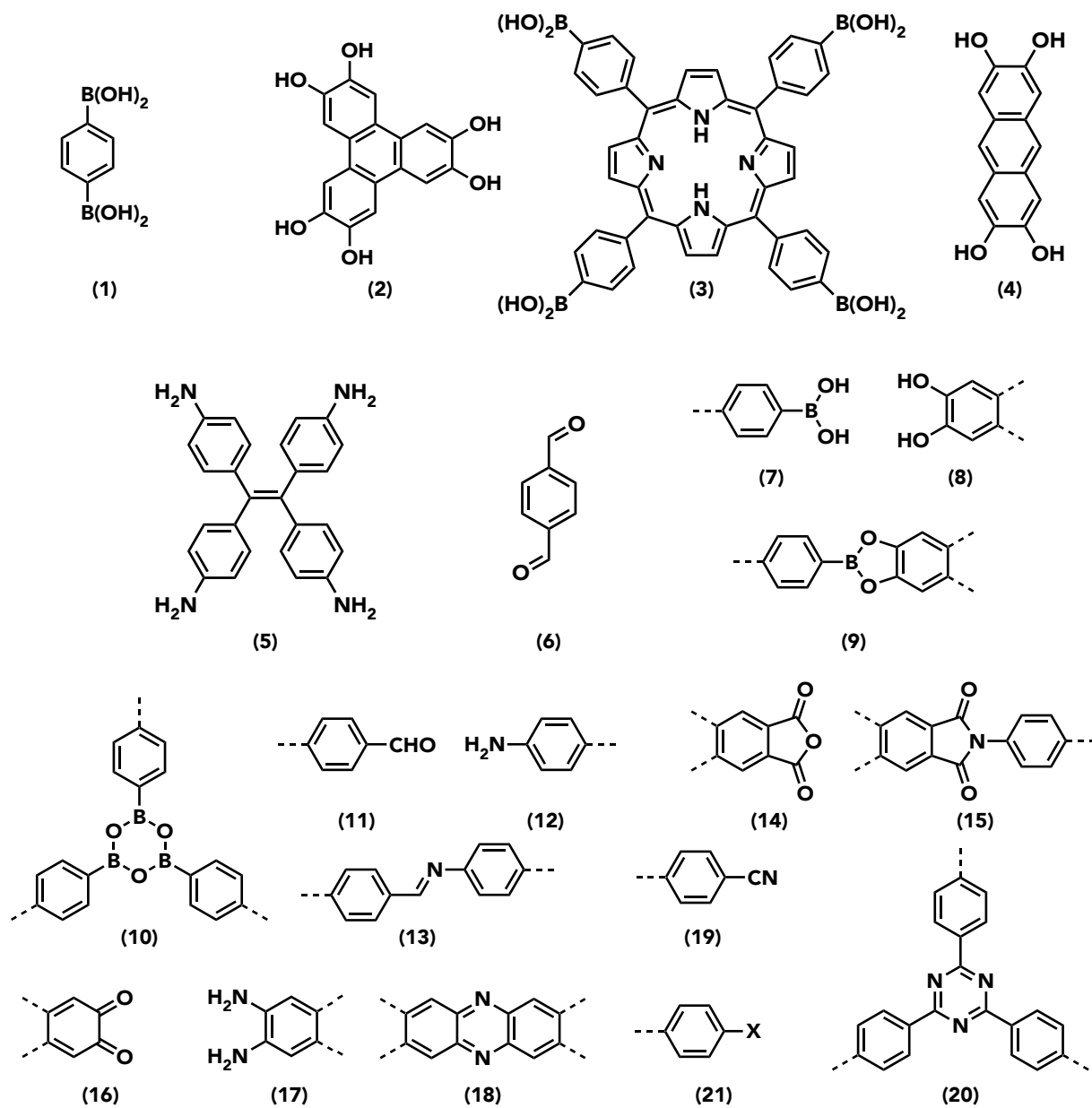
compound	eq.	n [mmol]	m [g]	V [mL]
ETE	1.00	0.48	0.175	
NBS	2.10	1.00	0.179	
THF				15.00

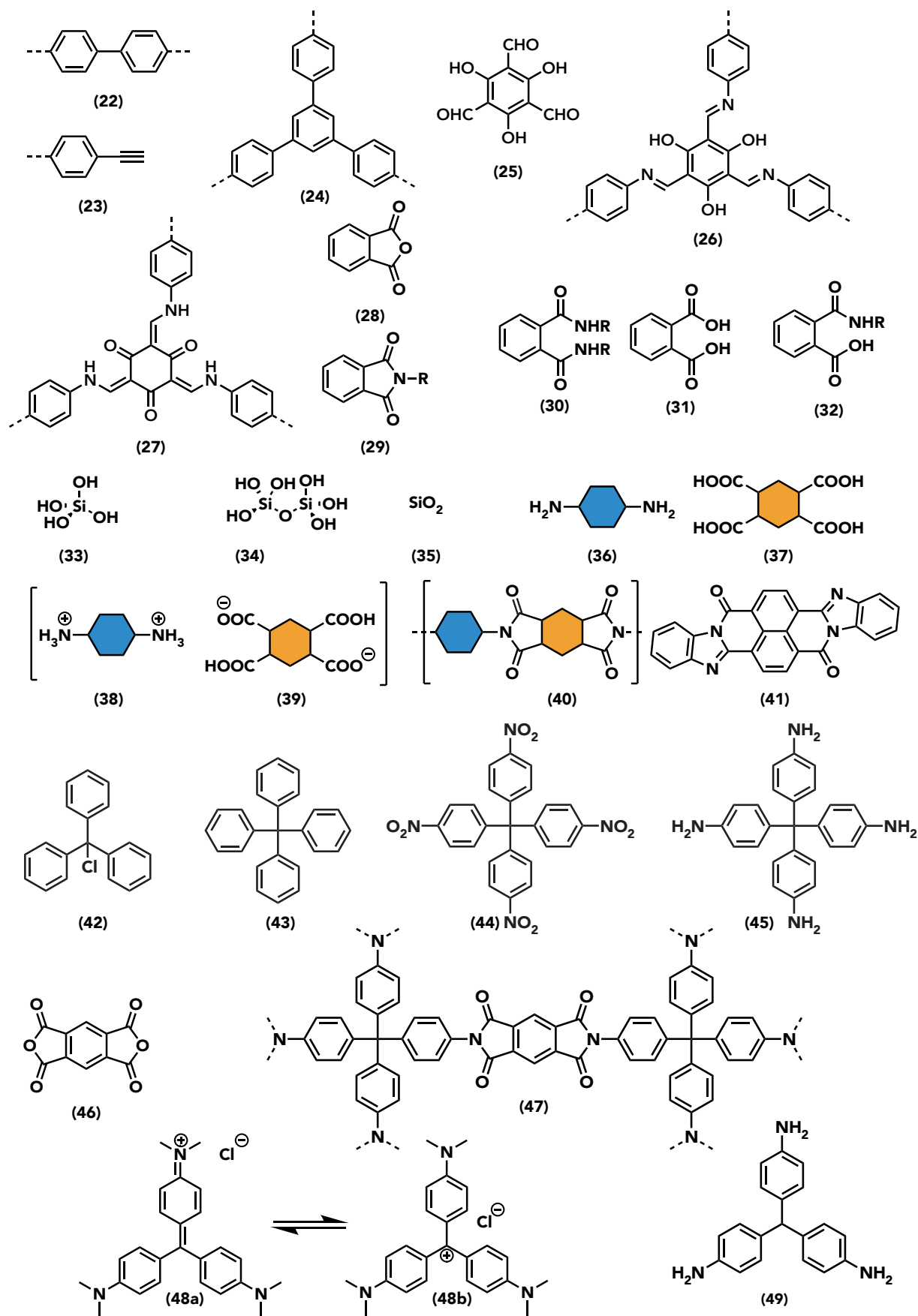
A 50 mL three-neck flask with a septum, an argon inlet and a gas washing flask was flushed with argon and charged with ETE and degassed THF. NBS was added in small portions over 10 minutes. The solution changed color from an initial yellow to dark green. A black precipitate separated at positions where NBS stuck to the flask wall. The reaction was stirred at RT for 4 hours and was monitored *via* GCMS before being quenched in 50 mL of saturated sodium thiosulphate. The solution was extracted with THF, washed with water and brine before being dried over magnesium sulphate. After reducing the volume to 10 mL some black particles separated and were filtered off. The remaining solution was stored in the freezer but yielded next to no product. NMR of the black precipitate showed, that oligomerization/polymersization occurred.

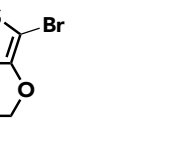
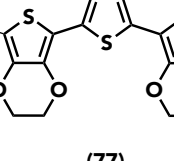
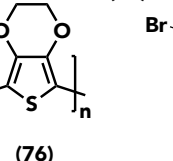
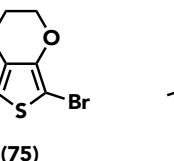
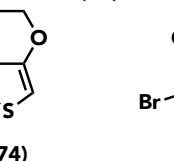
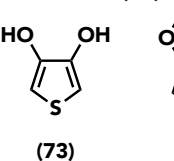
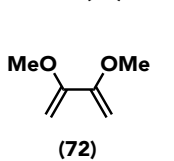
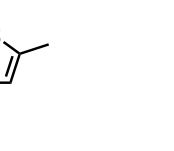
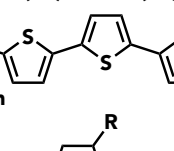
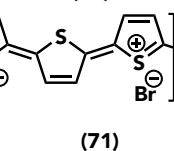
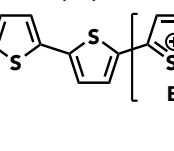
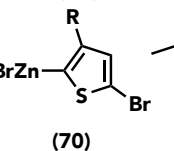
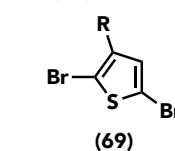
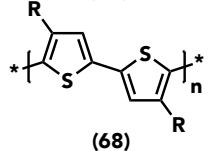
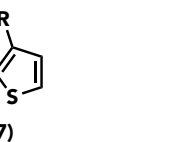
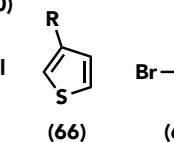
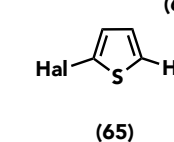
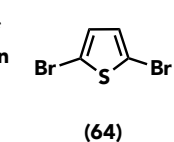
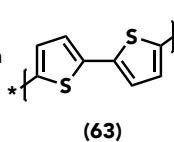
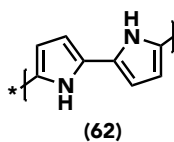
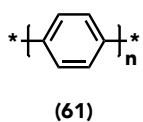
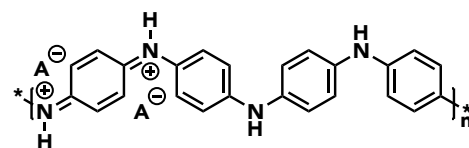
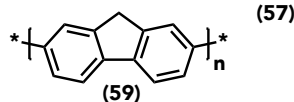
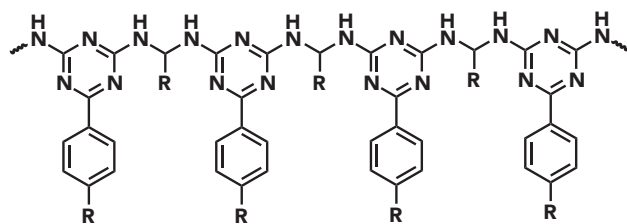
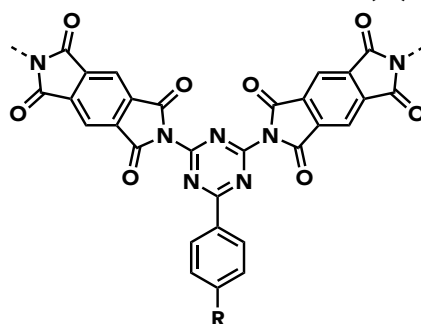
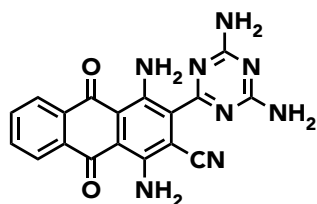
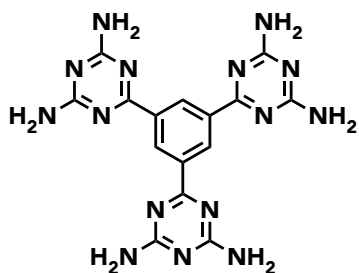
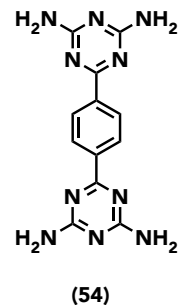
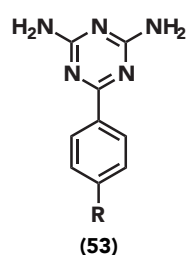
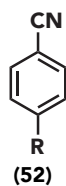
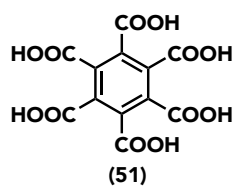
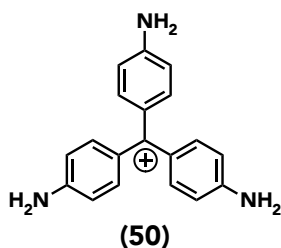
yield: 0%

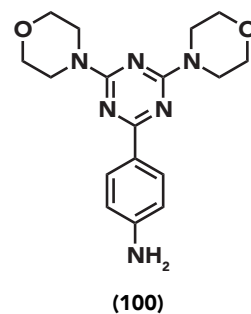
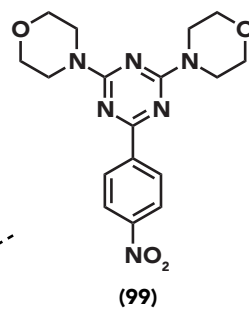
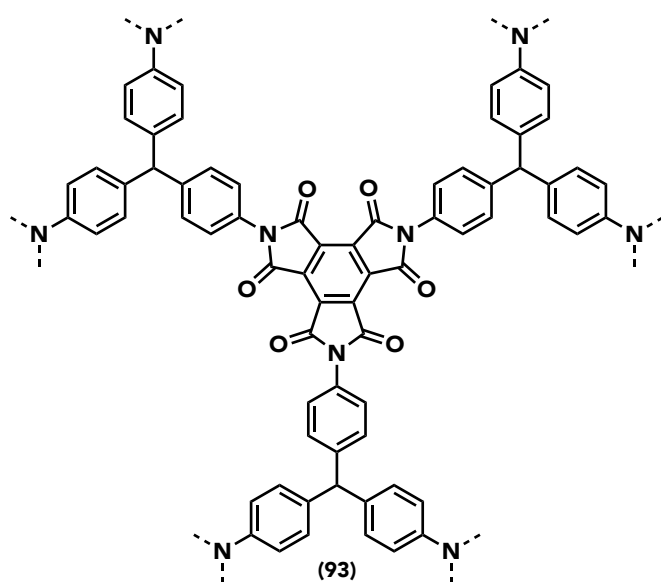
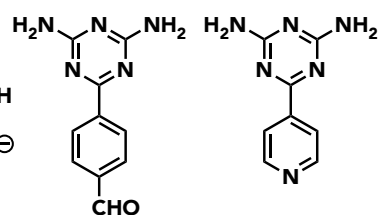
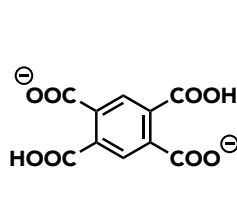
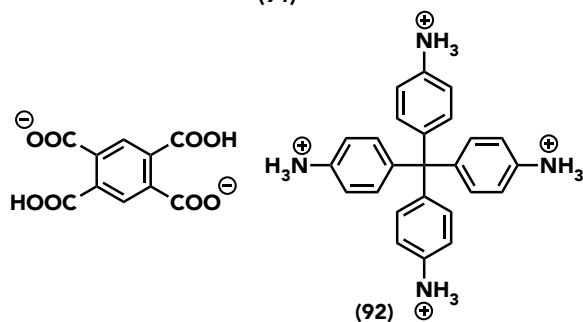
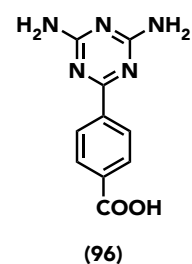
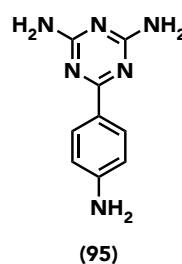
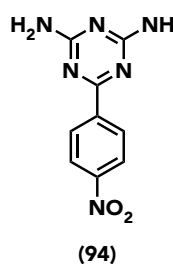
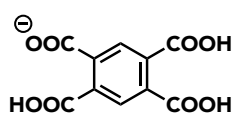
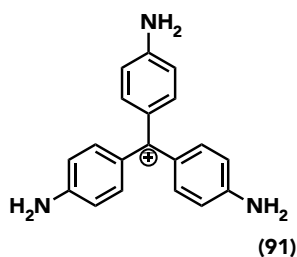
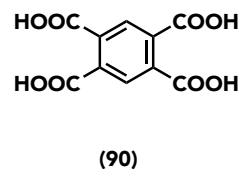
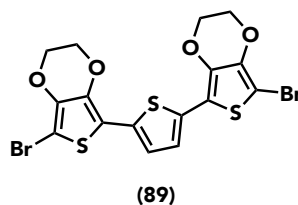
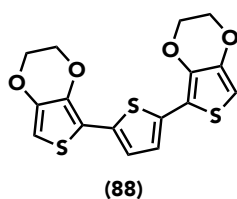
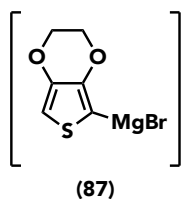
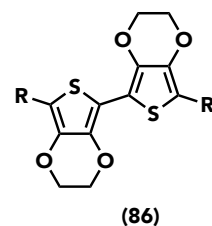
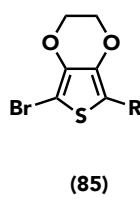
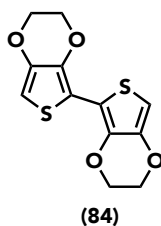
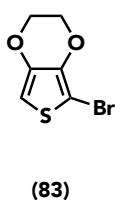
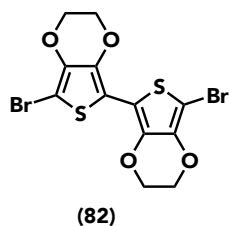
Appendix A

List of Structures









Appendix B

Polyimides

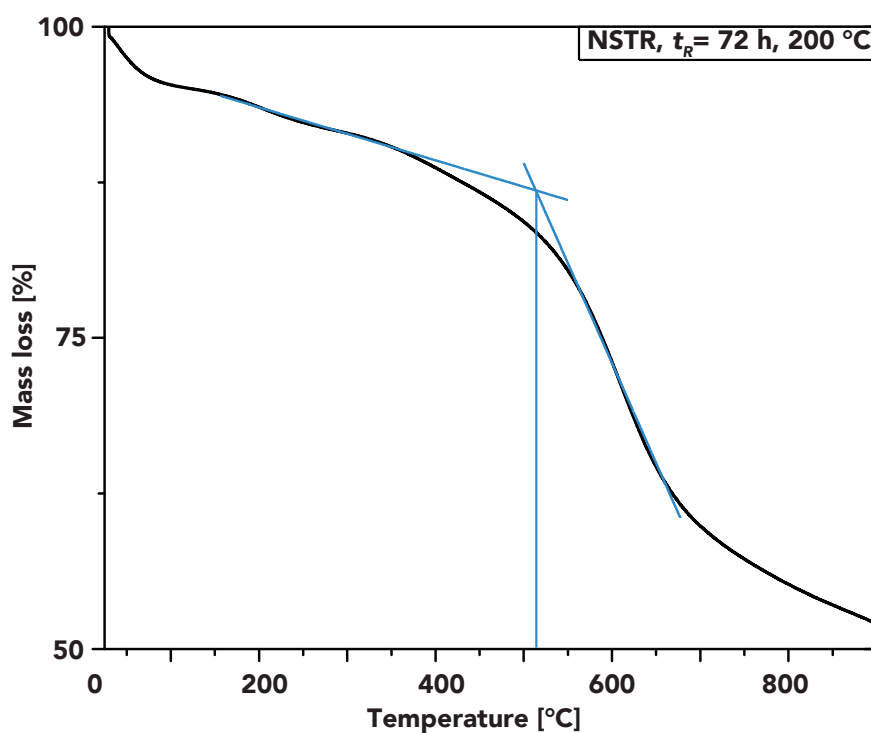


Figure B.1: TGA of TAPM:PMDA. $T_D \approx 515^\circ\text{C}$.

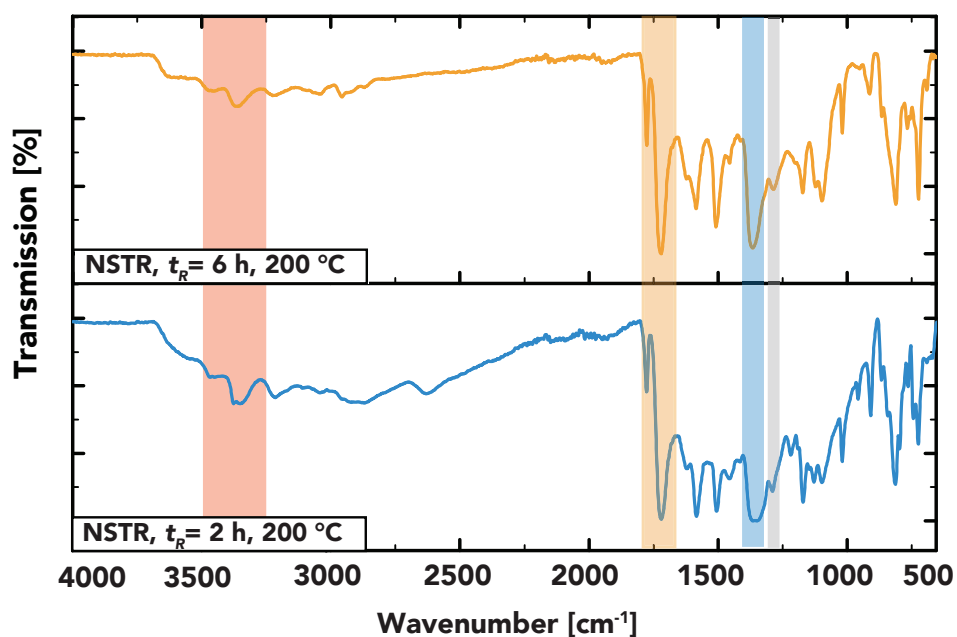


Figure B.2: ATR-IR of TAPM:PMDA at $t_R = 2$ h and 6 h. Red box indicates residual amines.

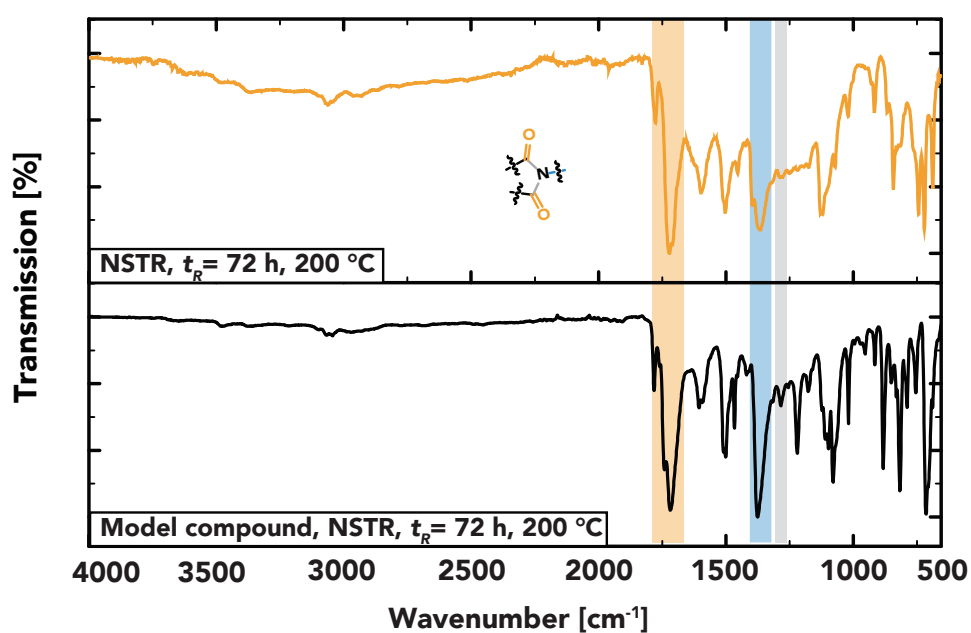


Figure B.3: ATR-IR of TAPM:PMDA at $t_R = 72$ h and the model compound obtained after HTS of TAPM with phthalic anhydride.

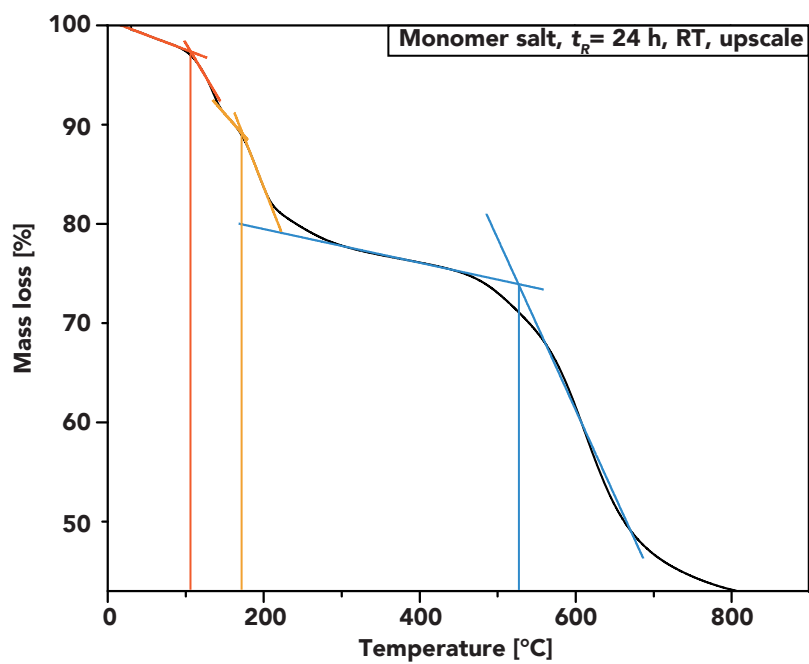


Figure B.4: TGA of the TAPM:PMA monomer salt A: SSP around 170 °C and $T_D \approx 530$ °C

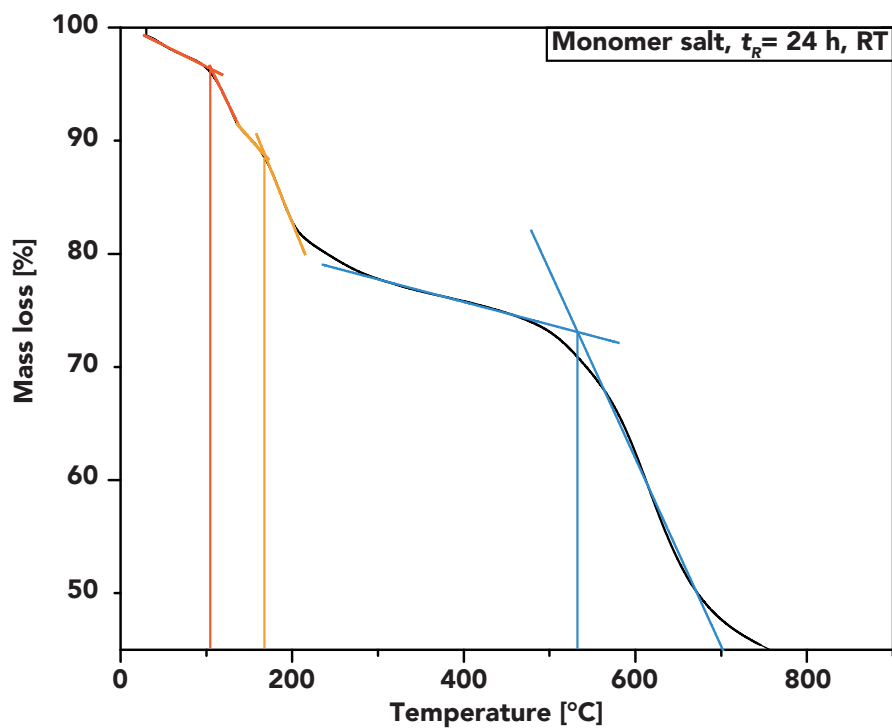


Figure B.5: TGA of the TAPM:PMA monomer salt B: SSP around 170 °C and $T_D \approx 530$ °C

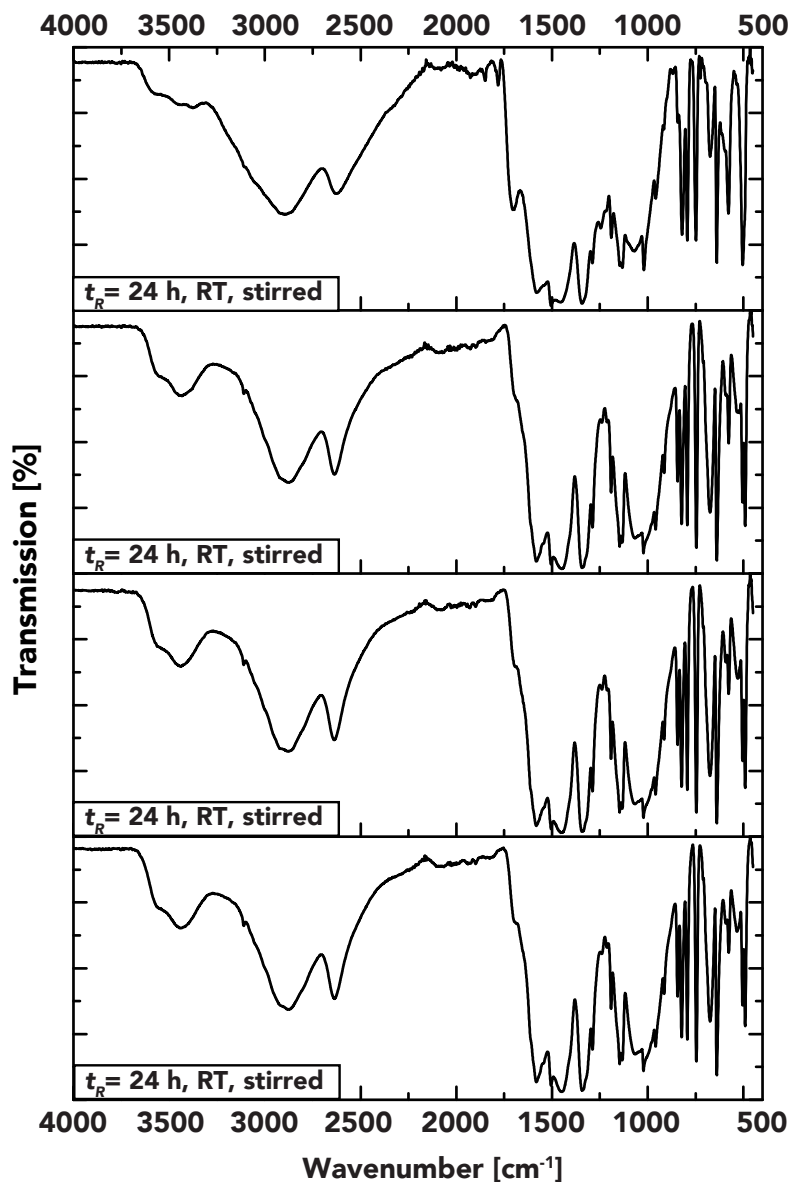


Figure B.6: IR of the TAPM:PMA monomer salt. The absence of amine moieties as well as imide modes indicates that no polymerization occurred, yet the amine moieties were successfully transformed to ammonium moieties.

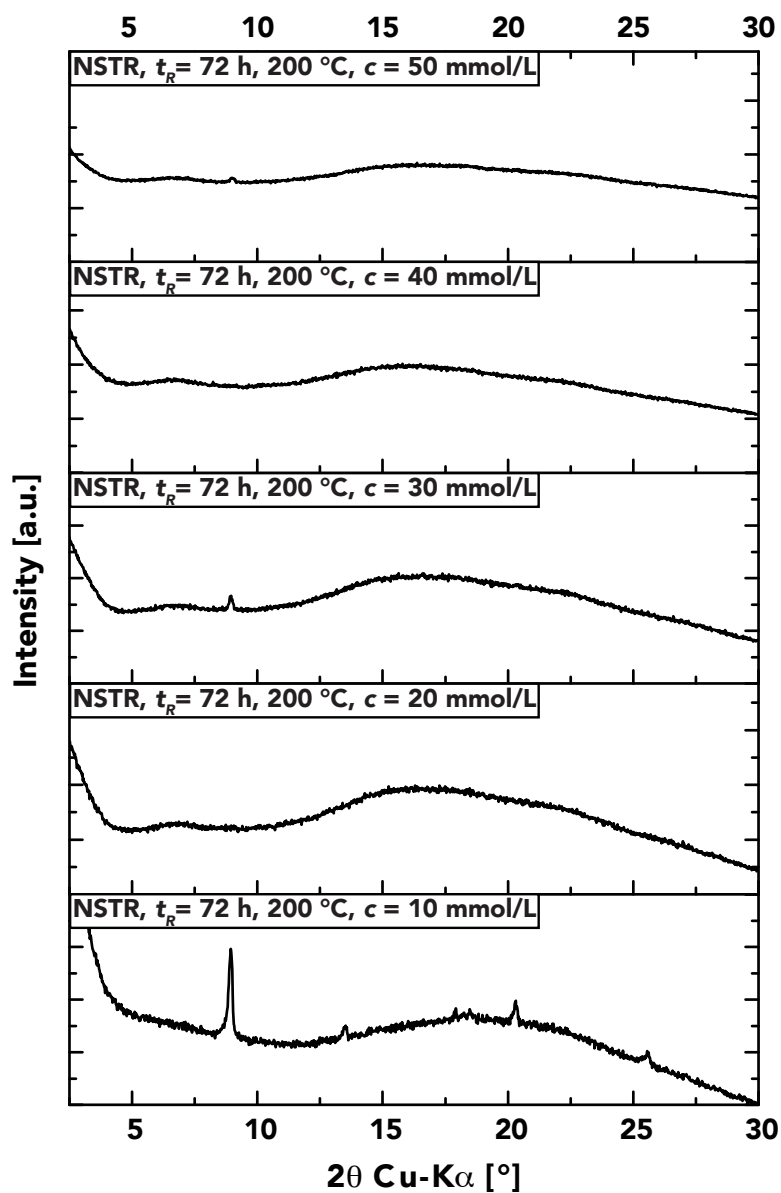


Figure B.7: PXRD of TrisAPM:PMDA. With increasing concentration, the amorphous background increased and crystalline reflections disappeared.

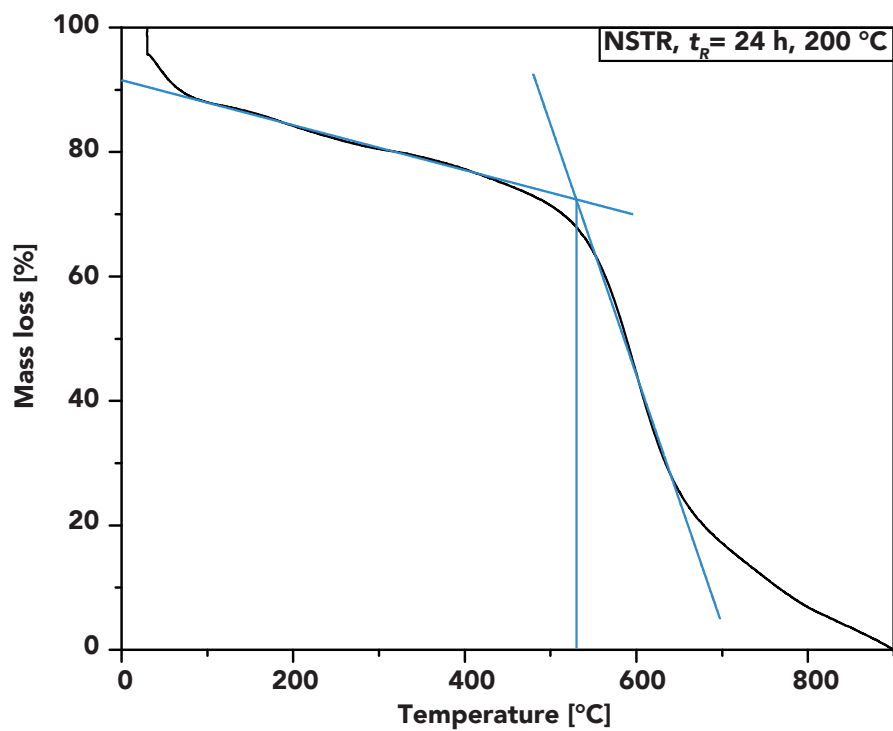


Figure B.8: TGA of the TrisAPM:PMDA. $T_D \approx 530$ °C

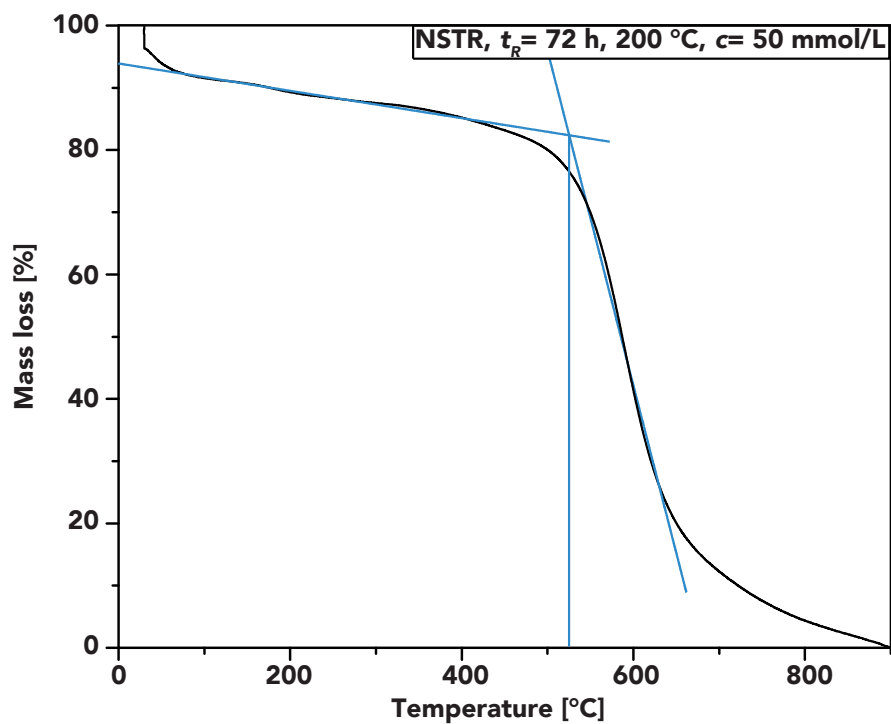


Figure B.9: TGA of TrisAPM:PMDA - conc. screen. $T_D \approx 530$ °C

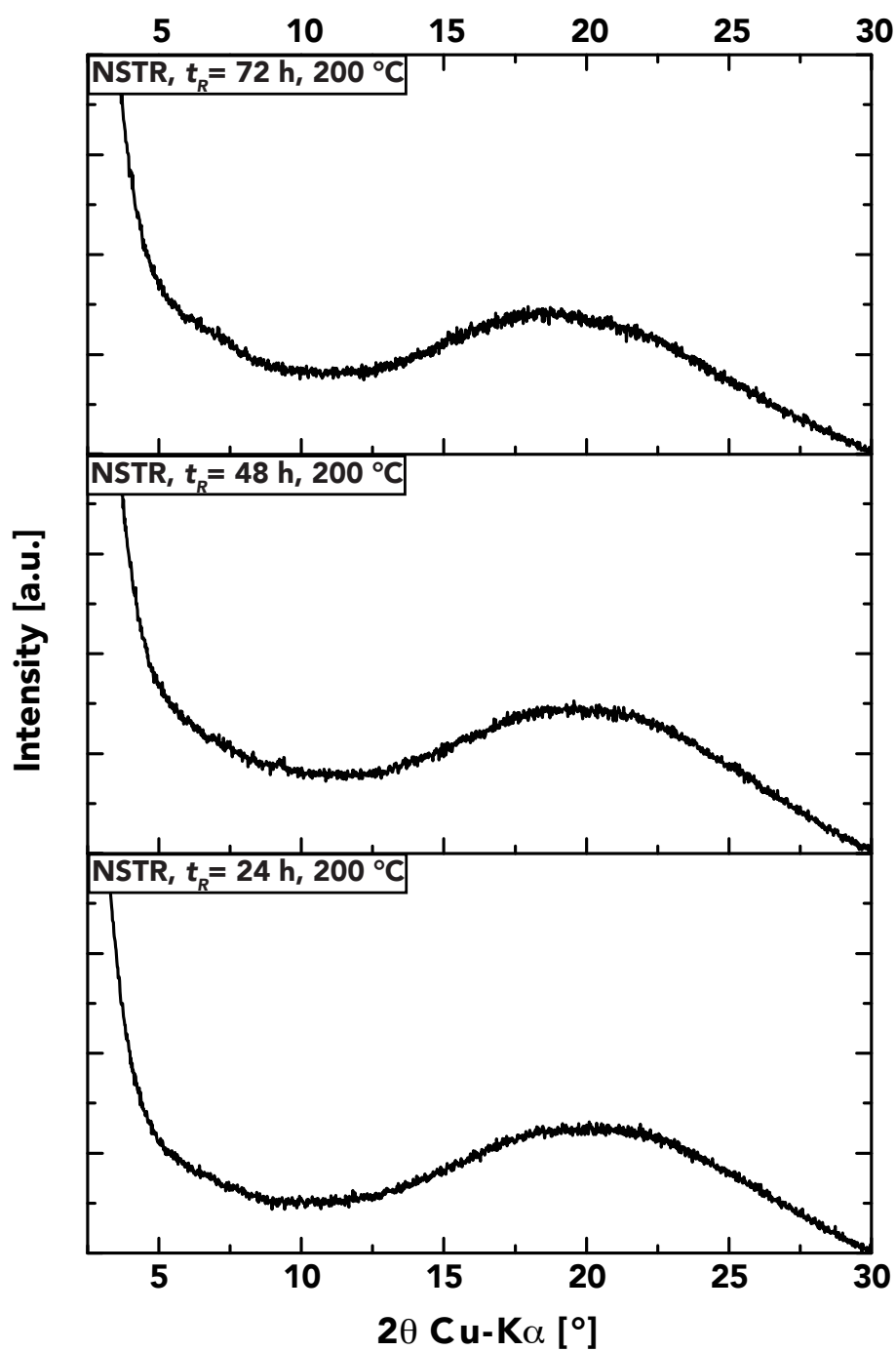


Figure B.10: PXRD of TrisAPM:MellA shows completely amorphous systems. $T_D \approx 530$ °C

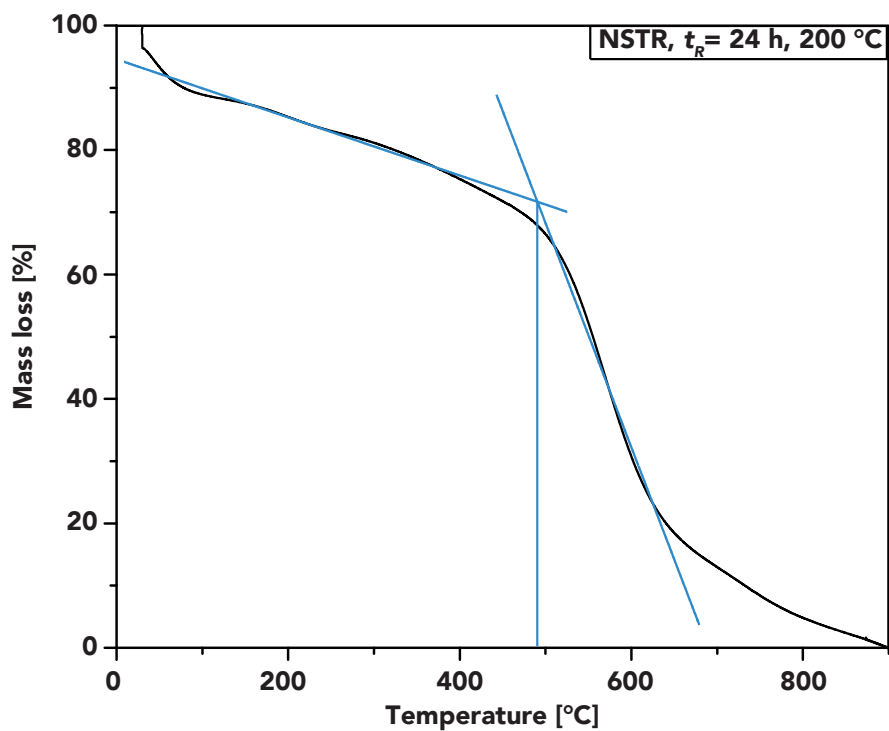


Figure B.11: TGA of TrisAPM:Mella. $T_D \approx 490$ °C. The continuous mass loss between 100 °C $\leq T \leq 400$ °C could indicate elimination of CO_2 .

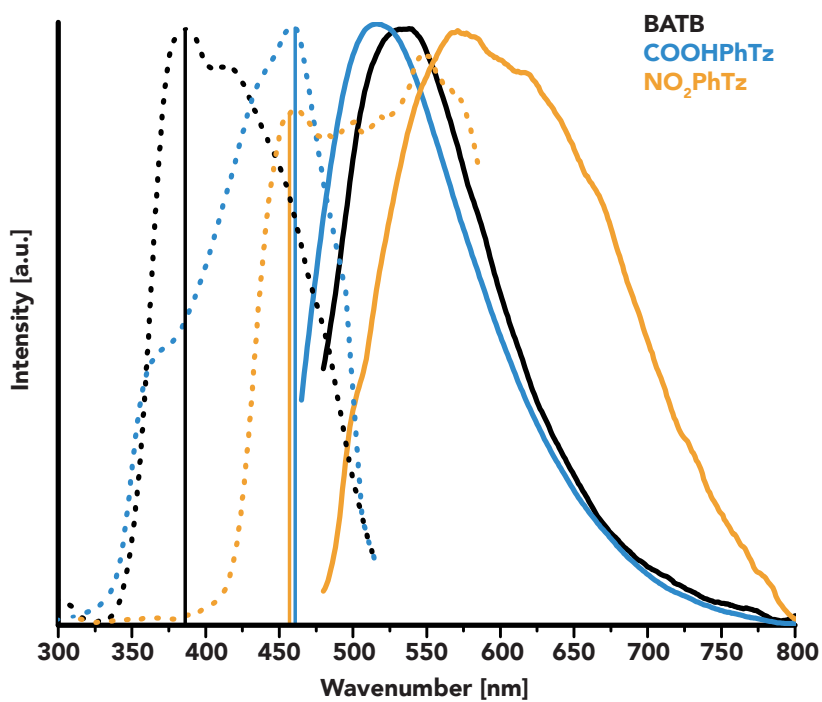


Figure B.12: UV/VIS measurements of DATz systems. As shown, UV/VIS properties can be tuned by tuning the para position.

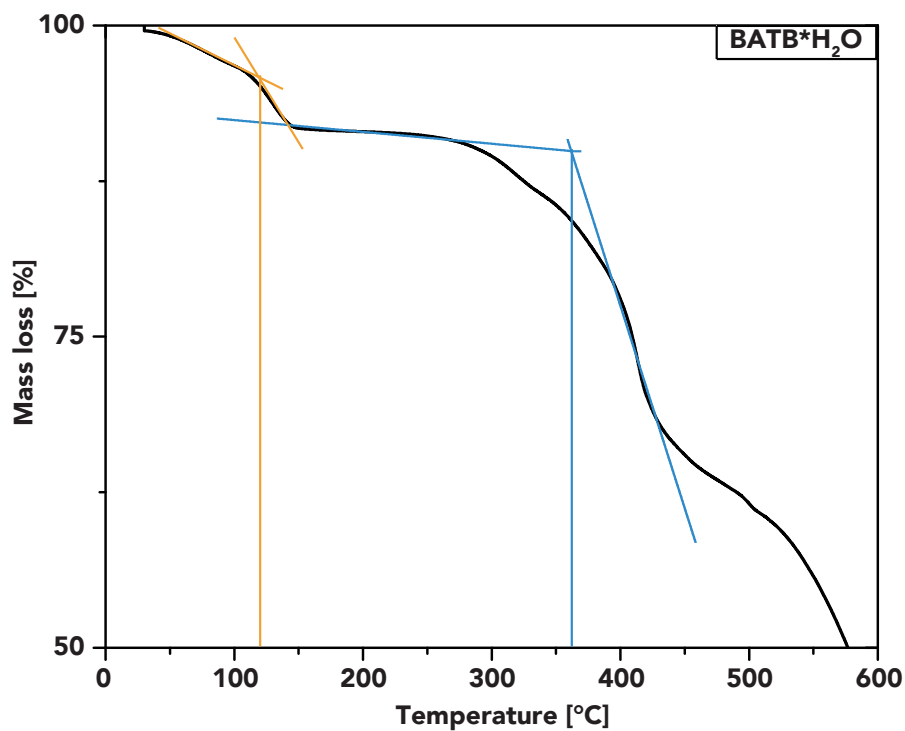


Figure B.13: TGA of BATB. The initial mass-loss can be accounted to the fact that BATB*H₂O was used for the measurement

Appendix C

Crystallization

BATB

_cell_length_a	3.6751(11)
_cell_length_b	11.628(4)
_cell_length_c	15.915(5)
_cell_angle_alpha	90
_cell_angle_beta	90
_cell_angle_gamma	90
symmetry_cell_setting	orthorhombic
_symmetry_space_group_name_H-M	'P n n m'
_symmetry_space_group_name_Hall	'-P 2 2n'
loop_	
_space_group_symop_id	
_space_group_symop_operation_xyz	
1	x,y,z
2	-x,-y,-z
3	-x+1/2,y+1/2,-z+1/2
4	x+1/2,-y+1/2,-z+1/2
5	-x,-y,-z
6	x,y,-z
7	x+1/2,-y+1/2,z+1/2
8	-x+1/2,y+1/2,z+1/2
loop_	
_atom_site_label	
_atom_site_type_symbol	
_atom_site_fract_x	
_atom_site_fract_y	
_atom_site_fract_z	
_atom_site_adp_type	
_atom_site_U_iso_or_equiv	
_atom_site_site_symmetry_multiplicity	
_atom_site_occupancy	
_atom_site_calc_flag	
_atom_site_refinement_flags	
_atom_site_disorder_assembly	
_atom_site_disorder_group	
O1	O 0.2050(4) 0.11833(11) 0 Uani 0.0179(4) 4 1 d . . .
N1	N 0.6054(3) 0.09753(8) 0.27982(6) Uani 0.0092(3) 8 1 d . . .
N2	N 0.5 0 0.14903(8) Uani 0.0101(4) 4 1 d . . .
N3	N 0.7473(3) 0.18213(9) 0.15290(7) Uani 0.0117(3) 8 1 d . . .
C1	C 0.5 0 0.31823(9) Uani 0.0081(4) 4 1 d . . .
C2	C 0.6169(3) 0.09097(9) 0.19475(7) Uani 0.0089(3) 8 1 d . . .
C3	C 0.5 0 0.41177(9) Uani 0.0079(4) 4 1 d . . .
C4	C 0.3547(3) -0.09345(9) 0.45634(7) Uani 0.0088(3) 8 1 d . . .
H1c4	H 0.254726 -0.157736 0.426348 Uiso 0.0106 8 1 d . . .
H1n3	H 0.847(5) 0.2422(14) 0.1799(10) Uiso 0.027(4) 8 1 d . . .
H2n3	H 0.781(5) 0.1772(15) 0.1002(14) Uiso 0.042(6) 8 1 d . . .
H1o1	H 0.277(6) 0.0734(19) 0.0481(13) Uiso 0.063(6) 8 1 d . . .

4NO2MPhTz

_cell_length_a	18.630(2)
_cell_length_b	4.7453(5)
_cell_length_c	9.4253(11)
_cell_angle_alpha	90
_cell_angle_beta	90
_cell_angle_gamma	90
symmetry_cell_setting	orthorhombic
_space_group_IT_number	31
_symmetry_space_group_name_H-M	'P m n 21'
_symmetry_space_group_name_Hall	'P 2ac-2'
loop_	
_space_group_symop_operation_xyz	
1	x,y,z
2	-x+1/2,-y,z+1/2
3	x+1/2,-y,z+1/2
4	-x,y,z
loop_	
_atom_site_label	
_atom_site_type_symbol	
_atom_site_fract_x	
_atom_site_fract_y	
_atom_site_fract_z	
_atom_site_adp_type	
_atom_site_U_iso_or_equiv	
_atom_site_occupancy	
_atom_site_calc_flag	
_atom_site_refinement_flags_posn	
_atom_site_refinement_flags_adp	
_atom_site_refinement_flags_occupancy	
_atom_site_disorder_assembly	
_atom_site_disorder_group	

O1	O	0.24608(6)	1.3745(2)	0.13649(14)	0.0213(2)	Uani	1	1	d
O2	O	0.44166(8)	-0.1066(3)	0.94392(15)	0.0286(3)	Uani	1	1	d
N1	N	0.5000	1.1956(3)	0.25452(18)	0.0118(3)	Uani	1	2	d	S	T	P	.	.	.
N2	N	0.43583(6)	0.9002(3)	0.41730(12)	0.0122(2)	Uani	1	1	d
N3	N	0.37631(6)	1.1885(2)	0.25737(13)	0.0135(2)	Uani	1	1	d
N4	N	0.5000	-0.0204(4)	0.90091(19)	0.0205(4)	Uani	1	2	d	S	T	P	.	.	.
C1	C	0.43954(7)	1.0937(3)	0.31152(13)	0.0110(2)	Uani	1	1	d
C2	C	0.5000	0.8141(4)	0.46353(19)	0.0106(3)	Uani	1	2	d	S	T	P	.	.	.
C3	C	0.37583(7)	1.4190(3)	0.15475(16)	0.0157(3)	Uani	1	1	d
H3A	H	0.4206	1.4161	0.0982	0.019	Uiso	1	1	calc	R	U
H3AB	H	0.3730	1.6020	0.2049	0.019	Uiso	1	1	calc	R	U
C4	C	0.31165(8)	1.3841(3)	0.05832(18)	0.0206(3)	Uani	1	1	d
H4A	H	0.3099	1.5432	-0.0095	0.025	Uiso	1	1	calc	R	U
H4AB	H	0.3170	1.2079	0.0031	0.025	Uiso	1	1	calc	R	U
C5	C	0.24684(7)	1.1389(3)	0.23065(18)	0.0175(3)	Uani	1	1	d
H5A	H	0.2506	0.9629	0.1747	0.021	Uiso	1	1	calc	R	U
H5AB	H	0.2011	1.1330	0.2841	0.021	Uiso	1	1	calc	R	U
C6	C	0.30911(7)	1.1541(3)	0.33464(16)	0.0168(3)	Uani	1	1	d
H6A	H	0.3021	1.3152	0.3999	0.020	Uiso	1	1	calc	R	U
H6AB	H	0.3109	0.9794	0.3919	0.020	Uiso	1	1	calc	R	U
C7	C	0.5000	0.6001(4)	0.57886(18)	0.0115(3)	Uani	1	2	d	S	T	P	.	.	.
C8	C	0.43506(7)	0.4995(3)	0.63307(15)	0.0149(2)	Uani	1	1	d
H8	H	0.3909	0.5696	0.5970	0.018	Uiso	1	1	calc	R	U
C9	C	0.43488(8)	0.2971(3)	0.73969(16)	0.0173(3)	Uani	1	1	d
H9	H	0.3909	0.2268	0.7767	0.021	Uiso	1	1	calc	R	U
C10	C	0.5000	0.1998(4)	0.7909(2)	0.0149(3)	Uani	1	2	d	S	T	P	.	.	.

Bibliography

- [1] A. Kekulé, *Ann. der Chemie und Pharm.* **1857**, *104*, 129–150.
- [2] F. Wöhler, *Ann. der Phys. und Chemie* **1828**, *88*, 253–256.
- [3] A. Baeyer, *Berichte der Dtsch. Chem. Gesellschaft* **1871**, *4*, 555–558.
- [4] J. R. McKee, M. Zanger, *J. Chem. Educ.* **1991**, *68*, A242.
- [5] H. Staudinger, *Berichte der Dtsch. Chem. Gesellschaft (A B Ser.)* **1920**, *53*, 1073–1085.
- [6] P. M. Hergenrother, *High Perform. Polym.* **2003**, *15*, 3–45.
- [7] B. Baumgartner, M. J. Bojdys, M. M. Unterlass, *Polym. Chem.* **2014**, *5*, 3771–3776.
- [8] B. P. Biswal, S. Chandra, S. Kandambeth, B. Lukose, T. Heine, R. Banerjee, *J. Am. Chem. Soc.* **2013**, *135*, 5328–5331.
- [9] O. M. Yaghi, M. J. Kalmutzki, C. S. Diercks, *Introduction to Reticular Chemistry*, **2019**.
- [10] A. P. Cote, *Science (80-.)* **2005**, *310*, 1166–1170.
- [11] F. Zhao, H. Liu, S. Mathe, A. Dong, J. Zhang, *Nanomaterials* **2017**, *8*, 15.
- [12] C. S. Diercks, O. M. Yaghi, *Science (80-.)* **2017**, *355*, eaal1585.
- [13] G. Zhu, H. Ren, *Porous Organic Frameworks*, Springer Berlin Heidelberg, Berlin, Heidelberg, **2015**.
- [14] Y. Zhu, S. Wan, Y. Jin, W. Zhang, *J. Am. Chem. Soc.* **2015**, *137*, 13772–13775.
- [15] Y.-B. Zhang, J. Su, H. Furukawa, Y. Yun, F. Gándara, A. Duong, X. Zou, O. M. Yaghi, *J. Am. Chem. Soc.* **2013**, *135*, 16336–16339.
- [16] F. J. Uribe-Romo, J. R. Hunt, H. Furukawa, C. Klöck, M. O’Keeffe, O. M. Yaghi, *J. Am. Chem. Soc.* **2009**, *131*, 4570–4571.
- [17] Q. Fang, J. Wang, S. Gu, R. B. Kaspar, Z. Zhuang, J. Zheng, H. Guo, S. Qiu, Y. Yan, *J. Am. Chem. Soc.* **2015**, *137*, 8352–8355.
- [18] Y. Jin, C. Yu, R. J. Denman, W. Zhang, *Chem. Soc. Rev.* **2013**, *42*, 6634.
- [19] S. Kandambeth, A. Mallick, B. Lukose, M. V. Mane, T. Heine, R. Banerjee, *J. Am. Chem. Soc.* **2012**, *134*, 19524–19527.
- [20] Q. Fang, Z. Zhuang, S. Gu, R. B. Kaspar, J. Zheng, J. Wang, S. Qiu, Y. Yan, *Nat. Commun.* **2014**, *5*, 4503.
- [21] J. Guo, Y. Xu, S. Jin, L. Chen, T. Kaji, Y. Honsho, M. A. Addicoat, J. Kim, A. Saeki, H. Ihee, S. Seki, S. Irle, M. Hiramoto, J. Gao, D. Jiang, *Nat. Commun.* **2013**, *4*, 2736.
- [22] P. Kuhn, M. Antonietti, A. Thomas, *Angew. Chemie Int. Ed.* **2008**, *47*, 3450–3453.
- [23] R. Gutzler, H. Walch, G. Eder, S. Klotz, W. M. Heckl, M. Lackinger, *Chem. Commun.* **2009**, 4456.
- [24] D. Schwarz, Y. Noda, J. Klouda, K. Schwarzová-Pecková, J. Tarábek, J. Rybáček, J. Janoušek, F. Simon, M. V. Opanasenko, J. Čejka, A. Acharjya, J. Schmidt, S. Selve, V. Reiter-Scherer, N. Severin, J. P. Rabe, P. Ecorchard, J. He, M. Polozij, P. Nachtigall, M. J. Bojdys, *Adv. Mater.* **2017**, *29*, 1703399.
- [25] J. R. Hunt, C. J. Doonan, J. D. LeVangie, A. P. Côté, O. M. Yaghi, *J. Am. Chem. Soc.* **2008**, *130*, 11872–11873.
- [26] L. M. Lanni, R. W. Tilford, M. Bharathy, J. J. Lavigne, *J. Am. Chem. Soc.* **2011**, *133*, 13975–13983.
- [27] L. Zhu, Y.-B. Zhang, *Molecules* **2017**, *22*, 1149.
- [28] S. Kandambeth, D. B. Shinde, M. K. Panda, B. Lukose, T. Heine, R. Banerjee, *Angew. Chemie Int. Ed.* **2013**, *52*, 13052–13056.
- [29] S. Kandambeth, A. Mallick, B. Lukose, M. V. Mane, T. Heine, R. Banerjee, *J. Am. Chem. Soc.* **2012**, *134*, 19524–19527.
- [30] L. Grill, M. Dyer, L. Lafferentz, M. Persson, M. V. Peters, S. Hecht, *Nat. Nanotechnol.* **2007**, *2*, 687–691.
- [31] X. Feng, X. Ding, D. Jiang, *Chem. Soc. Rev.* **2012**, *41*, 6010.
- [32] S. Ren, M. J. Bojdys, R. Dawson, A. Laybourn, Y. Z. Khimyak, D. J. Adams, A. I. Cooper, *Adv. Mater.* **2012**, *24*, 2357–2361.

- [33] J. F. Dienstmaier, A. M. Gigler, A. J. Goetz, P. Knochel, T. Bein, A. Lyapin, S. Reichlmaier, W. M. Heckl, M. Lackinger, *ACS Nano* **2011**, *5*, 9737–9745.
- [34] R. A. Laudise, A. A. Ballman, *J. Am. Chem. Soc.* **1958**, *80*, 2655–2657.
- [35] C. S. Cundy, P. A. Cox, *Chem. Rev.* **2003**, *103*, 663–702.
- [36] M. Fujita, Y. J. Kwon, S. Washizu, K. Ogura, *J. Am. Chem. Soc.* **1994**, *116*, 1151–1152.
- [37] D. G. Hawthorne, J. H. Hodgkin, M. B. Jackson, J. W. Loder, T. C. Morton, *High Perform. Polym.* **1994**, *6*, 287–301.
- [38] J. Chiefari, B. Dao, A. M. Groth, J. H. Hodgkin, *High Perform. Polym.* **2003**, *15*, 269–279.
- [39] L. Leimhofer, B. Baumgartner, M. Puchberger, T. Prochaska, T. Konegger, M. M. Unterlass, *J. Mater. Chem. A* **2017**, *5*, 16326–16335.
- [40] M. M. Unterlass, *Angew. Chemie Int. Ed.* **2018**, *57*, 2292–2294.
- [41] M. Uematsu, E. U. Frank, *J. Phys. Chem. Ref. Data* **1980**, *9*, 1291–1306.
- [42] W. L. Marshall, E. U. Franck, *J. Phys. Chem. Ref. Data* **1981**, *10*, 295–304.
- [43] B. Baumgartner, A. Svirikova, J. Binting, C. Hametner, M. Marchetti-Deschmann, M. M. Unterlass, *Chem. Commun.* **2017**, *53*, 1229–1232.
- [44] D. Laliberté, T. Maris, E. Demers, F. Helzy, M. Arseneault, J. D. Wuest, *Cryst. Growth Des.* **2005**, *5*, 1451–1456.
- [45] L. L. Koh, K. Eriks, *Acta Crystallogr. Sect. B Struct. Crystallogr. Cryst. Chem.* **1971**, *27*, 1405–1413.
- [46] B. Baumgartner, M. Puchberger, M. M. Unterlass, *Polym. Chem.* **2015**, *6*, 5773–5781.
- [47] M. Gomberg, *J. Am. Chem. Soc.* **1898**, *20*, 773–780.
- [48] Y. Zhang, S. Jin, *Polymers (Basel)* **2018**, *11*, 31.
- [49] L. Xu, R. Liu, F. Wang, S. Yan, X. Shi, J. Yang, *RSC Adv.* **2019**, *9*, 1586–1590.
- [50] J. Bi, W. Fang, L. Li, J. Wang, S. Liang, Y. He, M. Liu, L. Wu, *Macromol. Rapid Commun.* **2015**, *36*, 1799–1805.
- [51] P. Puthiaraj, Y.-R. Lee, S. Zhang, W.-S. Ahn, *J. Mater. Chem. A* **2016**, *4*, 16288–16311.
- [52] M. Liu, L. Guo, S. Jin, B. Tan, *J. Mater. Chem. A* **2019**, *7*, 5153–5172.
- [53] S. Hug, L. Stegbauer, H. Oh, M. Hirscher, B. V. Lotsch, *Chem. Mater.* **2015**, *27*, 8001–8010.
- [54] M. Ruiz-Osés, N. González-Lakunza, I. Silanes, A. Gourdon, A. Arnau, J. E. Ortega, *J. Phys. Chem. B* **2006**, *110*, 25573–25577.
- [55] M. J. Taublaender, F. Glöckhofer, M. Marchetti-Deschmann, M. M. Unterlass, *Angew. Chemie Int. Ed.* **2018**, *57*, 12270–12274.
- [56] X. Mu, J. Zhan, X. Feng, B. Yuan, S. Qiu, L. Song, Y. Hu, *ACS Appl. Mater. Interfaces* **2017**, *9*, 23017–23026.
- [57] G. Inzelt, *J. Electrochem. Sci. Eng.* **2017**, DOI 10.5599/jese.448.
- [58] J. A. Joule, *Thiophenes*, (Ed.: J. A. Joule), Springer International Publishing, Cham, **2015**.
- [59] K. Kaneto, K. Yoshino, Y. Inuishi, *Solid State Commun.* **1983**, *46*, 389–391.
- [60] S. Das, D. P. Chatterjee, R. Ghosh, A. K. Nandi, *RSC Adv.* **2015**, *5*, 20160–20177.
- [61] M. T. Dang, L. Hirsch, G. Wantz, *Adv. Mater.* **2011**, *23*, 3597–3602.
- [62] R. S. Loewe, S. M. Khersonsky, R. D. McCullough, *Adv. Mater.* **1999**, *11*, 250–253.
- [63] L. Groenendaal, F. Jonas, D. Freitag, H. Pielartzik, J. R. Reynolds, *Adv. Mater.* **2000**, *12*, 481–494.
- [64] M. Pomerantz, Y. Cheng, R. K. Kasim, R. L. Elsenbaumer, *J. Mater. Chem.* **1999**, *9*, 2155–2163.
- [65] H. Meng, D. F. Perepichka, F. Wudl, *Angew. Chemie Int. Ed.* **2003**, *42*, 658–661.
- [66] Y. Yin, Z. Li, J. Jin, C. Tusy, J. Xia, *Synth. Met.* **2013**, *175*, 97–102.
- [67] M. F. Pepitone, K. Eaiprasertsak, S. S. Hardaker, R. V. Gregory, *Org. Lett.* **2003**, *5*, 3229–3232.